STRUCTURE AND METAMORPHISM OF THE EASTERN BOUNDARY OF THE LABRADOR TROUGH NEAR KUUJJUAQ, QUEBEC, AND ITS TECTONIC IMPLICATIONS

by

Glenn Gerard Poirier

Department of Geological Sciences
McGill University, Montreal, Quebec

A Thesis submitted to the Faculty of Graduate Studies in partial fulfillment of the requirements for the degree Master of Science

March, 1989

Abstract

Geological mapping east of the Labrador Trough ($\approx 58°$ N, $62°$ $40'$ W) has delimited three distinct lithotectonic blocks which are, from west to east, the Lac Rachel-Lac Murray Block (LRLMB), the Lac Gabriel Block (LGB), and the Lac Berthet Block (LBB). The supracrustal succession of the LRLMB rests on the flanks of a series of doubly-plunging antiforms cored by reworked Archean gneiss. It is correlated with the Laporte "Group" and is believed to represent a distal equivalent of the Trough sediments, deposited on a continental rise. The LGB and LBB are considered correlative, and are believed to reflect sedimentation in a continental slope/shelf environment. The rocks of these blocks differ markedly from those of the Trough. A syntectonic intrusive complex (granodiorite to tonalite) in the LBB has petrological and geochemical characteristics consistent with calc-alkaline, "I" type volcanic arc granitoids.

The area records three phases of deformation, of progressively declining intensity. An early metamorphic event is recorded in the rocks of the LGB and LBB and was later overprinted by a second event which affected all the rocks in the area. Peak conditions of the second metamorphism were 750°C at 7 kbar.

The characteristics of the blocks indicate that the LBB and LGB may be exotic blocks which collided with the eastern margin of the Trough early in the orogeny, although they may simply be an uplifted portion of the eastern margin of the original sedimentary basin. The best modern analog for Hudsonian processes in the area is the Himalayan Orogen.

Résumé

La cartographie géologique de la partie est de la Fosse du Labrador ($\approx$ 58° N, 62°40' O) a permis de définir trois blocs lithotectoniques qui sont, de l'ouest vers l'est, le Bloc des Lacs Rachel et Murray (LRLMB), le Bloc du Lac Gabriel (LGB), et le Bloc du Lac Berthet (LBB). La succession supracrustale du LRLMB repose sur les flancs de séries de plis antiformes à double plongées contenant dans leur coeur des gneiss remobilisés Archéen. Ce bloc est corrélé avec le "Groupe" Laporte et il est considéré l'équivalent distal des sédiments de la Fosse qui se sont déposés sur une pente continentale. Les blocs LGB et LBB semblent corrélables entre eux et représenteraient un environnement de sédimentation de type plateau continental. Les roches de ces blocs sont très différentes de celles de la Fosse. Un complexe intrusif syntectonique (de granodiorite à tonalite) dans le bloc LBB a des caractéristiques pétrologiques et géochimiques similaires à celles des granitoïdes calco-alcalins de type "I" des arcs volcaniques.

La région a subi trois phases de déformation d'intensité décroissante. Le premier épisode métamorphique est préservé dans les roches des blocs LGB et LBB et elles ont subi par la suite la surimposition d'un second métamorphisme qui a aussi affecté toutes les roches de la région. Les conditions maximales atteintes lors du second épisode métamorphique furent de 750 °C à 7 kbar.

Les données géologiques semblent indiquer que les blocs LBB et LGB sont dérigine allochtone et seraient entrés en collision avec la marge est de la Fosse. Il est aussi possible qu'ils représentent la partie soulevée de la marge est du bassin sédimentaire d'origine. Le meilleur analogue moderne de cet évènement Hudsonien serait l'orogène Himalayen.

Traduit par Serge Nadeau

Table of Contents

Table of Contents (cont.)

Table of Contents (cont.)

Table of Contents (cont.)

List of Figures (cont.)

<u>List of Figures (cont.)</u>

List of Tables

Chapter 1. Introduction

1.1 Purpose and Scope

The Labrador Trough is the erosional remnant of a basin that was filled with Aphebian volcanic and sedimentary rocks and subsequently deformed and metamorphosed. This thesis concerns a suite of metamorphosed and multiply deformed sedimentary and igneous rocks on the eastern flank of the Labrador Trough near Kuujjuaq, Quebec. These rocks were deformed and metamorphosed with the Labrador Trough rocks during the early Proterozoic (Aphebian) Hudsonian Orogeny, but their relationship to the rocks forming the bulk of the Labrador Trough is uncertain.

Most of our present knowledge of the tectonic evolution of the Labrador Trough has been obtained through study of the mildly deformed and metamorphosed foreland fold-and-thrust belt that constitutes the Labrador Trough _sensu. stricto._ (e.g. Dimroth, 1972, Wardle and Bailey, 1981 and Lavoie and LeGallais, 1982), whose eastern margin is defined by the first occurrence of basement rocks east of the Superior province. Little attention has been given to the more highly deformed and metamorphosed "hinterland" regions east of it. Although the foreland fold-and-thrust belt provides excellent opportunities for the study of processes associated with the development of the sedimentary

basin, the hinterland regions may shed much light on the orogenic evolution of the Labrador Trough.

The first question to be addressed in this study concerns the relationship between the study area and the Labrador Trough _sensu stricto_. Is the study area simply an eastern extension of the Labrador Trough or was it juxtaposed to the Trough during the orogeny (_i.e._ is there an intervening suture)? Of equal importance are questions about the nature of the orogeny in the area. Studies of the stratigraphic, petrological and metamorphic evolution of the hinterland region will provide important constraints on the overall tectonic evolution of the orogen and allow comparison of processes of Proterozoic orogenies with modern ones. There is considerable controversy concerning when plate tectonic processes similar to those observed in modern orogenies first began (cf. papers in Kroner, 1981). Studies in the western portions of Laurentia (_e.g._ Lewry _et al._, 1985; Hoffman, 1980, 1988) have shown that early Proterozoic orogens have many similarities to modern ones, although other authors have pointed out differences (_e.g._ Glikson, 1982).

1.2 Location, Access and Physiography

The area studied in this work lies on the southwestern shores of Ungava Bay in Northern Quebec approximately 30 km west of Kuujjuaq (Fort Chimo). It is a long thin swath

2

approximately 58 km long extending from latitude 58°08' N to 58°33' N at longitude 68°42' W.

Although close to Kuujjuaq, the area is accessible only by float equipped aircraft or helicopter. In the month of June access is often limited to helicopter only, due to breakup of ice on the lakes. A year-round float/ski plane service is available in Kuujjuaq, but helicopter service is only sporadically available.

The area consists mainly of gently rolling ridge and valley type terrain whose average elevation increases from 50 meters above sea level in the east to 150 meters above sea level in the west (see Plate 1a). The highest point in the area occurs near Lac a Foin and has an elevation of 234 meters. The area contains abundant lakes of all sizes, the largest of which make up the Lac Berthet-Lac Gabriel system, which drains most of the region. The physiography is largely the result of the last glaciation which rounded and polished much of the outcrop (forming roches moutonnées) and deposited large amounts of glacial material ranging in size from house-sized boulders to the sand and gravel deposits which cover significant parts of the region. Glacial striae indicate movement in a north-south direction.

Despite the abundance of glacial deposits, the area offers excellent exposures of bedrock. Exposure in the area is typically greater than 25% and in some large areas can reach up to 100%. The best exposure is usually found on ridges made of rocks which

3

have a greater resistance to erosion (typically amphibolites) than those underlying valleys.

The tree line passes through the extreme southern parts of the study area, but isolated pockets of forest are found in sheltered valleys over much of the region. Ground cover consists mainly of a thick mat of caribou lichen with sporadic stunted conifers. Clumps of alder brush are commonly found in wet, low-lying locations.

The climate of the area is sub-Arctic, with frost and snow possible in any summer month. Average daytime temperatures for the months of July and August range from 10 to 15 ° C. Blizzards may occur until late June.

1.3 Previous Work

1.3.1 Tectonic Setting of the Labrador Trough

The Canadian Shield consists of at least six Archean provinces separated by a network of orogenic belts created in early Proterozoic times (Hoffman, 1988). The Archean provinces are the Nain in Labrador and Greenland, the Superior in Quebec, Ontario and Manitoba, the Slave in the Northwest Territories, the Wyoming in the northwest United States and the Hearne and the Rae recently proposed by Hoffman (1988) for the southeast and northeast parts respectively of the Canadian Shield between the Superior and Slave Provinces. Those parts of the Shield which were affected by early Proterozoic orogenies (the Trans-Hudson

Orogen, Hoffman, 1981) extend over 5000 km from the mid-continental United States through northern Saskatchewan, Manitoba, Ontario, Quebec and the Northwest Territories eastward into Greenland (Lewry et al., 1985; see Fig. 1). These areas are collectively known as the Churchill Province (Stockwell, 1963).

Although originally believed to be the product of a single orogeny between the proto-Churchill and Superior Provinces (cf. Dewey and Burke, 1973; Gibb, 1983), it is now apparent that the Trans-Hudson Orogen may be composite in nature, with orogenies occurring on all the borders of all the provinces. For example, Lewry (1981) presented evidence for intra-orogenic suturing and microplate collision in the Churchill in Saskatchewan. In a recent review paper (Hoffman, 1988) it has been suggested that the Trans-Hudson orogen is actually the result of at least five orogenies. These are the Thelon Orogeny, a Slave-Rae collision; the Snowbird Orogeny, a Rae-Hearne collision; the Trans-Hudsonian s.s., a Superior-Wyoming-Hearne collision; The Labrador Trough, a Rae-Superior collision and the Torngat Orogeny a Rae-Nain collision.

These orogenies are now generally believed to have involved extensive subduction of early Proterozoic oceanic crust (Dewey and Burke; 1973; Lewry et al., 1985; Thomas and Gibb, 1985; Hoffman, 1988) with attendant calc-alkaline magmatism (e.g. Stauffer, 1984; van der Leeden et al., in press) and volcanism (Lewry et al. , 1981; Stauffer, 1984; Hoffman, 1985), extensive basement remobilization (Lewry and Sibbald, 1980; Lewry et

Lower Proterozoic supracrustals

Volcanic and plutonic allocthonous terrains

Accreted early Proterozoic terrains

Ensialic mobile zones

Mildly reworked foreland zones

Archean cratons
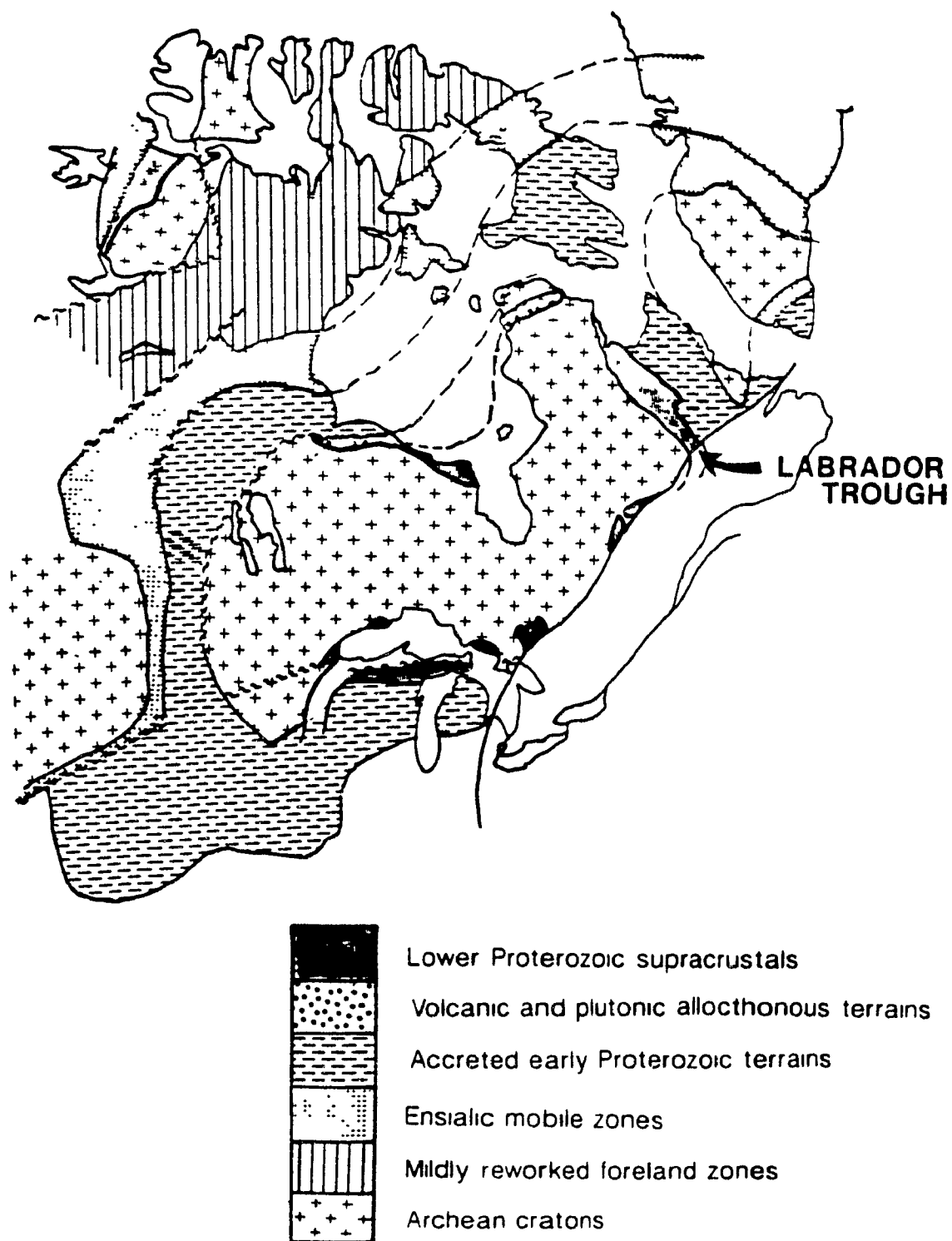
Figure 1. Simplified map after Van Schmus **et al.** (1987) showing lithotectonic elements and early Proterozoic terrains of North America. Wavy broken lines indicate major shear zones.

al.,1985) and high-grade metamorphism (cf. papers in Fraser et al., 1978).

Although the Labrador Trough has conventionally been considered part of the Trans-Hudson Orogen, Hoffman (1988) suggests that this may not be the case unless the Rae Province had already docked with the Hearne Province prior to the Rae-Superior collision. Since evidence for or against this proposal still is lacking, the orogeny responsible for the development of the Labrador Trough and its hinterland will be referred to as the Labrador Trough Orogeny in this paper.

The Labrador Trough is but one of a number of early Proterozoic fold belts in the eastern Churchill Province (see Fig. 2). The best known of these fold belts are the Cape Smith and Belcher Island fold belts, which both lie unconformably on Superior Province basement (Dimroth et al., 1972; Baragar and Scoates, 1981; Hynes and Francis, 1982). The Cape Smith belt is composed mainly of tholeiitic basalts, with subordinate iron formation, komatiitic flows, ultramafic sills and minor sediments (Hynes and Francis, 1982). The belt also contains small late-tectonic granodiorite plutons (Lucas and St. Onge, 1987). The Belcher Island Fold Belt is composed mainly of stable platform marine sediments and massive tholeiitic basalts (Dimroth et al., 1972; Baragar and Scoates, 1981).

The other fold belts in the region were first described by Jackson and Taylor (1972) and are known as the Fox (central Baffin Island and Melville Peninsula), Dorset (Southern Baffin
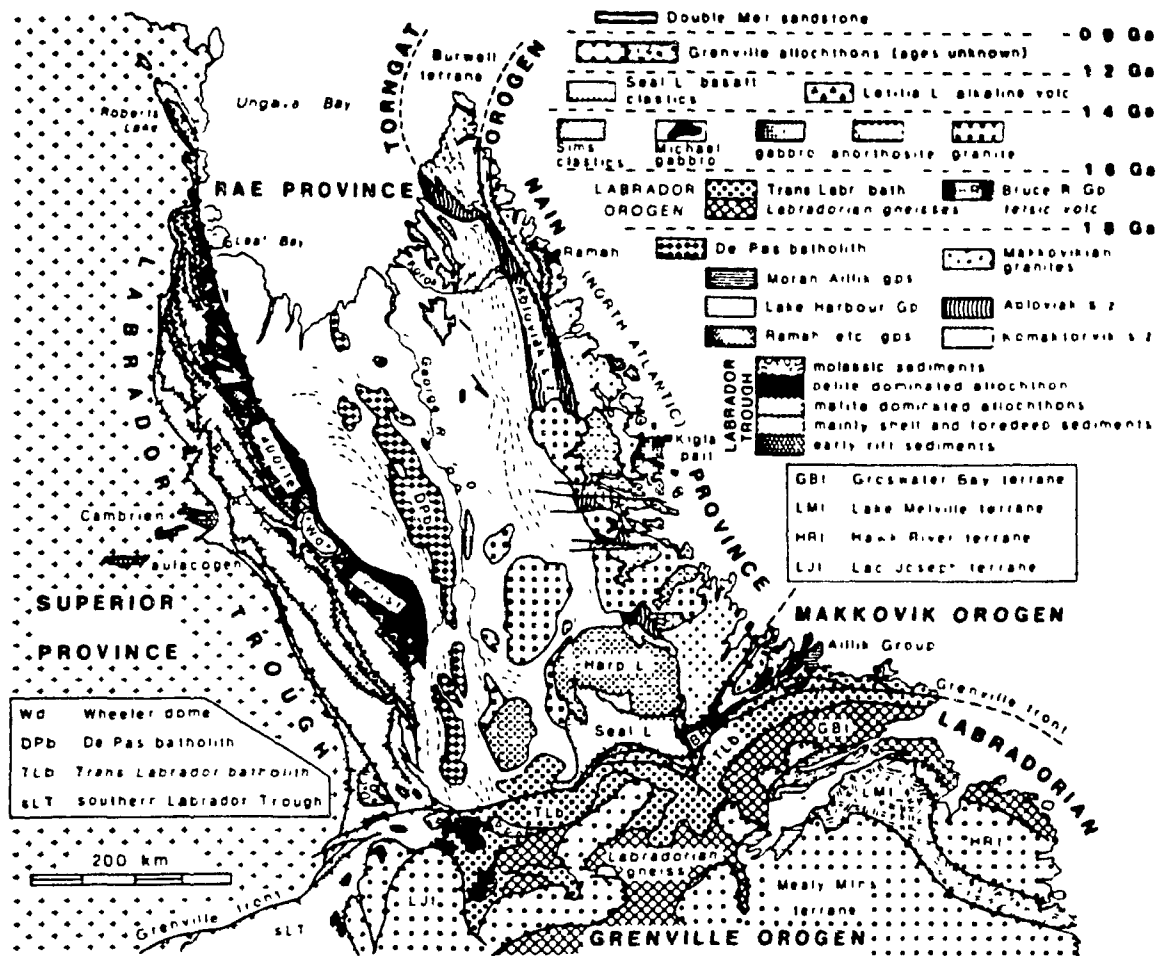
Figure 2. Geology of northern Quebec and Labrador, showing relationships between Precambrian provinces. From Hoffman, 1988.

Island) and Committee fold belts. The Fox and Dorset fold belts consist mainly of metased.ments with minor basic volcanics, while the Committee Fold Belt is composed mainly of basic Archean metavolcanics and minor sediments which were reworked during the Hudsonian. These three belts surround a 250,000 km² granite-charnockite batholith (Hoffman, 1988).

Correlations among these fold belts have been proposed by Bergeron (1957, Labrador Trough and Cape Smith Belt), Dimroth et al. (1972, Labrador Trough, Cape Smith and Belcher Island Fold Belts), Jackson and Taylor (1972, Labrador Trough, Cape Smith, Belcher Islands, Fox, Dorset and Committee Fold Belts) and Baragar and Scoates (1981, Labrador Trough, Cape Smith, Belcher Islands and smaller belts on the southern border of the Superior Province).

1.3.2 General Geology of the Labrador Trough and Environs

Since it was first described by A. P. Low in 1896, the Labrador Trough has been the subject of a great deal of study and exploration. The first real wave of exploration occurred during the late 1940's when large areas of the Trough were staked and drilled by mining companies searching for copper and nickel in the volcanic and intrusive rocks. During the late fifties and sixties most of the Labrador Trough was mapped at a scale of 1:63,360 by geologists from the Ministère de l'Energie et des Ressources du Québec. In the sixties and seventies large portions of the area east of the Labrador Trough were mapped at

9

a reconnaissance scale by the Geological Survey of Canada. The western parts of the study area were mapped by Gelinas (1958, 1959) at a scale of 1:63,360 and the remainder of the area was covered by Taylor and Skinner (1963) at a scale of 1:250,000.

Although fieldwork for this report was carried out to the east of the eastern limit of the Labrador Trough s.s., its conclusions will deal with the Labrador Trough and surrounding areas. Therefore a brief description of the Labrador Trough is in order. The Labrador Trough is a 900 km long, NW-trending belt of Aphebian volcanic and sedimentary rocks. The Trough stretches from the southwestern shores of Ungava Bay to the Grenville Front, and has been recognized for some distance into the Grenville Province (Dimroth et al., 1970). It is bounded to the west by the Archean Superior Province and to the east by the lesser known rocks of the Labrador segment of the Churchill Structural Province (name from Van Schmus et al., 1987)

The Labrador Trough is conventionally divided into three zones or lithotectonic domains which run parallel to its long dimension (Dimroth, 1972, 1978; Figure 3 this report) . The westernmost zone is made up of a series of autochthonous to para-autochthonous sediments and minor volcanic rocks resting unconformably on the Archean gneisses of the Superior Province. The western portions of this zone are undeformed, but minor deformation is observed in its eastern parts (LeGallais and Lavoie, 1982). This zone is followed to the east by a typical foreland fold-and-thrust belt consisting of thrust slices of

10
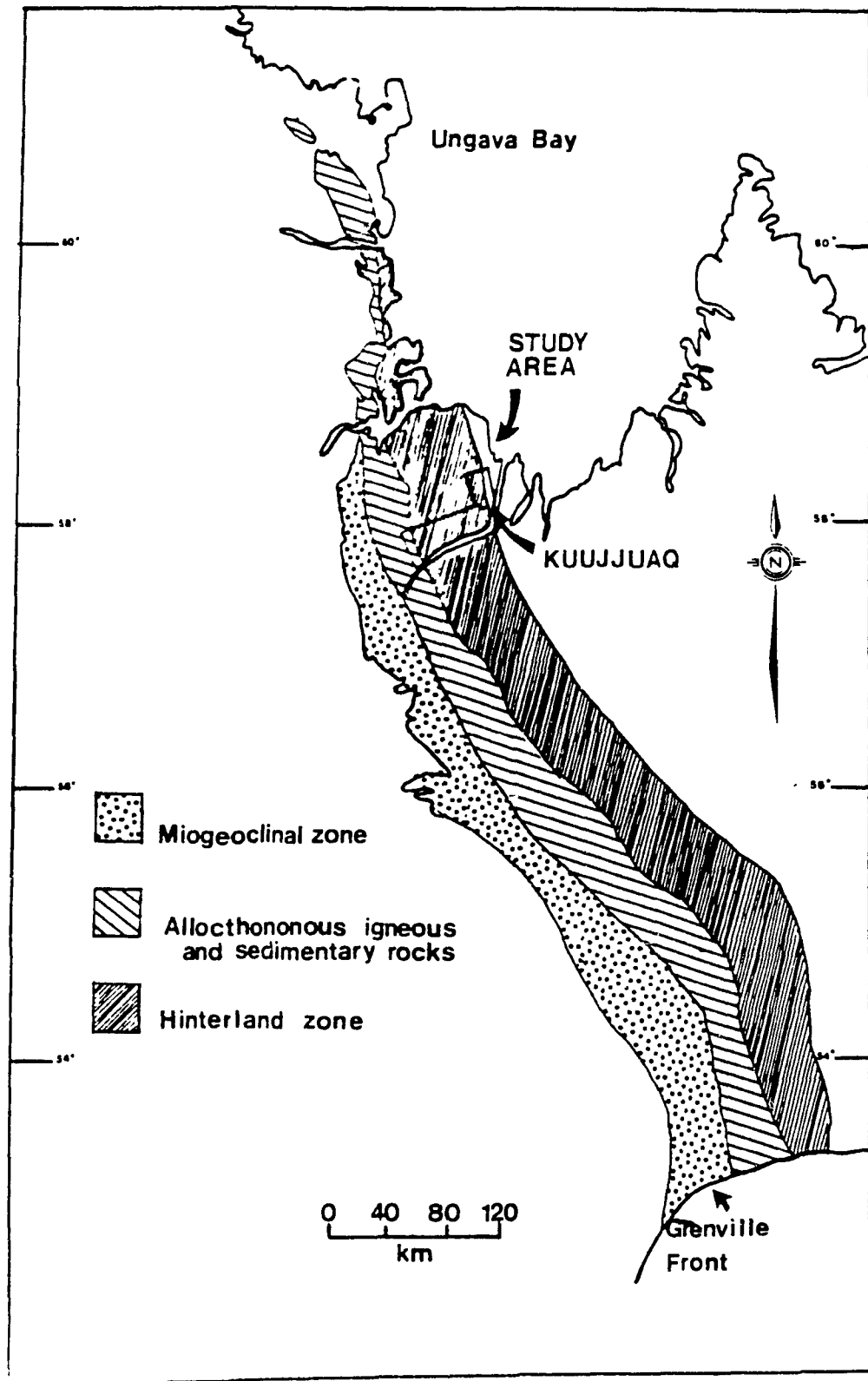
Figure 3. Major subdivisions of the Labrador Trough. Location of study area is outlined. Diagram modified after Dimroth and Dressler (1978)

sedimentary and basaltic volcanic rocks. There is no evidence of basement involvement in the deformation of this zone (Boone and Hynes, 1987 and in press). These two zones make up the Labrador Trough s.s. The sedimentary and volcanic rocks of the Trough belong to the Kaniapiskau Supergroup while the gabbroic and ultramafic intrusives make up the Montagnais Group (Frarey and Duffell, 1964).

The third, or "hinterland", zone contains sequences of volcanic and sedimentary rocks which were highly metamorphosed and deformed during the Hudsonian Orogeny. Although Dimroth's original hinterland zone referred only to those rocks on the immediate boundary of the Trough, in this report the term is used to refer to the entire area between the Labrador Trough s.s. and the Nain Province in Labrador. Relationships between this zone and the Labrador Trough s.s. are obscured by metamorphism and deformation, but some correlations have been made between the rocks of this zone and those of the Kaniapiskau Supergroup (Taylor, 1979; Wardle and Bailey, 1981; Moorhead and Hynes, 1986). The hinterland is generally separated from the rocks of the Labrador Trough s.s. by high angle faults (LeGallais and Lavoie, 1982).

The history of sedimentation and volcanism in the Labrador Trough has been the subject of a number of reports and papers (e.g. Dimroth, 1970; Dimroth, 1971, 1972, 1978; Wardle and Bailey, 1981; LeGallais and Lavoie,1982). Most authors believe that the sedimentary and volcanic rocks of the Trough, the

12

Kaniapiskau Supergroup (Frarey and Duffel, 1964), were deposited in an Aphebian rifting environment (Baragar and Scoates, 1981; Wardle and Bailey, 1981; LeGallais and Lavoie, 1982), although Hoffman (1987) has suggested that the sediments and volcanics were deposited in a foredeep. The first sediments deposited in the Trough were a series of arkosic sandstones and conglomerates, with minor associated alkali basalt (Baragar and Scoates, 1981). Later sedimentation had a distinctly cyclic nature, with cycles starting with stable platform sediments such as sandstone, carbonate and iron-formation and passing upwards into turbidite and shale. Tholeiitic volcanism is generally associated with the upper parts of the cycles (Baragar and Scoates, 1981). Two such cycles have been recognised (Dimroth 1981).

The hinterland to the Labrador Trough (or Rae Province as defined by Hoffman, 1988) is not as well known. At present, most of what is known about this region is from Taylor (1968, 1969, 1970, 1979) who mapped vast areas of this section of the Churchill at a scale of 1:250,000, and from continuing work by the MERQ as part of the Riviere George Project northeast of Schefferville (van der Leeden et al., in press).

The area to the east of the Labrador Trough contains both Archean and Aphebian rocks, with Aphebian rocks more common in the west (Taylor, 1979; Hoffman, 1988; van der Leeden et al., in press). The immediate hinterland of the Labrador Trough is characterized by a continuous belt of high-grade metamorphic

13

rocks consisting mainly of pelitic and semipelitic schist and amphibolite (metabasalt and metagabbro), with minor quartzite, marble, and conglomerate (Dimroth, 1972; Taylor, 1979; Wardle and Bailey, 1981; van der Leeden et al., in press). These rocks are variously known as the Laporte schists (Dimroth, 1972) or the Laporte "Group" (Wardle and Bailey, 1981)

East of the Laporte Group the hinterland consists largely of paragneiss, quartzofeldspathic gneiss, amphibolite, marble, quartzite and calc-silicate. Supracrustals in the northern parts of the hinterland in Labrador have been correlated with the Lake Harbour Group of Baffin Island (Jackson and Taylor, 1972; Taylor, 1979).

A significant feature of this region is the presence of a 500 km long batholith belt first mapped by Taylor (1979). The batholith is a composite body with granite/granodiorite and charnockitic-opdalitic portions and displays "I" type granitoid features and well defined calc-alkaline trends (De Pas batholith of van der Leeden et al., in press).

The extreme eastern regions of the hinterland near the Nain boundary contain a number of post-orogenic anorthosites and rapakivi granites which have been dated at 1.4 Ga (Elsonian) (van der Leeden et al., in press). U-Pb zircon dating of an intrusive body gives ages of 2.3 Ga. (van der Leeden et al., in press)

Metamorphic grades in this portion of the Churchill show an overall increase from west to east. Most of the Labrador Trough s.s. is of subgreenschist to greenschist facies, but in the

14

immediate hinterland metamorphic grade increases rapidly from lower amphibolite to upper amphibolite and in some cases granulite facies (Gelinas, 1965; Dimroth and Dressler, 1978; Fraser et al., 1978). Most of the rocks to the east of the Labrador Trough are metamorphosed to amphibolite facies, although substantial exposures of granulite facies rocks are found near the west side of the central batholith complex (Fraser et al., 1978; van der Leeden et al., in press) and near the western boundary of the hinterland (Taylor, 1979)

The structure of the Labrador segment of the Churchill Province, like that of the rest of the Churchill Province, is almost entirely due to deformation during the Hudsonian Orogeny. The structure of the Labrador Trough and its immediate hinterland is quite well known. The overall structural trend in the Trough is roughly NW to NNW. Deformation style changes significantly from west to east. The western parts of the Trough are characterized by both thrust faults which flatten out and merge into a basement decollement, and by open folding (Dimroth, 1981; Boone and Hynes, 1987). Deformation becomes increasingly intense and more ductile in nature to the east, where up to 5 sets of folds (Dimroth, 1981) have been recorded. The hinterland zones are characterized by remobilization of Archean basement and commonly exhibit westward vergent, overturned folds produced by early deformation (e.g. Hynes, 1978).

The structure of the easternmost parts of the hinterland is not as well known. As in the Labrador Trough, structural trends

are generally NNW. Taylor (1979) notes that folding of all types is present but that it is probably all attributable to the "Hudsonian Orogeny". Areas of migmatitic gneiss and granodiorite are characterized by "chaotic" deformation   (Taylor, 1979). Two major shear zones have been mapped in the southern of the hinterland on either side of the De Pas batholith (van der Leeden et al., in press). The Lac Tudor shear zone is a 150 km long and up to 20 km wide shear zone on the east side of the batholith. Motion on this shear is dextral with a west directed thrusting component. The Riviere George shear zone, on the east side of the batholith is approximately 200 km long and has a complex motion history.

The deformation at the border between the Nain craton and the Churchill province has the opposite sense to that in the Labrador Trough and immediate hinterland. Thrusting is east directed (Morgan, 1975) and major shear zones record sinistral motion (Taylor, 1979; Hoffman, 1988).   This deformation is associated with the Nain Orogeny.

1.3.3 Tectonic models for the development of the Labrador Trough and the eastern Churchill Province

Models for the development of the Labrador Trough may be grouped into two main types; those invoking a plate tectonic origin and those invoking an ensialic origin.

The main proponent of an ensialic orogeny in the Labrador Trough was Dimroth, who rejected a plate tectonic origin and

instead proposed several ad hoc models for its development. This rejection of a plate tectonic model for the Trough stems from the lack of a number of features usually found associated with modern orogenic belts. He argued that the absence of ophiolites precluded any involvement of oceanic crust in the orogeny and that the lack of tectonic melanges, blueschist facies metamorphism and calc-alkaline intrusive/volcanic suites indicated that no subduction had taken place. He also pointed out that Archean basement is found in all the zones of the trough and was continuous around its northern closure, indicating ensialic development (Dimroth, 1972). He did not, however discount the possibility that the Labrador Trough developed in response to plate tectonic activity in the far hinterland, although he thought that it was unlikely.

Many workers now believe that the Labrador Trough represents a foreland fold-and-thrust belt. If this is the case, then some of the features cited by Dimroth as lacking, should actually be found in the hinterland of the Trough. The calc-alkaline plutons found 150 km east of it may, for example, reflect the development of a Peruvian style plate margin between the Superior and Churchill Provinces (van der Leeden et al., in press).

It is only now, when considerably more data are becoming available about the hinterland to the Labrador Trough, that true constraints on its tectonic evolution can be established. Some of the most recent data have recently been presented, on a large scale, by van der Leeden et al. (in press). This thesis is

17

concerned with a more detailed study of a small area of the northern hinterland, but with the same object in mind - to determine whether the geological record is compatible with the operation of modern geological processes and to determine where this part of the hinterland may fit into the tectonic scheme.

Chapter 2. Lithology and Stratigraphy

2.1 Introduction

The rocks of the study area may be divided into three main classes: 1) remobilized Archean basement, 2) Aphebian supracrustals and 3) Hudsonian intrusives. There is also a volumetrically insignificant series of diabase dykes. Remobilized Archean basement and Hudsonian intrusives are relatively minor but important parts of the study area. Most of the area (approximately 90%) is underlain by Aphebian supracrustals.

The area may be divided into three fault-bounded blocks, each with a different lithological character. These blocks are, from east to west, the Lac Rachel-Lac Murray Block, the Lac Gabriel Block and the Lac Berthet Block (Fig. 4).

The supracrustals of the Lac Rachel-Lac Murray Block rest on the Archean basement forming the cores of the doubly-plunging antiforms making it the structurally lowest block. The block is composed of pelitic to semipelitic schists and amphibolites with minor marble and metaconglomerate. The block is juxtaposed with the Lac Gabriel Block along the Lac Turcotte Fault. The Lac Gabriel Block consists of a wide variety of gneissic metasandstones, amphibolites and pelitic gneisses. It also contains a complex suite of syntectonic granitoid and

19
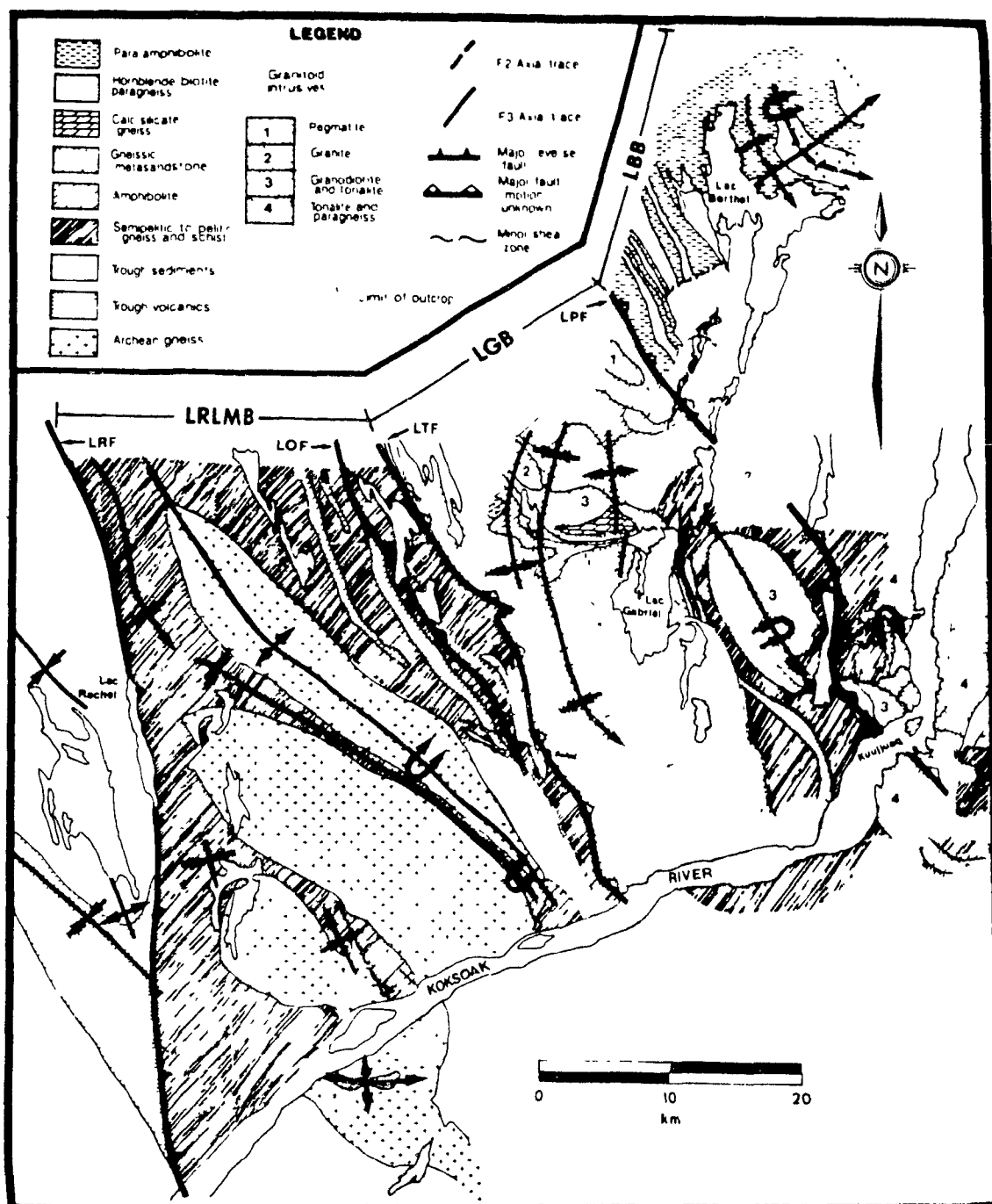
Figure 4. Map of study area showing major lithological units. **LRLMB:** Lac Rachel-Lac Murray block; **LGB:** Lac Gabriel block; **LBB:** Lac Berthet block; **LRF, LOF, LTF** and **LPF:** Lac Rachel, Lac Olmstead, Lac Turcotte and Lac Pingiajjulik Faults. Map includes data from Gélinas (1958, 1959, 1960) Taylor and Skinner (1963) and Perreault (1987, 1988).

associated gabbroic rocks. The Lac Berthet Block, which is separated from the Lac Gabriel Block by the Lac Pingiajjulik Fault, consists of a thick series of epiclastic amphibolites and arkosic paragneisses mixed with minor amounts of calc-silicate gneiss, quartzite, marble and semipelitic gneiss.

This chapter is devoted to describing the lithology of the rocks in the study area. The high-grade metamorphism characterizing the area has obliterated most primary features making stratigraphic relationships, and in some cases protoliths, difficult if not impossible to establish with any degree of certainty. Because of these difficulties, no formal stratigraphy has been introduced. The recognizable primary features (mainly graded bedding) indicate that the study area is NE younging and homoclinal.

2.2 Archean rocks

Archean basement is exposed in at least two and probably three areas in the region. The westernmost exposure of Archean rock occurs in the cores of three doubly-plunging, westward-overturned antiforms (the Renia, Moyer and Boulder antiforms), found at the western limit of the study area. They consist mainly of medium-grained microcline gneiss that is weakly layered and has a poorly to well developed foliation (Sauvé and Bergeron, 1965). Migmatites are common. Thin amphibolitic lenses are also occasionally found within the antiforms. The gneisses have been

dated at 2850 ±5 Ma using U-Pb zircon methods (Machado et al., 1987).

A second unit of Archean rocks is found on the shores of Lac Turcotte in the Lac Rachel - Lac Murray Block. These rocks are very different from other Archean rocks in the area and their origin is somewhat problematical. The unit is very homogeneous and mainly of a leucotonalitic composition. The main minerals are quartz and plagioclase, with minor biotite and rare sillimanite. The unit is weakly foliated. An interesting feature is the presence of large (up to 10's of square meters) "xenoliths" of foliated rock very similar in appearance to the surrounding supracrustals. These "xenoliths" led to the original interpretation of the unit as a late-to post-tectonic Hudsonian intrusive. Subsequent U-Pb dating of these rocks, however, has yielded ages of 2717 Ma (Machado et al., 1988), indicating that they are Archean.

A third unit of granitoid gneiss in the area has not yet been confirmed as Archean basement, but dating is in progress. These rocks are interpreted as basement on the basis of their lithological features, which are similar to those of confirmed Archean rocks and very different from those of the surrounding supracrustals. The gneisses are found northeast of Lac Berthet in two separate exposures separated by a four kilometer strip of supracrustal rocks.

The exposure nearer to Lac Berthet is predominantly highly migmatized tonalitic to granodioritic gneisses. The gneisses

consist mainly of quartz, alkali feldspar and plagioclase with minor biotite and accessory retrograde muscovite. Rare biotite-rich lenses are interpreted as restite. The gneisses are highly deformed and are cut in places by rare syntectonic tonalite dykes. Contacts between these gneisses and the surrounding supracrustal rocks are generally poorly defined due to extensive migmatization of the contact. When contacts are observed, they are commonly characterized by a rusty zone composed of a garnetiferous quartz-rich paragneiss. Shearing is occasionally observed on the contacts. The structure of the area indicates that the "basement gneisses" are structurally above the supracrustals.

The other unit of basement gneiss in the area consists for the most part of a very coarse-grained alkali-feldspar gneiss with quartz and minor plagioclase and biotite. The rocks are very poorly foliated and sporadically migmatized. Contact relationships between this unit and the supracrustals are unknown. Rare bands of well-layered rocks occur in places within these gneisses. Recent mapping by S. Perreault (pers. comm., 1988) has shown that the two gneiss units join up to the east and continue to the Koksoak estuary and perhaps farther.

2.3 Supracrustals

In this section the supracrustals successions of the three

blocks are described separately. Schematic "stratigraphic" sections are depicted in Figure 5.

2.3.1 Lac Rachel-Lac Murray Block

The supracrustals of the Lac Rachael-Lac Murray Block (LRLMB) rest on the flanks of the doubly-plunging basement antiforms. In the study area the contact between the gneisses and supracrustals is not exposed, but farther west it is commonly marked by a highly brecciated marble unit. The bedding-parallel foliation in the supracrustals wraps around these antiforms, but it is not known if they were deposited unconformably on these gneisses or were transported into place on a basement-cover decollement. Although the LRLMB as originally defined includes all the supracrustals between Lac Rachel and Lac Turcotte (Poirier et al., 1987) this section will deal only with those supracrustals east of the basement antiforms.

The majority of the eastern section of the LRLMB is underlain by pelitic and semipelitic schists. The two schist types are classified on the basis of mineralogy; the pelitic schists contain muscovite and sillimanite, which are absent in the semipelitic schist. Most of the semipelitic schist is found in the western section of the LRLMB, but minor amounts are found in the east. The contacts between pelitic and semipelitic schist are commonly gradational.

The major minerals in both types of schist are quartz, biotite and plagioclase. Quartz and plagioclase commonly exhibit

24
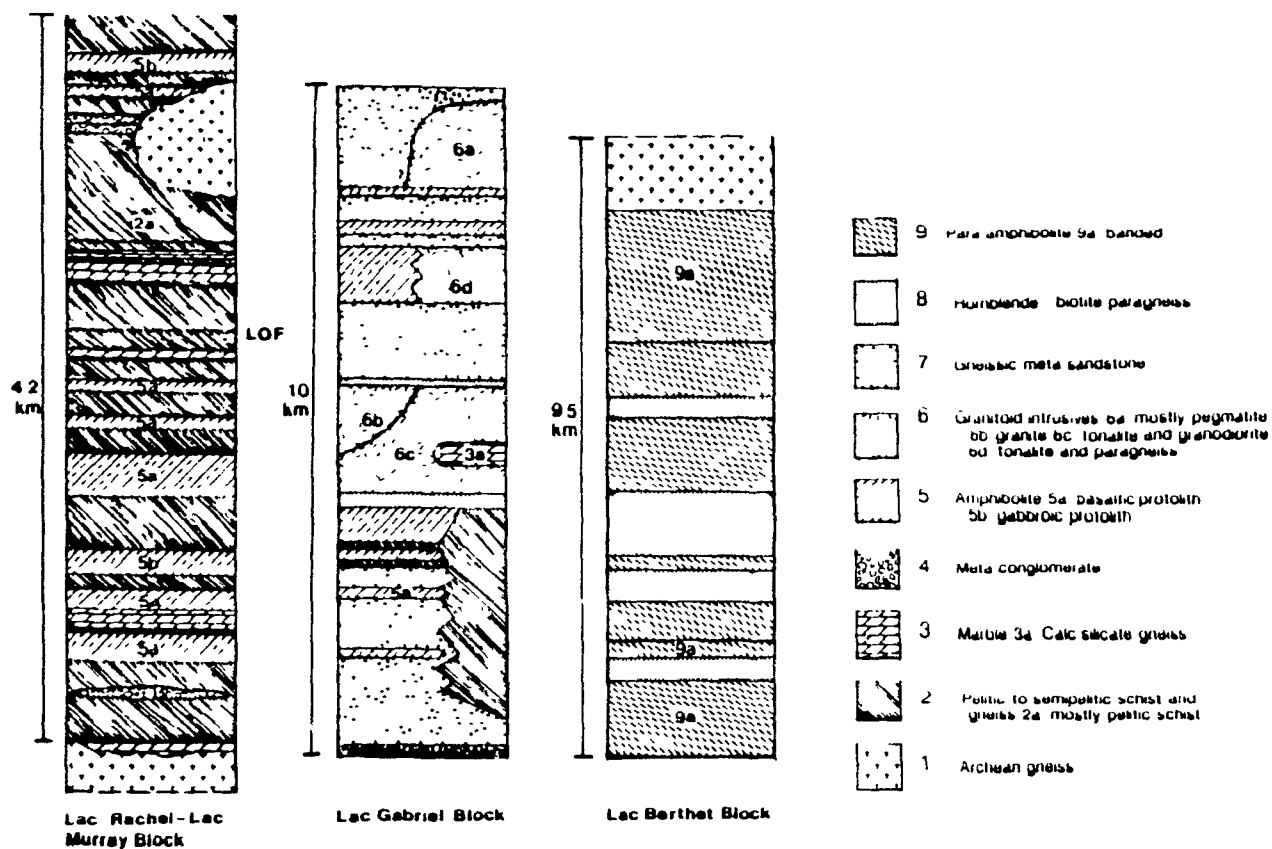
Figure 5. Simplified "stratigraphic" columns for the three tectonic blocks. LOF: Lac Olmstead Fault.

granoblastic textures. The plagioclase is generally unzoned oligoclase, but in some cases, especially when garnet is present, it may exhibit pronounced reverse zoning (i.e. increasing anorthite content towards crystal rims).

Biotite is a major phase in all schists and defines the foliation. Muscovite is restricted to pelitic schists. Some muscovite, especially that found with sillimanite, is probably retrograde, but in this block most muscovite is part of the typomorphic assemblage. Muscovite (retrograde) commonly crosscuts the biotite-defined foliation.

Sillimanite is also restricted to pelitic schists. It generally has a radiating, fibrolitic texture and is commonly found as 1-3 cm nodules with cores of garnet or muscovite. On outcrop surfaces these nodules form positive-relief features (Plate 4c.).

Garnet is found in both types of schist, but is restricted to the cores of sillimanite nodules in pelitic schist. Grains range in diameter from 1 mm to several cm, with larger crystals commonly riddled with ilmenite and quartz inclusions. Crystals are generally subhedral.

Alkali-feldspar (microcline) and tourmaline are common accessories in pelitic schists. Ilmenite, apatite and zircon are common accessories in all schists.

The modal mineralogy of the schists is highly variable and they have been observed grading into quartzofeldspathic gneiss as

modal quartz increases and biotite decreases. Thin quartz lenses and layers are commonly found in both types of schist unit.

Major portions of the LRLMB are also underlain by amphibolites. They are concordant with the surrounding rocks and are almost always relatively fine-grained and very well foliated. The major phases of the amphibolites are hornblende and plagioclase. Hornblende is usually elongated and defines the foliation. Plagioclase is found as equant grains between hornblende-rich domains. It is invariably zoned with anorthite content increasing towards the rim of plagioclase crystals. Biotite is a common minor phase and is generally associated with hornblende and oriented parallel to the foliation. Quartz is commonly found in the plagioclase-rich domains. Common accessories are ilmenite and apatite, with garnet and diopside occurring more rarely.

The eastern parts of the LRLMB contain two thin (100-200 m thick) marble units. The units are for the most part pure dolomite with minor plagioclase and are generally poorly foliated. The marbles contain numerous calc-silicate layers ranging in thickness from several centimeters to several meters (Plate 1b.). These layers are distinctly banded, with cores of diopside rimmed by successive layers of tremolite and calcite. This banding is the result of prograde metamorphic reactions between the dolomite and quartz rich beds within it (Gelinas, 1965). These features make it possible to delineate structures within the marbles (Plate 1c.)

The LRLMB is capped by a sequence of quartz-rich metasediments that are locally conglomeratic. The unit is medium to coarse-grained with variable foliation development. It is composed mainly of quartz and plagioclase with minor biotite. The conglomeratic quartzose gneiss consists of clasts of granitic gneiss and subsidiary clasts of dolomite marble, amphibolite and pelitic schist in a matrix of quartz and plagioclase. The quartzose gneiss also contains minor units of calc-silicate, amphibolite and schist.

2.3.2 Lac Gabriel Block

The base (westernmost parts) of the Lac Gabriel Block (LGB) consists of a thick (approximately 3 km) sequence of gneissic metasandstones with a basal conglomerate. The clasts in the conglomerate are mainly of granitic gneiss, with subsidiary amounts of amphibolitic and pelitic clasts, in a matrix of quartz and plagioclase. The metasandstone is composed mainly of quartz and plagioclase with variable amounts of alkali-feldspar (which may form porphyroblasts), biotite and hornblende. Gradational increases in the amount of biotite over small intervals are interpreted as being inherited from graded bedding and give younging directions to the NE (Plate 1d.). Sphene, calcite and iron oxides are common accessories. The unit contains minor amounts of amphibolite, calc-silicate gneiss and silicate iron-formation. The metasandstones become finer-grained to the east

28

(top of the sequence) where they pass into a series of semipelitic gneisses.

Another thick gneissic metasandstone unit is found above the Lac Gabriel Complex (See section 2.4 for a description of the complex). The unit is similar to the one previously described, but in general it is coarser grained and may contain garnet and prismatic sillimanite. It is also generally very rusty, probably due to the oxidation of iron sulphides.

The LGB contains numerous amphibolite units of various types. The most common type of amphibolite is medium to fine-grained with a strong foliation defined by hornblende and a well defined compositional layering (i.e. alternating hornblende and plagioclase-rich layers). Hornblende and plagioclase are the major phases in these amphibolites. Plagioclase composition is generally in the labradorite range and single crystals commonly show reverse zoning. Quartz is commonly found in plagioclase-rich layers. Biotite, garnet, diopside and calcite are occasional minor phases, with ilmenite occurring as a common accessory phase. Rare deformed pillow structures are observed in these amphibolite units (Bosdachin, 1986).

A distinctive amphibolite unit found to the north of Lac à Foin has essentially the same mineralogy as the previously described amphibolites, but is much coarser grained with a correspondingly coarser compositional layering. This unit is believed to be epiclastic or pyroclastic and contains a tuffaceous horizon.

Another sequence of amphibolites has been mapped near the top of the LGB. These amphibolites are variable in composition (mainly in hornblende content). They are generally well foliated with a good compositional layering and are medium to fine-grained. The main phases are hornblende, plagioclase, quartz and biotite. The most hornblende-rich of these amphibolites commonly contain irregular veins and layers of plagioclase and quartz.

Two thin layers of pelitic schist are observed north of Lac à Foin. The mineralogy of these units is essentially the same as that of those observed in the LRLMB except that most muscovite is probably retrograde. These schists weather to a rusty red color.

The only remaining major units of the LGB are made up of hornblende-biotite paragneisses. These rocks are composed of variable amounts of hornblende, biotite and quartzofeldspathic components, and are transitional between amphibolite, mica schist and quartzofeldspathic gneiss. One of these units is found between the uppermost amphibolite unit at Lac à Foin and the Lac Gabriel Complex, and the other caps the block. Although highly variable, the gneisses are generally medium-grained with a good compositional layering and a well defined foliation (Plate 1e.). Graded bedding in this unit gives a younging direction towards the NE.

Scattered throughout the block are various minor calc-silicate and marble units. Three of these units are mappable. A thin marble unit is found between the upper amphibolite units at Lac à Foin and consists of calcite and diopside with minor

30

plagioclase, sphene and quartz (Bosdachin, 1986). The thickest calc-silicate unit in the LGB is associated with the Lac Gabriel Complex. The mineralogy of this unit is variable but in general it consists mainly of diopside and plagioclase, with subsidiary calcite, epidote and tremolite, and accessory garnet, sphene and clinozoisite. This unit is typically a dull green color.

The hornblende-biotite gneiss unit at the top of the block contains two and possibly three thin (roughly 3-15 m) calc-silicate/ marble units. The thicker units are zoned, with a core of calcite marble containing approximately 20 percent forsterite and surrounded by rims of almost pure tremolite and diopside.

The block also contains two minor silicate iron-formations just north of Lac à Foin. One of these is well banded, consisting of bands of hornblende, diopside and iron oxides alternating with quartz-rich bands. This unit is commonly garnetiferous. The second iron formation is unlayered and weathers a rusty red color.

2.3.3 Lac Berthet Block.

The Lac Berthet Block (LBB) is the northernmost of the three blocks and extends from the Lac Pingiajjulik fault to the overlying granitic gneiss, and perhaps beyond. The stratigraphy of this block is the least well known of the three. The block is underlain by a large variety of probably epiclastic metasediments, which are highly variable at all scales, making it

31

difficult to trace most units confidently for any distance along strike.

One of the most easily traced units is found at the base of the block. It is a coarse-grained gneiss containing variable amounts of biotite and amphibole (hornblende and/or cummingtonite). The degree of foliation development varies throughout the unit, but a reasonably well developed compositional layering is generally present. It is commonly porphyroblastic, with either plagioclase and alkali-feldspar (up to 3 cm in diameter) or garnet (up to 2 cm in diameter), but rarely both (plate 1f). Alkali-feldspar porphyroblasts are generally surrounded by thick (up to one third of the diameter of the porphyroblast) myrmekite rims. These gneisses are commonly rusty red.

Large areas of the LBB are underlain by a heterogeneous unit composed of a variety of rock types which occur as closely spaced layers throughout the unit. The most common rock type in this unit is a medium grained biotite-quartz-plagioclase paragneiss with about 15-20 percent biotite. The unit is generally well foliated with a good compositional layering, Amphibole is a common minor phase. Other rock types in this unit are quartzofeldspathic gneisses, metaquartzites and amphibolites with variable amphibolite contents. The unit is typically a buff grey.

The block also contains several major amphibolite units. Like the majority of units in this block they are variable in composition. Generally they are very rusty and composed mainly of

hornblende and or cummingtonite, plagioclase, biotite and quartz. Garnet is a common phase. These amphibolites are generally poorly foliated but occasionally have a good compositional layering.

Minor calc-silicates and marble units are scattered throughout the block. The calc-silicate units are composed of diopside and plagioclase with associated tremolite and hornblende s.l. Marbles are calcitic and usually contain forsterite.

A distinctive unit is found on the SW shores of Lac Berthet, where a series of outcrops composed of a clinopyroxene and orthopyroxene gneisses were mapped. These outcrops are highly serpentinized on their contacts with the surrounding metasediments, and form a series of elliptical outcrops extending in a line parallel to regional strike.

2.4 Hudsonian Intrusives

An important feature of the study area is the presence of a series of Hudsonian intrusive rocks ranging in composition from granitic to tonalitic. The rocks occur in three main complexes which form an east-trending belt and have been named the Lac Gabriel Complex, the Lac Stewart Complex and The Elbow Island Complex. These complexes are all restricted to the same general stratigraphic level and all contacts are roughly parallel to the local foliation. This discussion will be restricted to the Lac Gabriel Complex which was mapped as part of this study.

(Descriptions of the other complexes will be published in Poirier et al., in press.)

The Lac Gabriel Complex is located west of Lac Gabriel and approximately 2 km north of Lac à Foin, and is composed of rocks ranging in composition from granitic to gabbroic. Structural relationships indicate that the complex was emplaced early in the tectonic history of the area (see section 3.4 for more detailed discussion) and was subsequently deformed and metamorphosed.

The complex consists predominantly of granodioritic and tonalitic gneisses with lesser amounts of granitic gneiss, hornblende diorite and gabbro. The gabbroic rocks are composed mainly of hornblende with minor amounts of biotite. Interstitial plagioclase, apatite and magnetite are found as accessories. A zone of layered rock consisting of a 10-20 cm thick layer of magnetite which apparently grades up(?) into a hornblende gabbro was found in one outcrop and is traceable for at least 300 m along strike.

The granodioritic and tonalitic rocks consist of plagioclase, hornblende, and quartz with interstitial biotite and alkali-feldspar. These rocks vary in color index from 20 to 50. Magnetite is a common accessory mineral in all rock types, but also occurs as irregular blobs up to 20 cm in diameter in the tonalitic rocks. Xenoliths in the complex are commonly gabbro or hornblende diorite but a few metasedimentary xenoliths are observed. The complex shows no clear evidence of zoning, but a general increase in the mafic content of the granitoids is

observed as the southern (lower) side of the complex is approached. Crosscutting relationships indicate that the gabbroic and dioritic intrusives generally predate the granodiorites and tonalites. At the northern margin of the complex there is a large exposure of alkali-feldspar-megacrystic granite.

The rocks of the complex show variable amounts of deformation depending on position in the complex. At its edges the intrusives are well foliated and interleaved with the surrounding metasediments. Toward the centre of the complex very little foliation is evident but the rare xenoliths of country rock are well foliated. The non-foliated intrusives very commonly have a pronounced lineation defined by the long axes of hornblende grains.

Uranium-lead zircon studies (Machado et al., 1988) yield an age of 1833 ±2 Ma for the Lac Stewart Complex. The Elbow Island complex has three zircon populations which give ages of 1845 ±2, 1840 ±2 and 1829 ±2 Ma. The 1840 and 1845 dates are believed to be igneous ages, while the 1833 and 1829 ages are interpreted as metamorphic.

The most widespread Hudsonian intrusives in the study area are the syn to post-tectonic pegmatites found throughout the area. The LRLMB contains minor amounts of pegmatite in its upper portions. They are coarse-grained and composed essentially of equal proportions of plagioclase, quartz and microcline. Tourmaline and muscovite are common accessories. The pegmatites

are exposed as elliptical pods oriented roughly parallel to the regional foliation.

The majority of pegmatite in the area is found near the border between the LGB and LBB. In this region there are several large areas in which pegmatite veins constitute up to 50 percent of the bedrock. Within this region are several areas (up to 1 sq. km) in which 100 percent of the bedrock is pegmatite.

The pegmatites are composed mainly of quartz, plagioclase and microcline, with minor muscovite and biotite. Garnet is a rare accessory mineral and occurs as small (1-2 mm) euhedral crystals.

The pegmatites exhibit variable amounts of deformation. Some are so deformed that foliation development has occurred. Others are tightly folded and many are undeformed. Both deformed and undeformed pegmatites may be found in the same outcrops suggesting episodic or continuous pegmatite intrusion both during and after deformation. U-Pb dating of late undeformed pegmatites gives an age of 1775 ±4 Ma (Perreault et al., 1988).

2.5 Diabase Dykes and Sills

The youngest rocks in the area are a series of diabase dykes and sills, which range in thickness from several centimeters to several tens of meters. The undeformed state of these rocks and the presence of chilled margins at their contacts with the supracrustals indicates that they are post-orogenic. Similar dykes found to the east of the study area (Taylor, 1979;

S. Perreault, pers. comm., 1988) have been dated (K/Ar ages) as Neohelikian (Taylor, 1979).

The chilled margins of the dykes and sills are generally aphanitic, but the centers of the intrusives may be quite coarse-grained. The diabase is composed mainly of plagioclase, with interstitial olivine, clinopyroxene and recrystallized glass and displays intergranular textures (Williams et al., 1954).

CHAPTER 3. Structural Geology

3.1 Introduction

The structural geology of the hinterland of the Labrador Trough has received little detailed attention (with the exception of Hynes, 1978). Information on the nature and relative timing of structural features in the region are of major importance in developing a model for the area.

The study area experienced multiple deformation during the Hudsonian Orogeny, which left it marked by various ductile and brittle strain features. Structural examination of the study area has revealed at least three sets of folds. Their order of formation, overprinting relationships and style are consistent and they may well reflect three separate episodes of deformation varying both in intensity and regional distribution. In general the most intense deformation occurred early in the tectonic history of the area. This chapter provides a description of the deformation in the study area. A discussion of the significance of these features is deferred to the final chapter.

3.2 Folds and Foliations

D_1

The earliest deformation episode (D_1) is recorded in all pre-Hudsonian rocks in the area as a well defined foliation commonly associated with compositional layering and or

gneissosity. Rarely observed primary sedimentary features (mainly in the form of graded bedding in paragneisses) indicate that S_1 is bedding-parallel. Major differences in bulk chemistry, as indicated by modal mineralogy parallel to the foliation (_e.g._ garnet-or cummingtonite- rich layers in an otherwise garnet- or cummingtonite free-rock) are consistent with this. The foliation is generally defined by preferred orientation of [001] planes in layer-silicates and long dimensions of amphiboles and other elongate minerals (Plates 2a, 2b.).

Folds associated with D_1 (F_1) are characteristically isoclinal, with axial planes parallel to S_1. The vast majority of F_1 folds observed are rootless and intrafolial and typically have wavelengths of tens of centimeters (Plate 2c.). Larger F_1 folds are rare or unrecognized due to their isoclinal nature and a lack of facing indicators. In single outcrops it is common to F_1 find fold axes that plunge in opposite directions (_i.e._ 180° difference in trend of plunge), possibly indicating a later isoclinal folding event. This could not be verified however, due to the difficulty of measuring fold axis orientations on flat outcrops. Evidence for a similar early isoclinal folding event has also been noted to the northwest of the study area (Hynes, 1978). One F_1-F_2 interference pattern has been observed, defining a well-formed mushroom-type interference pattern (Plate 2d.).

$\underline{D_2}$

Although not as intense as D_1 deformation, the effects of

D_2 on regional structure are much more prominent, with most of the regional scale folding due to D_2 (see Fig. 6). The most obvious effect of D_2 deformation is the presence of F_2 folds at all scales throughout the study area. F_2 folds occur with a wide variety of styles and orientations, depending on lithology and competency contrast between folded layers. Most commonly, F_2 folds are intermediate between tight and open, have rounded closures and have a parallel style (Plate 2e, 2f, and 3a.). There is much departure from this basic style throughout the area, especially where lithologies of contrasting competency are deformed by the same fold. For example, in the Lac Murray area most of the folds in biotite schist units are simple, tight to open, parallel folds (Plate 2f.). However, where the folded schists contain quartz layers or veins, folds develop a very distinctive concentric style. A distinctive style of folding is also observed in the Lac a Foin area, where chevron-style folds are observed in amphibolite units.

In the Lac a Foin area there is evidence for two sets of folds associated with D_2 deformation. In the amphibolites of this area, the limbs of larger F_2 folds are commonly folded by a later set of more open coaxial folds with axial planes that dip more steeply to the SE than the earlier set.

The orientations of F_2 fold axes vary throughout the study area. In the extreme northern parts of the LBB F_2 fold axes are commonly rotated about the NE-plunging fold axis of a later major fold (F_3) and plot on a small circle on a stereographic
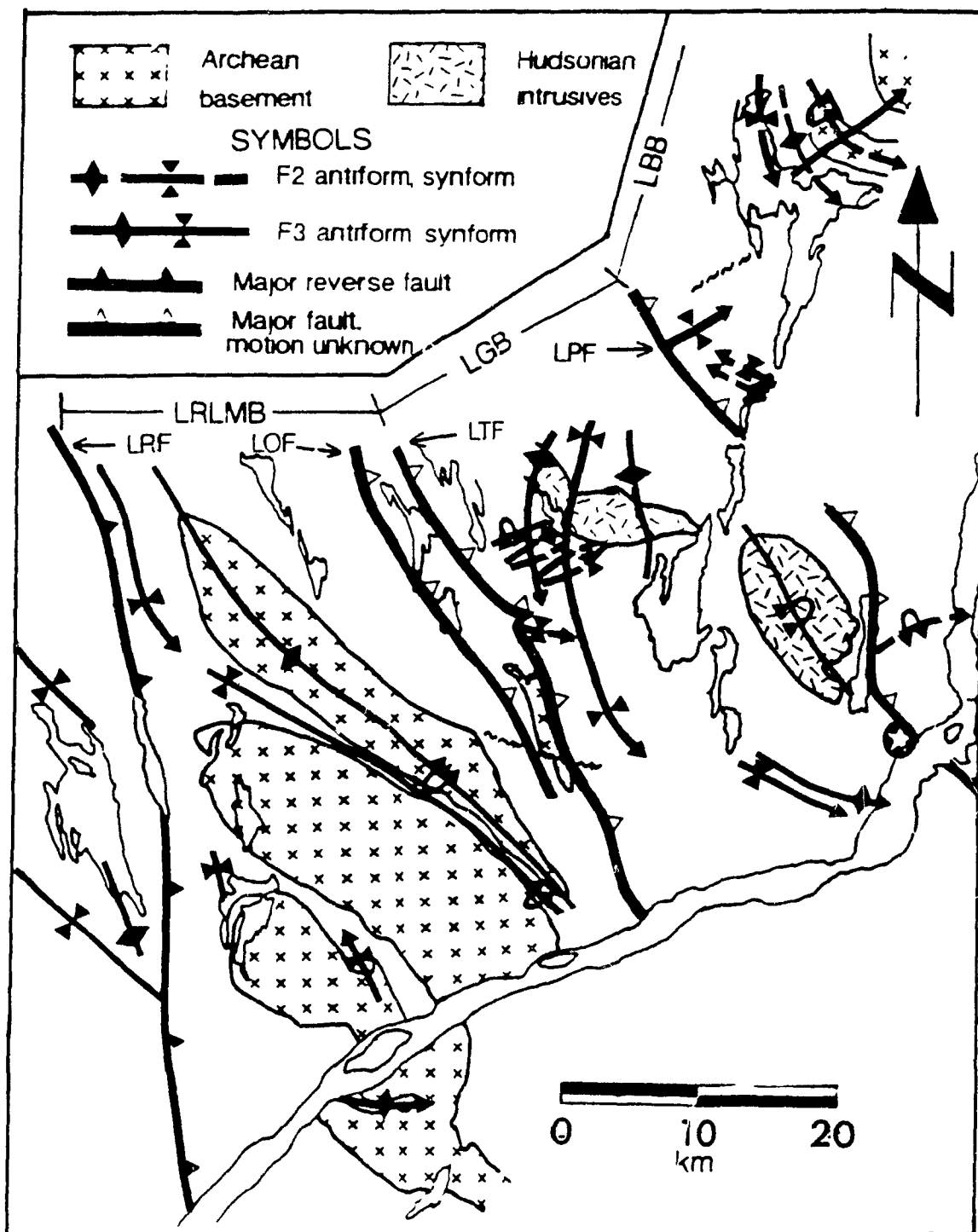
Figure 6. Map of study area showing major structural features. Abbreviations as in Figure 4. Map includes data from Perreault (1987).

41
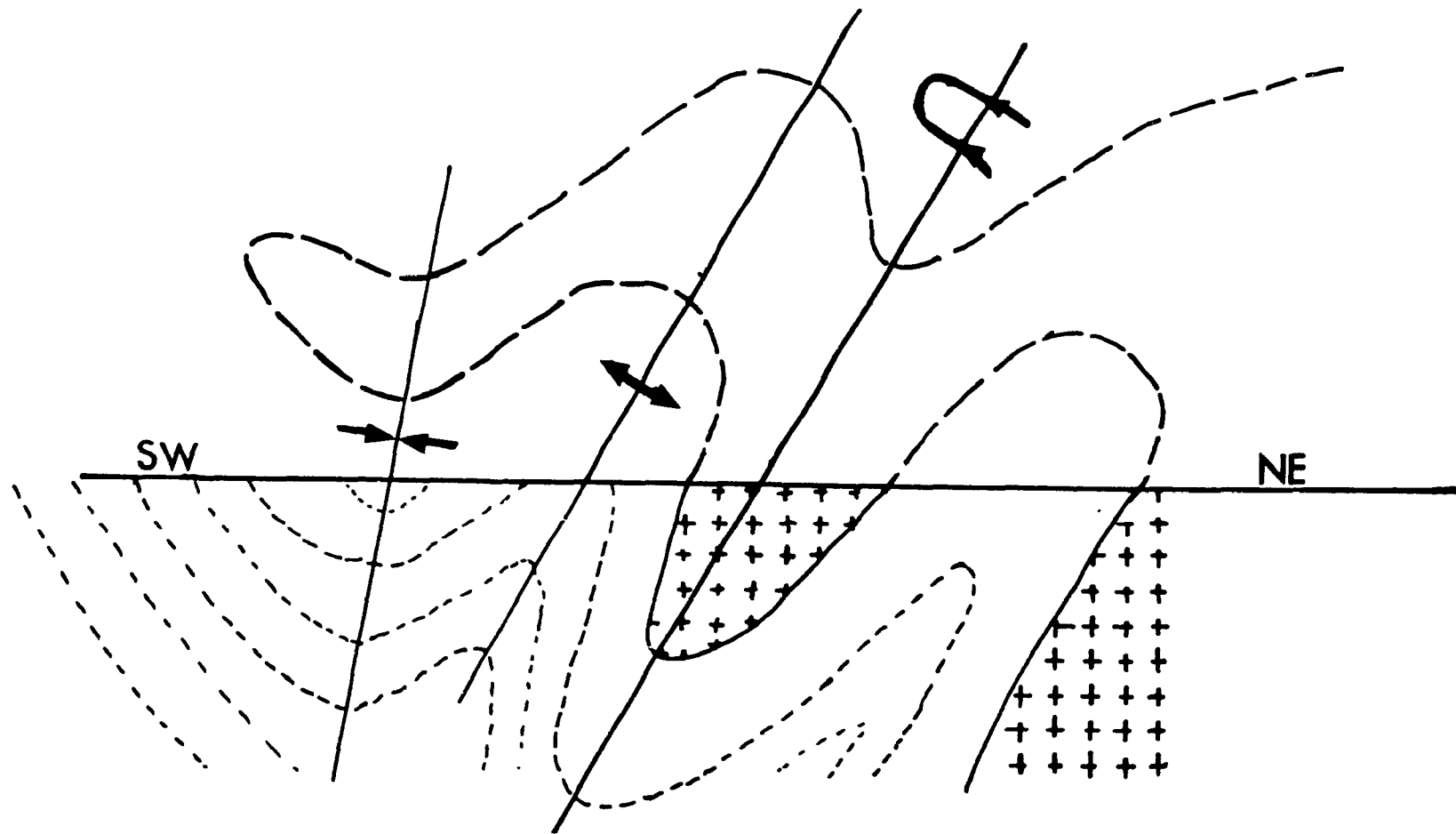
Figure 6b. Cartoon showing structural relationships between the Lac Berthet "basement" gneisses and supracrustal rocks. Line of section is approximately parallel to the axial trace of the regional F_3 fold. Stippled pattern indicates "basement" rocks.

projection (Fig. 7). In northern areas not affected by D_3 folding F_2 folds plunge to the SSW and have W-dipping axial planes. In more southerly parts of the study area, where D_3 deformation is less pronounced, F_2 folds generally plunge to the east (trend 65-120, plunge 20-60) and have south-dipping axial planes.

Foliation associated with D_2 is not as   widespread or pronounced as S_1 and is restricted to the Lac Murray area. The most common type of S_2 foliation is spaced (2-3 cm in wavelength) crenulation cleavage found in micaceous schists. The crenulations have axes and axial planes parallel to those of F_2 folds in the area (Plate 3b.). This crenulation is not associated with folding on the outcrop scale, which probably indicates that it is   due to either macroscopic folding or more simply a regional homogeneous shortening. Similar crenulations   are occasionally observed in amphibolites in the area, but are restricted to the closures of outcrop-scale folds (Plate 3c.). Petrographic   examination also reveals that there is some development of a   preferred orientation of [001] planes in biotite parallel to the axial planes of small (1-4 cm) F_2 folds in biotite schist units (Plate 3d.).

$\underline{D_3}$

In most of the Labrador Trough s.s., the last deformation event (D_3) produced the most intense deformation. In the study area, however, the intensity of D_3 deformation is highly variable. In some regions there is no evidence of D_3, while in
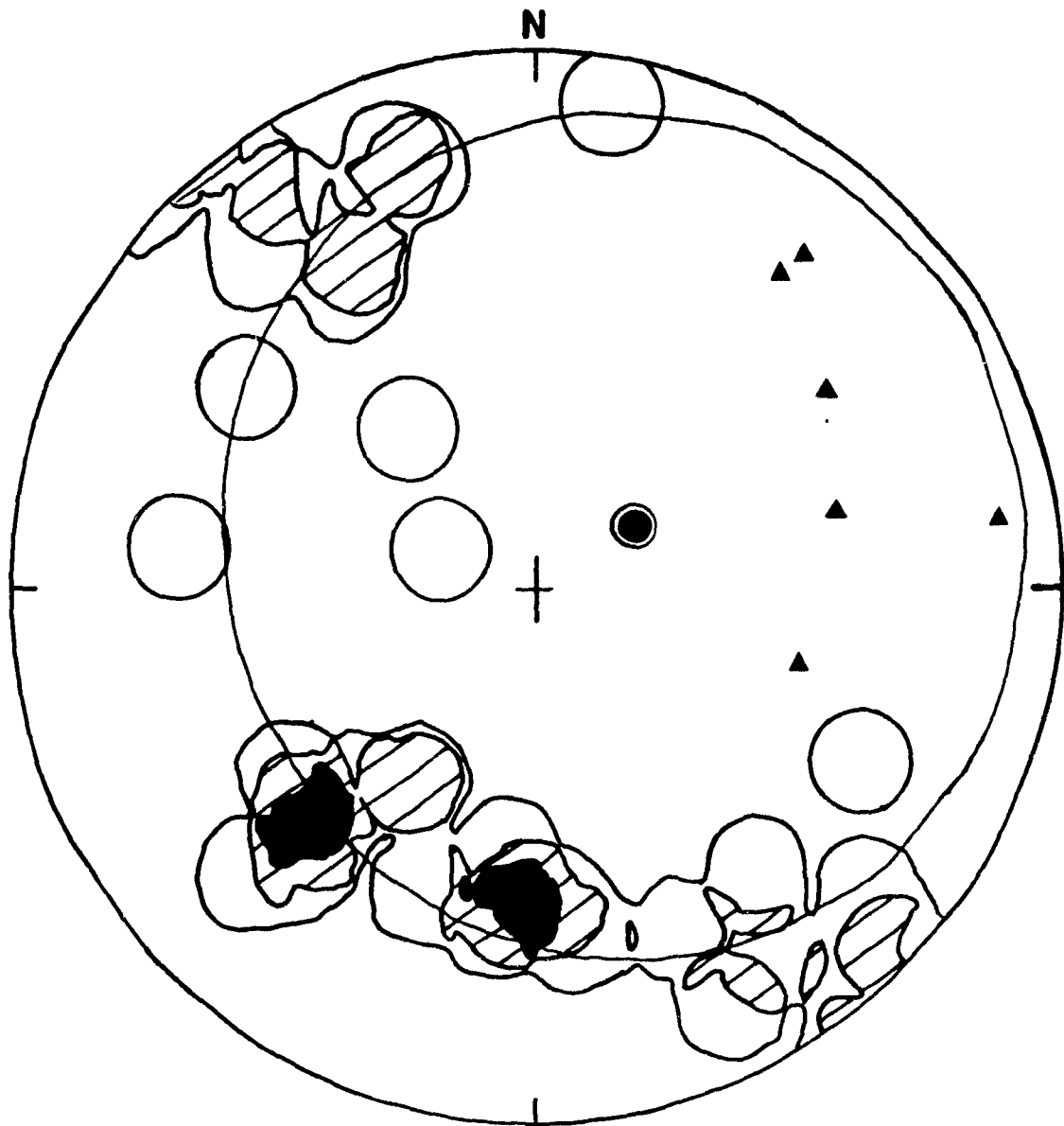
Figure 7. Contoured stereoplot of F_2 fold axes rotated about F_3 axes at Lac Berthet. Large dot: axis of fitted small circle, Triangles: Measured F_3 fold axes. Data contoured at 2, 5, and 10 % /1% area

others it is responsible for the regional tectonic grain (see Fig. 6). D_3 is usually evident as F_3 folds and in a few cases faults. No evidence for foliation development during this event has been observed.

In general, F_3 folds are open, with upright axial planes that trend roughly NNW and have shallowly plunging fold axes that are occasionally doubly-plunging. D_3 is strongest in the Lac Berthet area, where, as mentioned previously, all earlier structures show considerable rotation about a regional F_3 fold (Fig. 7). In this area F_3 folds are upright and open and plunge shallowly towards 240 or 060. F_3 folds are also observed in the Lac a Foin area where they are similar to those at Lac Berthet. Interference between F_2 and F_3 folds in this area produces minor, elongate dome and basin patterns with long axes parallel to F_2 axial traces (Plate 3e, 3f.). Minor F_3 folding is also observed in the Lac Pingiajjulik area where a gentle warping of the S_1 foliation on a scale of 5 to 10 meters is observed. The axes of these warps plunge to the NE at 40 to 60 degrees.

An inspection of the regional structural map (Fig. 6) reveals that F_3 axial surface traces undergo an anticlockwise rotation of approximately 90° from the Lac Berthet region to the Koksoak River where they are parallel to those in the Labrador Trough s.s. This rotation is apparently gradual (i.e. there are no abrupt changes in axial trace orientation) over the length of the study area, although data are scarce in the region between Lac Berthet and Lac Pingiajjulik.

3.3 Faults.

The area is cut by at least three major faults and a number of minor ones. The earliest recognized fault is the Lac Turcotte Fault (LTF). The LTF is a prominent, NNW trending, linear feature in the southern part of the study area. This fault is parallel to S_1, which in this area dips approximately 45° NE. The assignment of this fault to D_1 is based on its parallelism to the S_1 foliation (and bedding) and to the observed folding of its surface trace by a fold associated with D_2 (Fig. 6). Local mylonites are observed along the surface trace of this fault (S. Perreault, pers comm.,1987).

Another relatively early fault is the Lac Pingiajjulik fault. This fault separates the LGB from the LBB and extends from the NE side of Lac Pingiajjulik to the NE side of the Lac Stewart Complex (S. Perreault, pers. comm., 1988). The fault is characterized by a broad zone of highly recrystallized mylonite, separating two blocks of contrasting lithology. The timing and type of motion on this fault is not well constrained, but several features allow tentative dating with respect to regional metamorphism and deformation. Folding of the surface trace of this fault by an F_3 fold indicates it is pre-D_3. The highly recrystallized nature of the mylonite suggests that metamorphic conditions after motion were such that annealing and static recrystallization could occur. These features are consistent with

motion on this fault pre-dating both D_3 deformation and peak metamorphism. This fault marks the southwestern limit of granulite facies rocks produced during the early metamorphic event (see Chapter 4.).

The youngest major fault occurs just east of Lac Murray and is believed to be a southern extension of the Lac Olmstead Fault (LOF) mapped by Goulet (Goulet et al., 1987). The fault zone is characterized by an approximately 1 km wide zone of discontinuous shear zones which commonly display mylonitic and C-S fabrics. The motion on the fault, as determined from C-S fabrics and displacement of planar markers in mylonites (Ramsay, 1981; Simpson and Schmidt, 1983) was dextral (Plate 4a, 4b.). F_2 fold axes measured on either side of the fault exhibit no observable change in orientation, indicating no rotation in the fault plane. Geothermobarometry on either side of the fault indicates a temperature increase from 600 °C. on the west side of the fault to 700 °C on the east side with no corresponding increase in pressure (estimated to be 8 kb) (Perreault et al., 1987). This lack of increase in pressure suggests that there was little or no dip-slip motion on the fault. (Errors in P and T are estimated to be 50 °C and 1000 bars, respectively.) The timing of this fault is less certain. C-S fabrics associated with this fault contain deformed fibrolite nodules, in contrast to those observed outside the fault zone which are undeformed. If the sillimanite grew during peak metamorphism, as is likely (see Chapter 4) this indicates that motion on this fault coincided with or post-dated

peak metamorphism. The lack af any major retrogression associated with fault zones indicates that motion occurred on the fault before the rocks had time to cool significantly from peak metamorphic conditions.

There are several faults of lesser importance in the area. The south side of the LGC is marked by an eastward trending, 200 meter wide band of highly sheared and lineated rocks which extends from the north end of Lac Gabriel to the area north of Lac à Foin. The lineation associated with this fault plunges to the east at 40° and parallel to the F_2 fold axes in the area. The fault terminates just north of Lac Gabriel, but the timing and extent of offset on it are unknown.

The other minor fault in the area runs parallel to the long dimension of Lac Pingiajjulik. This fault is not exposed, but several features in the area indicate the presence of a fault. The most suggestive feature is major lithological change on either side of Lac Pingiajjulik. Examination of aeromagnetic maps for the area reveal dogleg patterns suggesting sinistral fault offset. A jog is also observed in the regional foliation in the area immediately to the south of the fault.

3.4 Features of Special Interest

There are a number of features in the area that deserve a more detailed discussion due to their importance in the overall history of the study area. These features are the Lac Gabriel

Complex and the gneiss-cored synform on the eastern side of Lac Berthet.

The "basement" gneisses of the Lac Berthet area are geometrically on top of the surrounding metasediments. The overall structure of the area consists of a tight keel of highly deformed gneiss resting on the metasediments. The contact between the gneisses and the surrounding rocks is poorly exposed and often obscured by migmatization. Local shearing is also observed on the contact at some points. The folding of this contact by D_2 deformation indicates that the basement rocks were placed above the metasediments during D_1. There are two possible explanations for the event. The first possibility is that both gneisses and metasediments were overturned by recumbent F_1 folding and subsequently deformed by D_2 and D_3. Alternatively, basement was thrust over the metasediments by a D_1 thrusting event. Differentiation between these two possibilities is not feasible with the limited number of reliable facing indicators observed in the area.

Structural features associated with the Lac Gabriel Ccomplex play a major role in determining its time of emplacement. The deformation of the complex is highly heterogeneous in nature. In its central part there is no foliation or folding. As the southern contact is approached, however, deformation becomes more obvious. The first evidence of deformation is the presence of an eastward plunging lineation ($\approx$ 090/40°). Continuing southward, a foliation is developed and F_2 and F_3 folds are observed. Very

48

intense local deformation is also observed in the area of the fault described in section 3.3. In this area intrusives are interleaved with the country rock. In the more deformed portions of the complex, and in the rocks on the edge of the complex, linear fabric elements (_i.e._ lineations, fold axes and rare mullion structures) have very similar orientations (Fig. 8) and lie approximately in the plane of the regional foliation. The colinearity of the lineations and fold axes with F_2 fold axes outside the shear zone indicate that the shearing is possibly a D_2 feature.

The timing of the intrusive event can be determined with a fair degree of certainty. The absence of S_1 foliation, the presence of well foliated country rock xenoliths within the complex and the common observation of associated gabbroic dykes crosscutting well foliated country rocks suggest intrusion post-dated D_1. F_2 and F_3 folds in the complex suggest that intrusion was post D_1 and pre-to syn-D_2.
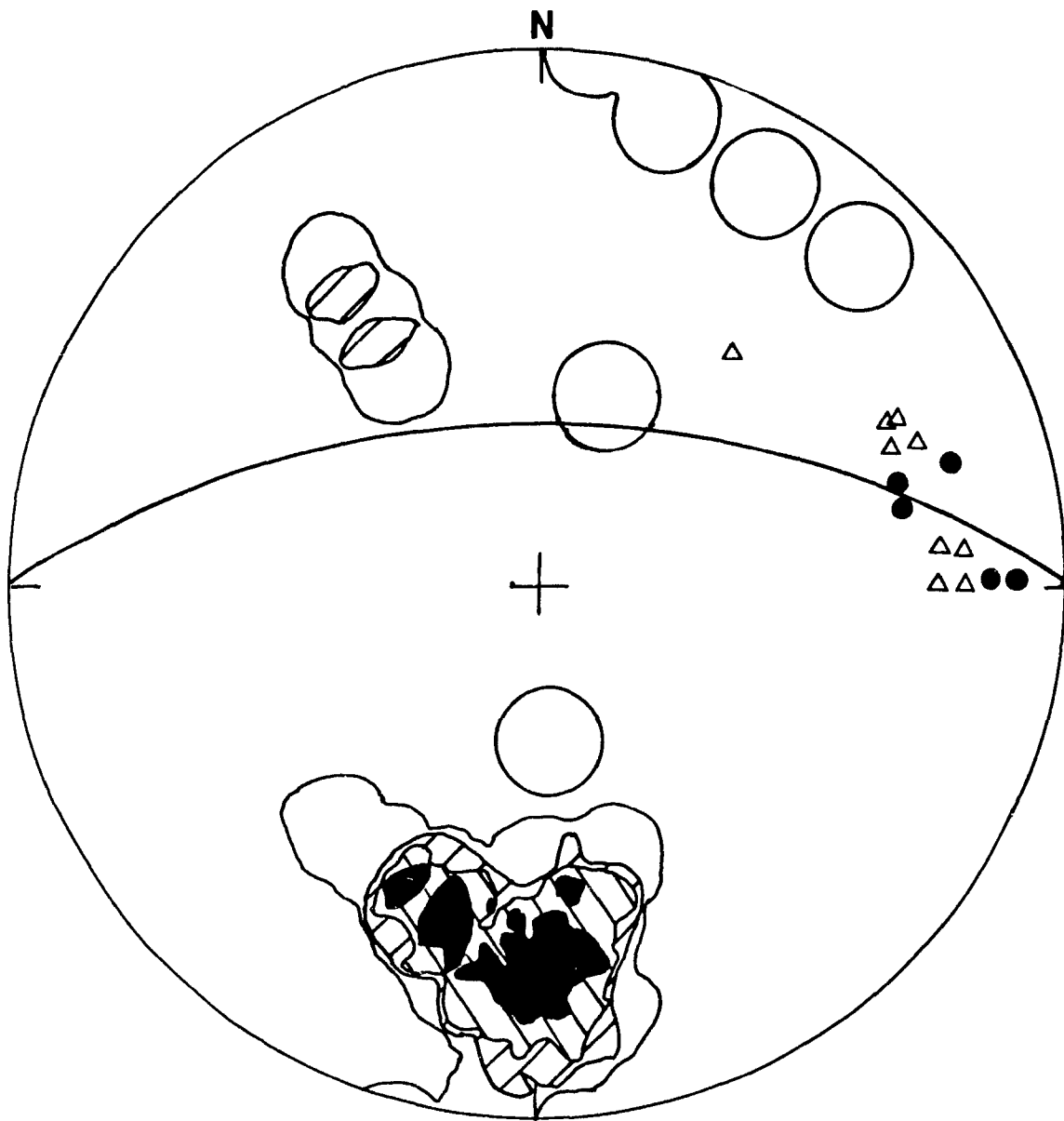
Figure 8. Stereoplot of poles to foliation (S_1), lineations (L_1) and fold axes (F_2) from LGC shear zone. Circles: Fold axes. Triangles: Lineations. Great circle is best fit to foliation data. Data contoured at intervals of 2, 5, 10, and 15 % per 1% area.
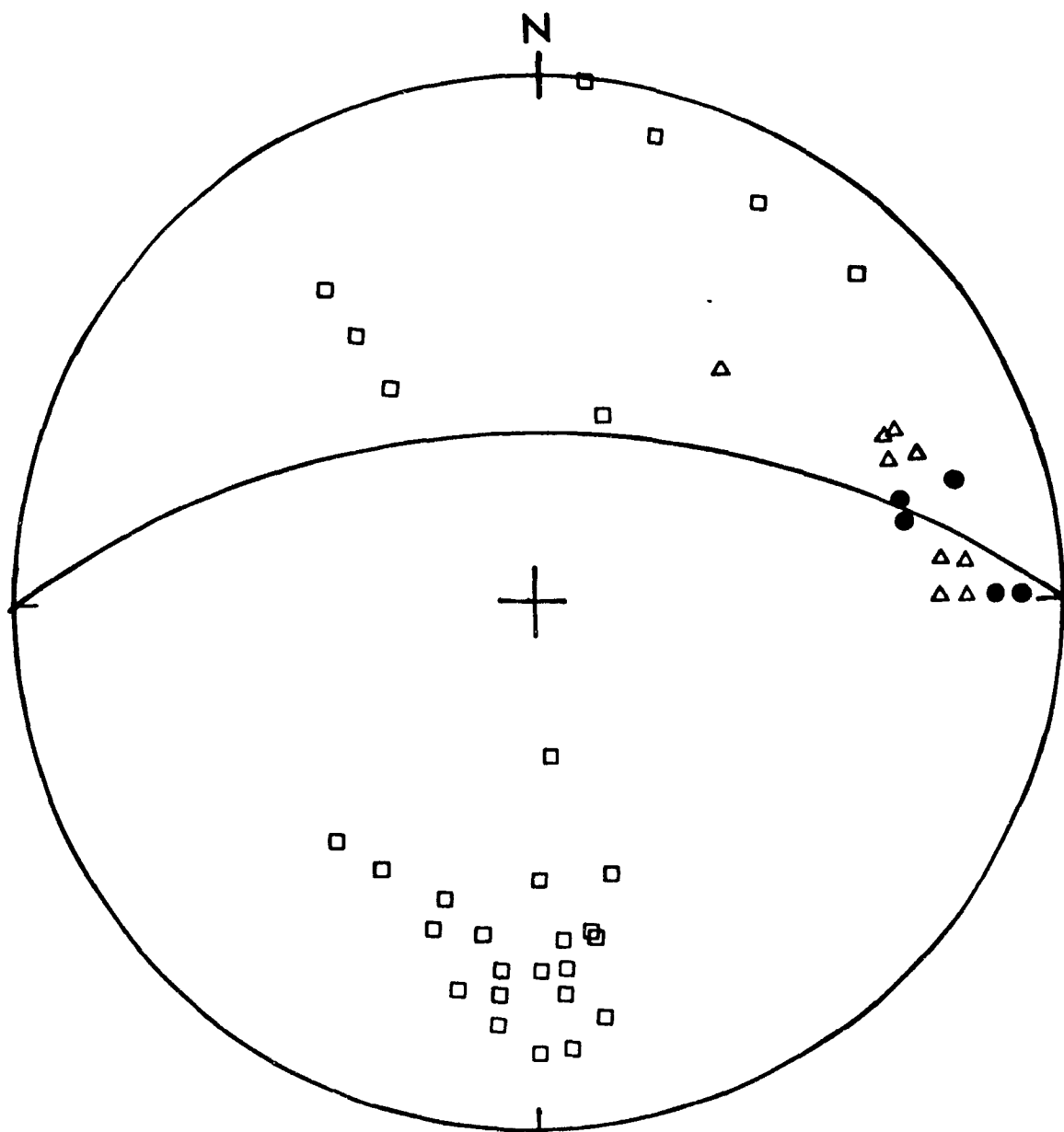
Figure 8b. Raw data used to prepare Fig. 8. Squares : poles to S_1; Triangles : L_2; Dots : F_2 fold axes.

CHAPTER 4. METAMORPHISM and GEOTHERMOBAROMETRY

4.1 Introduction

The study of metamorphism and metamorphic petrology is an essential part of the investigation of any orogenic belt. The aim of this sort of study is to use techniques such as geothermometry and geobarometry to determine the changes in pressure and temperature to which the rocks of the belt have been subjected during the orogeny. By combining data of this sort with information from structural studies and available isotopic dates of various intrusive and metamorphic events it may be possible to develop a comprehensive history of the orogeny.

4.2. Previous Work

Although the Labrador Trough and its environs have been the subject of a large number of studies dealing with structure and stratigraphy, little attention has been given to detailed examination of the regional metamorphism. The two most detailed accounts to date are by Gélinas (1965), dealing with the Kuujjuaq area, and by Dimroth and Dressler (1978), which is a review of the metamorphism of the entire Labrador Trough. The following general description of metamorphism in the Trough is drawn mainly from the latter source.

The oldest metamorphic imprint in the Labrador Trough is that recorded in the Archean basement gneisses which now

51

underlie most of the Trough s.s.. These rocks commonly show the effects of a pre-Hudsonian thermotectonic event (the Kenoran Orogeny, ca. 2700 Ma) which metamorphosed them to amphibolite or granulite facies. This Kenoran metamorphism has been extensively overprinted by subsequent Hudsonian metamorphism. Pre-Hudsonian metamorphic imprints preserved in the low-grade portions of the Trough are contact metamorphism of sediments intruded by gabbro and load metamorphism in thick volcanic sequences (Dimroth and Dressler, 1978).

Metamorphism due to Hudsonian tectonism in the Trough ranges from sub-greenschist at the extreme western boundary of the Trough to granulite facies in the hinterland, with isograds striking NNW to NW (Fig. 9). The dip of the isogradic surfaces varies systematically from shallowly westward dipping in the low-grade portions of the Trough to steeply westward dipping farther east. This steepening is believed to be the result of the greater amount of uplift experienced by the rocks of the hinterland (Dimroth and Dressler, 1978). The transition between greenschist and amphibolite facies closely parallels the eastern margin of the Labrador Trough s.s. and is roughly parallel to the eastern limit of exposed volcanic units (Dimroth and Dressler, 1978, Boone, 1987).

The timing of peak metamorphism with respect to deformation varies in a systematic way across the Trough. Where the metamorphic grade is sub-greenschist (i.e. in the miogeoclinal zone), peak metamorphic conditions predate deformation. Moving

52
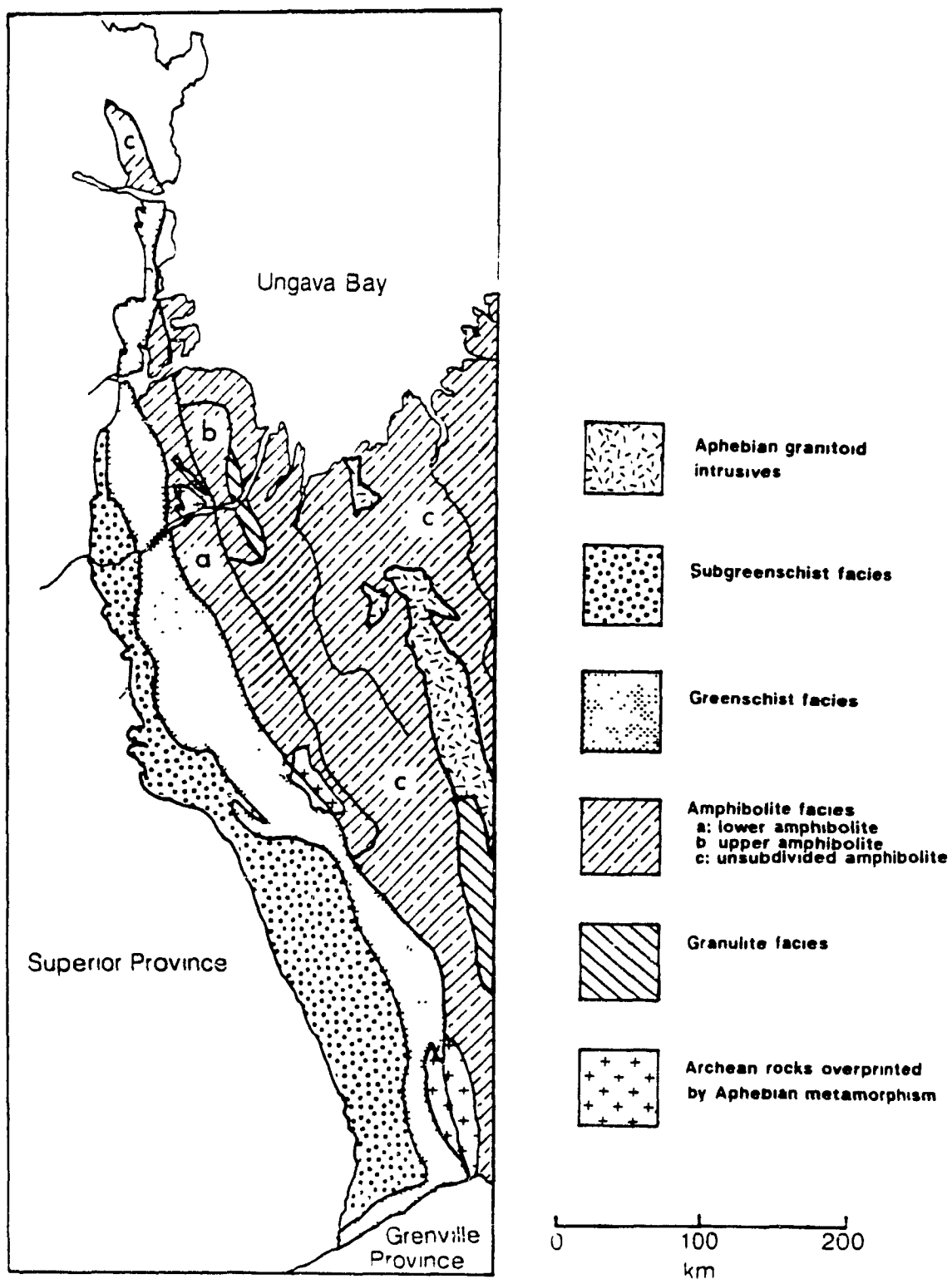
Figure 9. Regional metamorphic map of Labrador Trough and hinterland. After Fraser _et al_. (1978).

east across the Trough, lower greenschist facies metamorphism is syntectonic, upper greenschist and amphibolite metamorphism is late-tectonic and upper amphibolite and granulite metamorphism is post-tectonic (Gélinas, 1965; Dimroth and Dressler, 1978; Moorhead and Hynes, 1986; and this study).

A more detailed report on the metamorphism of part of the study area (south of Lac a Foin) is given in a D. Sc. thesis prepared by Gélinas (1965). The following section, which gives a general overview of metamorphism in the region, is compiled mainly from this source and from personal communications with S. Perreault (1987-8).

As in the Labrador Trough s.s., metamorphic grades in the study area increase from lower amphibolite in the west to upper amphibolite in the east with isograds striking approximately N to NNW. The area contains four major isograds and three minor ones which are defined mainly in pelitic rocks (Fig. 10). The first major isograd encountered is defined by the appearance of oligoclase in place of albite which occurs approximately four kilometers west of the Lac Rachel Fault (LRF) (Boone, 1987). This isograd marks the transition between upper greenschist and lower amphibolite facies metamorphic conditions and is sub-parallel to the LRF.

The next isograds encountered are marked by the successive appearance of garnet (almandine-rich), staurolite and kyanite in pelitic rocks, all within five kilometers of the LRF. Following this is the sillimanite-in isograd which occurs approximately
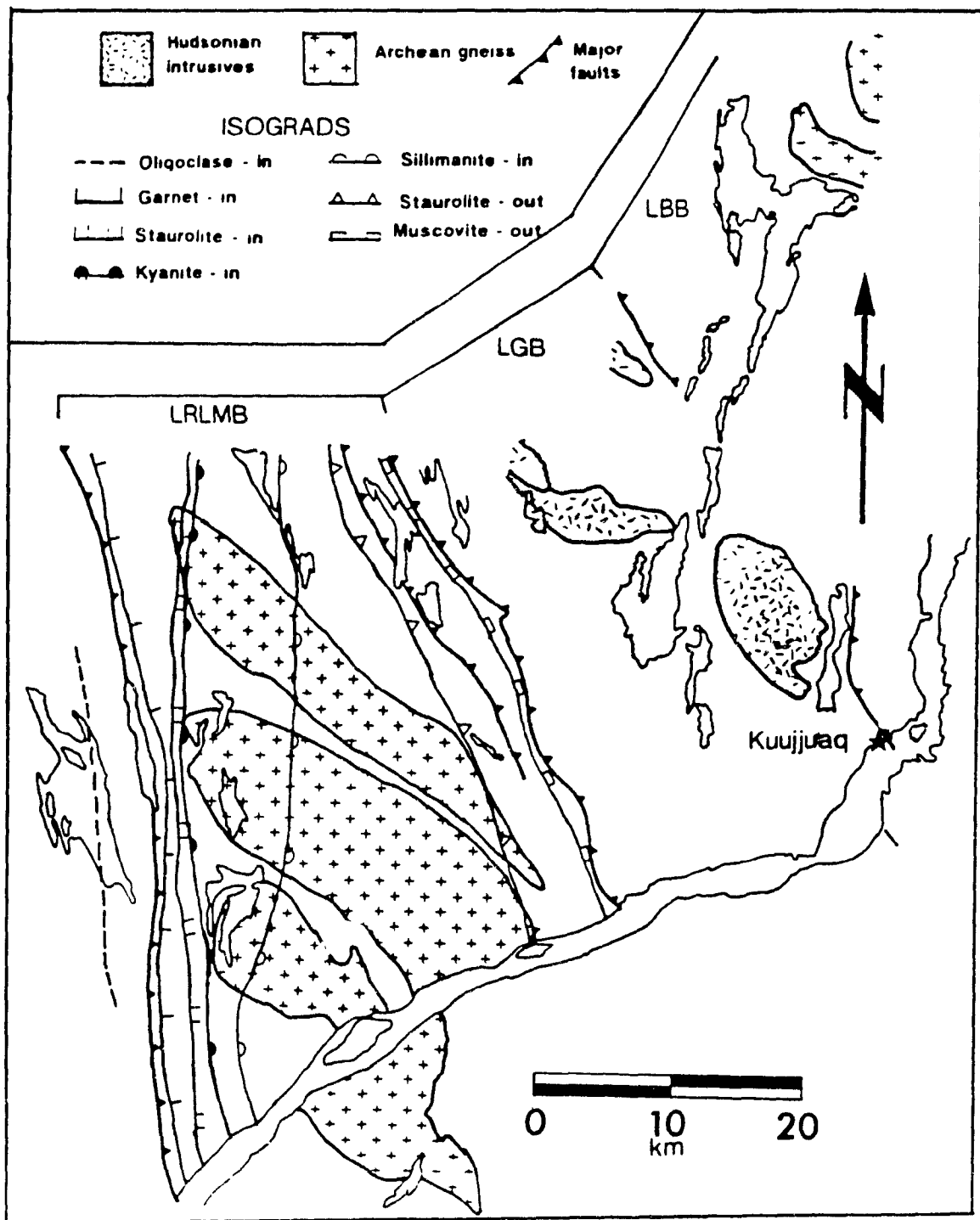
Figure 10. Isograd map of study area and surroundings. After Perreault et al. (1987). Abbreviations as in Figure 4.

10 km to the east of the LRF and marks the onset of upper amphibolite facies metamorphism. The disappearance of staurolite occurs approximately two and a half kilometers west of the Lac Olmstead Fault (LOF; S. Perreault, pers com., 1988). The next isograd occurs approximately 20 km to the east of the LRF and is marked by the disappearance of prograde muscovite (retrograde muscovite is found up to the southern boundary of the Lac Gabriel Complex). This is the only well defined isograd in the study area, its western limit occurring just west of the staurolite out isograd

In contrast to the pelitic rocks, the marble, calc-silicate and amphibolite units in the area exhibit only minor changes in mineral assemblages between the kyanite-in isograd and the onset of upper amphibolite facies metamorphism.

Isograds in the area commonly cross surface traces of D_3 structures (i.e. gneiss cored antiforms (Fig. 10)) and provide further evidence that peak metamorphism in the area occurred after the last episode of ductile deformation.

Recent work (Perreault et al., 1988) has shown that the LBB and LGB were subjected to an earlier metamorphic event. Relict assemblages indicate that the early metamorphism (M_1) reached granulite facies conditions in the LBB and upper amphibolite conditions in the LGB. No evidence for M_1 has been found in the LRLMB (Perreault et al., 1988). This event has been dated at approximately 1830 $\approx$ ±2 Ma (Perreault et al., 1988; Machado et al., 1988). The extensive overprinting of this event by the main

Hudsonian metamorphic event (M_2) has made it very difficult to determine the nature of this early event. U-Pb dating of sphene and monazite has shown that peak M_2 conditions occurred between 1770 and 1790 in all three blocks (Perreault et al., 1988)

4.3 GENERAL PETROLOGY

Although most specimens in the study area have mineral assemblages characteristic of upper amphibolite facies, one of the specimens collected (7e11) contains the assemblage:

Hb-Plag-Cpx-Gt-Opx

which is characteristic of granulite facies (Turner, 1981). This is the only occurrence of a granulite facies assemblage in the area. As mentioned in the previous section, there is some evidence for an early, syn-tectonic granulite event in the northern part of the study area. The SW limit of M_1 is apparently collinear with the trace of the LPF and extends in a SE direction along the north side of the Lac Stewart Complex (S. Perreault pers. com, 1987). It is difficult to determine whether this specimen crystallized during the M_2 event or is a relic from the earlier granulite event which escaped retrogression. Hornblende, plagioclase, garnet and clinopyroxene all appear to be in stable equilibrium, and hornblende composition is similar to granulite facies hornblende composition (i.e. high Ti, Na, K; Raase, 1974; Raase et al., 1986), but it is difficult to determine whether Opx

57

is a stable phase. If Opx was stable during the later event then it has implications discussed further below (see section 4.6).

Apart from this specimen, the only major metamorphic changes observed across the area studied for this thesis are 1) the disappearance of prograde muscovite near the LTF and 2) the change in the habit of sillimanite from fibrolite (with minor associated prismatic material) to prismatic sillimanite north of the LGC. The mineral assemblages of the major rock types of the area are given in Table 1.

Sillimanite has several modes of occurrence south of the LGC. Particularly noteworthy are the garnet-cored sillimanite nodules which occur in pelitic schists (Plate 4c, 4d.). The nodules range from one to two centimeters in diameter. They have cores of extremely ragged garnet which is usually rich in inclusions of biotite (occasionally retrograded to chlorite), quartz and ilmenite. Immediately surrounding the garnet is a quartz-rich rim containing fresh biotite and crystalline sillimanite. These rims are in turn surrounded by a mat of almost pure fibrolite with minor amounts of biotite and ilmenite. The fibrolite is commonly stained brown and small amounts of biotite are commonly observed between fibers. Muscovite, which is a common phase in sillimanite-free portions of the rocks, is absent in the vicinity of these nodules.

These features indicate that the textures may result from a prograde reaction between garnet and muscovite. In a more detailed study of similar textures Pigage (1982) derived the

Table 1. Metamorphic Assemblages

South of LGC	North of LGC

Pelitic Rocks

Qtz - Olig - Bi - Mu $\pm$ Tour   Qtz - Olig - Bi - Sill - Ksp $\pm$ Gt
Qtz - Olig - Bi - Mu - Fib $\pm$ Tour

Accessories: ilmenite, apatite

Semipelitic Rocks

Qtz - Olig - Bi - Gt   Qtz - Olig - Bi - Gt
Qtz - Olig - Bi - Ksp   Qtz - Olig - Bi - Ksp

Amphibolite

Hb - Pl $\pm$ Bi $\pm$ Qtz $\pm$ Gt   Hb - Pl - Bi $\pm$ Cumm $\pm$ Qtz $\pm$ Gt

Accessories: Sphene, ilmenite, apatite, calcite

Quartzose Gneiss

Qtz - Bio - Pl - Mu $\pm$ Ksp   Qtz - Bio - Pl - Ksp $\pm$ Sill $\pm$ Gt

Paragneiss

Qtz - Pl - Bi - Hb $\pm$ Ksp $\pm$ Cumm $\pm$ Gt

Accessories: Sphene, ilmenite, apatite, zircon, allanite

Abbreviations used in table and text:

Ab   = albite
An   = anorthite
Bi   = biotite
Cumm = cummingtonite
Cpx   = clinopyroxene
Fib   = fibrous sillimanite
Gt   = garnet
Hb   = hornblende
Ilm   = ilmenite
Ksp   = alkali feldspar
Mu   = muscovite
Olig = oligoclase
Opx   = orthopyroxene
Pl   = plagioclase (greater than An_{30})
Qtz   = quartz
Rt   = rutile
Sill = sillimanite
Tour = tourmaline

the following reaction (not balanced)

Gt + Rt + Mu —-> Sill + Qtz + An + Bi + Plag + Ilm.

This reaction is consistent with the ragged appearance of the garnet, the quartz rich rims around the garnet, the concentration of ilmenite in the quartz-rich regions and the absence of muscovite. The presence of biotite in the fibrolite also supports the operation of this reaction.

Some amphibolites and paragneisses north of the LPF contain coexisting cummingtonite and hornblende. Cummingtonite is clear, monoclinic, nonpleiochroic and commonly displays extensive lamellar twinning. The hornblende is a smoky blue-green with a strong pleiochroism. There are several ways in which these two amphiboles coexist. The most common modes are 1) fine lamellae of hornblende parallel to twin lamellae in cummingtonite (Plate 4e), 2) a patchy intergrowth of blue-green hornblende and cummingtonite with no distinct grain boundaries (Plate 4f) and 3) an apparently stable intergrowth of the two types of amphibole with distinct grain boundaries (Plate 4g). More than one of these textures is commonly found in the same section, especially modes 1 and 2.

These textures are quite similar to those described by Stephenson and Hensel (1979). These authors suggest that type 3 intergrowths are the result of simultaneous growth during metamorphism. They also suggest that type 1 and 2 intergrowths are the result of exsolution of hornblende during cooling, with type 2 possibly being the result of some sort of exsolution

coarsening process. In any case, the textures of hornblende-cummingtonite intergrowths (type 3) probably indicate that they coexisted stably during prograde and peak metamorphism. The other textures could possibly be the result of the exsolution of a calcic phase from the cummingtonite on cooling from peak M_1 conditions.

A fourth type of hornblende-cummingtonite intergrowth is more difficult to interpret. In many of the sections cummingtonite is rimmed by a zone of blue-green hornblende where it was originally in contact with plagioclase (Plate 4h). The hornblende rims of these crystals are generally poikiloblastic with quartz and have poorly defined grain boundaries with the cummingtonite. Cummingtonite in these intergrowths commonly displays a set of fine "hornblende" exsolution lamellae which terminate at the contact with the rimming hornblende. These textures indicate that the rims may result from a reaction of the type:

$$Cumm + Plag \longrightarrow Hb + Qtz.$$

Though the reaction itself may be fairly obvious, its timing is not. The observation that the reaction has not gone to completion (i.e. there is still cummingtonite remaining) suggests that the reaction is a retrograde one (Vernon, 1976). Evidence of the stable coexistence of hornblende and cummingtonite at peak metamorphic conditions is difficult to reconcile with a retrograde reaction of this nature. A possible explanation is that the hornblende rims represent a reaction which occurred during retrogression from the early granulite event. When peak

61

conditions of the later Barrovian event were reached the assemblage became stable and reaction ceased.

4.4 GEOTHERMOBAROMETRY

4.4.1 Introduction

Mineralogic thermometry and barometry are very important tools in the study of metamorphism and metamorphic terrains. The use of appropriate, well calibrated geothermometers and geobarometers allows reasonably accurate estimation of peak pressures and temperatures of metamorphism and may permit the elucidation of various portions of P-T paths followed by rocks. The following section is a short review of geothermometers and geobarometers and their application.

4.4.2 Geothermometers

The most commonly used geothermometers in high grade metamorphic terrains are based on the exchange of isovalent cations between coexisting mineral pairs. Reactions of this sort are well suited for geothermometry because of their small volume change and their resistance to retrograde resetting (Essene, 1982). The small volume change of intercrystalline cation exchange means that these reactions are only slightly or not at all affected by differences in pressure, and therefore the equilibrium composition of minerals used in these geothermometers is for the most part a function of temperature.

The most commonly used exchange geothermometers are based on Fe-Mg exchange reactions such as:

Almandine + Phlogopite <---> Pyrope + Annite

$$Fe_3Al_2Si_3O_{12} + KMg_3AlSi_3O_{10} \longleftrightarrow Mg_3Al_2Si_3O_{12} + KFe_3AlSi_3O_{10}$$

(Ferry and Spear, 1978). Fe-Mg exchange geothermometers have also been calibrated for garnet-clinopyroxene (Ellis and Green, 1979; Saxena, 1979; and Dahl, 1979), garnet-cordierite (Currie, 1974; Thompson, 1976; Perchuk and Lavrent'eva, 1983; Holdaway and Lee, 1977; Martignole and Sisi, 1981), garnet-hornblende (Graham and Powell, 1984) and garnet-ilmenite (Pownceby et al., 1987) exchange pairs. The very common use of garnet as one member of a geothermometry exchange pair is due both to its common presence in rocks of widely variable bulk composition and to its refractory nature, which makes it relatively resistant to retrograde compositional changes (Loomis, 1983).

4.4.3 Geobarometers

The most commonly used geobarometers in metamorphic studies are based on solid-solid reactions involving the breakdown of low density minerals in favour of higher density phases (i.e. negative volume change). Ideally this type of barometer is calibrated by locating the endmember reaction in P-T space (either by experimental, empirical or theoretical means) and extrapolating this over a range of K_ds (equilibrium coefficients) for the pressures and temperatures of interest. Because these barometers often have a significant temperature

63

dependence, an independent estimate of temperature is usually required for their use.

Examples of solid-solid reaction geobarometers useful in high-grade metamorphic terrains are Garnet-Rutile-Ilmenite-Plagioclase-Silica (GRIPS; Bohlen and Liotta, 1986), Garnet-Rutile-Aluminosilicate-Ilmenite (GRAIL; Bohlen et al., 1983) Garnet-Aluminosilicate-Silica-Plagioclase (GASP; Ghent, 1976, Newton and Haselton, 1981; Koziol and Newton, 1988), garnet-plagioclase-clinopyroxene-quartz (Perkins and Newton, 1981) and garnet-plagioclase-orthopyroxene-quartz (Perkins and Newton, 1981; Newton and Chipera, 1985).

4.4.4 Application

All geothermometers and geobarometers are based on the assumption that chemical equilibrium exists among the minerals used. In most cases this is ensured simply by working with assemblages in mutual contact. When using minerals from high grade metamorphic rocks, however, minerals in contact have commonly undergone retrograde re-equilibration after peak metamorphism and so record retrograde rather than peak metamorphic conditions. Fortunately, mineral zoning provides a way to look back into a rock's past. In almost all metamorphic rocks garnet is zoned (Tracy, 1982; Loomis, 1983). Because diffusion of cations through the garnet lattice is relatively slow compared to other minerals, garnet crystals can maintain large composition gradients between their rims and cores,

64

allowing the garnet rims to remain in chemical equilibrium with minerals in the matrix while the core retains the composition it had earlier in the metamorphic history of the rock. In rocks of medium metamorphic grade the composition of the core of zoned garnets is generally believed to reflect the composition of garnet in equilibrium with matrix minerals at an early stage of its growth (Trzcienski, 1977; Loomis, 1983). At higher metamorphic grades (i.e. T > 650°C Woodsworth, 1977; Yardley, 1977) volume diffusion in garnets becomes fast enough that chemical gradients can no longer be maintained between the garnet rim and core and the crystal may become compositionally homogeneous (given enough time at or above temperatures required for rapid volume diffusion; Anderson and Olimpio, 1977; Woodsworth, 1977; Yardley, 1977; Loomis, 1983). Garnets from rocks above the second sillimanite isograd, therefore, are generally unzoned. As the rocks cool however, the rims of these garnets maintain chemical equilibrium with the minerals in the surrounding matrix, while the core of the garnet maintains the composition it had at peak metamorphic conditions. Knowing the significance of zoning in garnets from high grade rocks, it is possible to obtain information about peak metamorphic conditions if an assumption is made. If the volume of matrix Fe-Mg phases is large compared with the volume of retrograded garnet rims the matrix Fe-Mg minerals act as a sink of cations and their composition is only very slightly changed by retrograde reactions in garnet (i.e. lever principle, Ferry and Spear, 1978). By

65

using the core composition of garnet and the composition of matrix ferromagnesian minerals as input for geothermometers or geobarometers it should therefore be possible to estimate peak metamorphic pressures and temperatures (cf. Indares and Martignole, 1985; Bohlen, 1987).

4.4.5 Sources of Error

Most calibrations of geothermometers and geobarometers include a calculated estimate of error (usually in the area of $\pm$ 50°C and $\pm$ 1 kbar respectively). These calculated errors however, are based only on uncertainties in the calibration (systematic errors) and are often "overly optimistic" (Hodges and Mackenna, 1987). Examples of this type of error include extrapolation of the geothermometer/barometer to conditions far removed from those at which it was calibrated (Essene, 1982) and use of the calibrations on minerals with compositions significantly different from those used in the calibration.

One of the major sources of non-systematic error is the possibility that the minerals used for calculating pressure and temperature are not in chemical equilibrium. Although it is difficult to prove that an assemblage was ever in equilibrium, the risks of error due to non-equilibrium assemblages can be minimized in several ways. The most important way of doing this is by careful microscopic examination of textures for evidence of non-equilibrium. Such evidence includes 1) the presence of obviously retrograde minerals such as chlorite and muscovite, 2)

textures indicating the breakdown of one mineral in favour of another, 3) the lack of stable grain boundary and inclusion shapes, 4) violations of the phase rule or 5) varying compositions of grain edges for crystals of the same mineral (all from Vernon, 1976). The chances of using non-equilibrium assemblages can also be minimized by using only minerals from a small volume of rock so that possible complications due to possible bulk chemical inhomogeneity are avoided.

Another potential source of error is the presence of ferric iron in the minerals used for geothermobarometers. Electron microprobe analysis cannot distinguish ferrous from ferric iron. If a mineral used for geothermobarometry contains significant amounts of ferric iron, it may cause large errors in calculated temperatures and pressures. Even though neglecting the presence of ferric iron may lead to significant errors, the lack of an adequate way to estimate ferric iron contents of minerals accurately from microprobe data (especially minerals such as biotite, hornblende and clinopyroxene) has made it common practice to assume all iron is ferrous when calculating pressure and temperature.

Errors may also be associated with thin-section effects. If a zoned garnet is sectioned off-center, the apparent core composition will differ from the actual core composition. Errors from this source can be minimized in several ways. If it is assumed that garnets in a sample are of a uniform size, then the largest garnet(s) in the thin section are cut closest to the

67

core of the garnet. This source of error may be ignored when homogenized high-grade garnets or assemblages found on garnet rims are used for geothermometry or geobarometry.

4.4.6 Procedure

Thin sections of over 200 samples were made to determine the mineralogy of the specific rock units and to provide a check of metamorphic grades and mineral assemblages. Polished thin sections were prepared from a number of samples to allow more detailed study of the metamorphism using an electron microprobe.

The sections were prepared for microprobe analysis by carbon coating to prevent charge buildup. Analyses were carried out on a Cameca-Camebax wavelength-dispersive electron microprobe with specimen currents of between eight and 10 nanoAmps and counting times of 20 to 30 seconds. Raw intensity data were converted into oxide weight percentages using various silicate standards (depending on the minerals being analyzed) and corrected using the ZAF procedure. A microcomputer-based recalculation program was used to recast the oxide weight percent results into structural formulae.

The diversity of rock types in the study area makes it possible to use a variety of different thermometers and barometers and compare the results from each. This section describes the thermometers and barometers used and how they were

applied (see Table 2 for summary). Where possible thermometers and barometers were used on both rim and core-matrix assemblages.

Four different Fe-Mg exchange thermometers were used for this work. The most frequently employed thermometer was the garnet-biotite geothermometer.

Several calibrations are available for this thermometer (e.g. Thompson, 1976; Ferry and Spear, 1978; Hodges and Spear, 1982; Perchuk and Lavrent'eva, 1983; Indares and Martignole, 1985) and although temperatures were calculated using all of them, only that of Perchuk and Lavrent'eva produced reasonable results throughout the area (see section 4.5.1)

The garnet-hornblende thermometer was also frequently employed. The calibration of Graham and Powell (1984) as modified by Powell (1985) was used in this study.

The two other thermometers used are garnet-clinopyroxene and garnet-cordierite. These thermometers were used on only one sample each, due to the scarcity of the required assemblage in the study area. For the garnet-clinopyroxene thermometer, Powell's (1985) modification of Ellis and Green's thermometer (1979) was chosen in order to maintain consistency with the garnet-hornblende thermometer, which had been calibrated using the same data set (Graham and Powell, 1984). The calibration of Perchuk and Lavrent'eva (1983) was chosen for the garnet-cordierite thermometer because it had been calibrated using the same set of experimental runs as their garnet-biotite thermometer.

Table 2. Geothermometers and Geobarometers

ASSEMBLAGE	REACTION	REFERENCE
GARNET BIOTITE	Almandine + Phlogopite = Annite + Pyrope $Fe_3Al_2Si_3O_{12} + KMg_3AlSi_3O_{10} = KFe_3AlSi_3O_{10} + Mg_3Al_2Si_3O_{12}$	Perchuk and Lavrent'eva,1983
GARNET HORNBLENDE	3 FerroPargasite + 4 Pyrope = 3 Pargasite + 4 Almandine $3\ NaCa2Fe_4Al_3Si_6O_{22}(OH)_2 + 4\ Mg_3Al_2Si_3O_{12} = 3\ NaCa2Fe_4Al_3Si_6O_{22}(OH)_2 + Fe_3Al_2Si_3O_{12}$	Graham and Powell, 1984[1]
GARNET CLINOPYROXENE	3 Pyrope + Hedenbergite = 3 Almandine + Diopside $3\ Mg_3Al_2Si_3O_{12} + CaFeSi_2O_6 = 3\ Fe_3Al_2Si_3O_{12} + CaMgSi_2O_6$	Ellis and Green, 1979[1]
GARNET CORDIERITE	3 Mg-Cordierite + 2 Almandine = Fe-Cordierite + Pyrope $3\ Mg_2Al_4Si_5O^1_8 + 2\ Fe_3Al_2Si_3O_{12} = 3\ Fe_2Al_4Si_5O_{18} + 2\ Mg_3Al_2Si_3O_{12}$	Perchuk and Lavrent'eva,1983[2]

ASSEMBLAGE[3]	REACTION	REFERENCES
GRIPS	Garnet(gr_1al_2) + Rutile = Ilmenite + Anorthite + Quartz $CaFe_2Al_2Si_3O_{12} + TiO_2 = FeTiO_3 + CaAl_2Si_2 + SiO_2$	Bohlen and Liotta, 1986
GRAIL	Ilmenite + Aluminosilicate + 2 Quartz = Almandine + 3 Rutile $FeTiO_2 + Al_2SiO_5 + 2\ SiO_2 = Fe_3Al_2Si_3O_{12} + 3\ TiO_2$	Bohlen et al., 1983
GARNET-ALUMINOSILICATE PLAGIOCLASE-QUARTZ	Anorthite = Grossular + Sillimanite + Quartz $CaAl_2Si_2O_8 = Ca_3Al_2Si_3O_{12} + Al_2SiO_5 + SiO_2$	Newton and Haselton, 1982
GARNET-CLINOPYROXENE PLAGIOCLASE-QUARTZ	Anorthite + Diopside = Grossular + Pyrope + Quartz $CaAl_2Si_2O_8 + CaMgSi_2O_6 = Ca_3Al_2Si_3O_{12} + Mg3Al_2Si_3O_{12} + SiO_2$	Perkins and Newton, 1981

---

[1] As modified by Powell (1985)

[2] Pressure effects ignored

[3] ACTIVITY MODELS
  GARNET: Ganguly and Saxena, (1984) in GRIPS and GRAIL
          Newton and Haselton, (1981) in Gt-Sill-Pl-Qtz
  PLAGIOCLASE : Newton et al., 1980.
  CLINOPYROXENE: Ideal two site mixing.
  ALL OTHER MINERALS: Ideal mixing assumed.

Pressures were calculated using four mineralogical barometers. For most of the specimens the GRIPS barometer (Bohlen and Liotta, 1986) was used. For this geobarometer garnet activities were calculated using both the ternary solution models of Perkins (1979, as reported in Bohlen et al., 1983) and the quaternary models of Ganguly and Saxena (1984). Plagioclase activities for this barometer (and for all others using plagioclase) were calculated using the aluminum avoidance model of Newton et al., (1980).

The use of the remaining geobarometers (GRAIL, Garnet-AlSi-Plag-Qtz, Garnet-Cpx-Plag-Qtz) was restricted to single samples. The activities of phases involved in these barometers were calculated as in Table 2.

4.5 Thermobarometry Results

4.5.1 Temperatures

Among the garnet-biotite geothermometers used, the calibration of Perchuk and Lavrent'eva (1983) was found to be the most useful for this study. At the lower temperature range in the study area (e.g. LRLMB), all tested garnet-biotite thermometers, with the exception of the Hodges and Spear (1982) calibration, produce results which are practically indistinguishable. At higher metamorphic grades, however, there is considerable disparity between the calibrations. In many cases some of the calibrations gave unrealistic results (i.e. temperatures of 850-1000°C). The results of the Perchuk and

Lavrent'eva thermometer were found to give results that are more realistic and consistent with other types of geothermometers use in the area, in agreement with a study by Chipera and Newton (1988) who used a more statistically significant method (trend surface analysis) to compare calibrations. These authors suggested that lack of knowledge of the effect of minor components (e.g. Ca and Mn in garnet and Ti and Al_{VI} in biotite) may lead to significant errors in those calibrations which attempt to correct for the effects of these components (e.g. those of Hodges and Spear, 1982; Indares and Martignole, 1985).

Temperatures calculated using the garnet-hornblende thermometer were found to be quite consistent with those calculated using the Perchuk and Lavrent'eva calibration. When both thermometers could be used in the same specimen the results rarely differed by more than 50°C.

Results from the garnet-clinopyroxene and garnet-hornblende calibrations were also found to be very similar. The results of garnet-cordierite geothermometry (approximately 700°C for core-matrix pairs) cannot be compared directly with the results of the other thermometers, as there is no other thermometer available for that specimen (OC40). When compared with results from nearby samples however, the results from this thermometer appear to be approximately 50°C lower than garnet-biotite or garnet-hornblende temperatures

Temperatures calculated from rim pairs across the entire study are remarkably consistent, even when results from different

thermometers are compared. Temperatures range from 510 to 600°C with average garnet-biotite temperatures of 550 (σ = 29°C) and average garnet-hornblende temperatures of 550°C (σ = 31°C).

This consistency is not observed in temperatures obtained from core-matrix pairs. The core-matrix results can be divided into two distinct groups. The three southernmost samples give core-matrix results which are the same as or slightly lower than those obtained for rim pairs in the same sample. The northern group of samples record relatively higher temperatures for core-matrix pairs (e.g. over 650°C). The results for garnet-biotite thermometers are quite variable, ranging from 650 to 850°C. The garnet-hornblende results are more consistent, averaging 760°C (σ = 22°C).

4.5.2 Pressures

Most of the samples collected contain no assemblage amenable to geobarometry. In the LRLMB there are a number of specimens containing the assemblage garnet-plagioclase-sillimanite-biotite-quartz, but these assemblages are rare elsewhere. Although most specimens contain no rutile, the only barometer which can be applied to specimens across the area is the GRIPS barometer of Bohlen and Liotta (1986). The absence of rutile means that pressures calculated using this barometer are maximum possible estimates.

Pressures were calculated using the garnet activity models of Perkins (1979, in Bohlen et al., 1983) and Ganguly and Saxena (1984). The results calculated using the Ganguly and Saxena model

73

were found to be preferable to those calculated using the Perkins model. The use of the Perkins model results in pressures up to one kilobar higher than for the Ganguly and Saxena model, giving pressures in the field of kyanite stability at calculated temperatures (Sillimanite is the stable aluminosilicate over the entire study area.).

As with temperatures, pressures calculated using rim pairs are quite consistent across the entire study area. Average rim pressures are about 6.3 kbar (σ = 0.38 kbar).

Pressures calculated using core-matrix pairs are much more variable. As with temperatures, results from the three southern samples give pressures which are similar to those obtained from rim assemblages ($\approx$ 6.5 kbar). The remainder of the samples give results which are significantly higher, but show more variability. Much of the variability is due to the results obtained from the GRAIL and garnet-aluminosilicate-plagioclase-quartz barometers, which give pressures significantly lower (6.7 - 7.0 kbar) than most of the GRIPS pressures. The results from GRIPS barometry range from 7.1 kbar to 9.1 kbar, with the majority of the results between 7.7 and 8.2 kbar.

4.6 Discussion

This section is devoted to a discussion of the observations and results presented in the previous sections and their

implications for the overall metamorphic history of the study area.

A major feature of the results is the striking consistency of rim temperatures for both garnet-biotite and garnet-hornblende pairs from specimens throughout the study area. This similarity suggests that similar late stage events occurred in all parts of the study area. Almost without exception, microprobe traverses across garnet porphyroblasts show that the rims of these crystals are quite different in composition from the cores (Fig. 11). Concentrations of Mn and Fe increase sharply while Mg decreases sharply at a small distance from the rim (Ca profiles change from sample to sample, see Fig. 11). Profiles such as these are generally believed to be the result of retrograde changes in garnet composition (Grant and Weiblen, 1971; Tracy, 1982). Compositional changes of this nature have been ascribed to two processes. In one process, the garnet breaks down in favor of another ferromagnesian phase (e.g. biotite ; Grant and Weiblen, 1971; Tracy, 1982). The other process involves simple cation exchange between garnet and a co-existing ferromagnesian phase (Lasaga et al., 1977). Evidence of garnet resorption has been observed only in gp10i and gp26A and is thought to be of minor importance in this region. If most of these rim changes are due to cation-exchange, the calculated rim temperatures correspond to the temperature at which diffusion in garnet was so slow that it was no longer able to maintain local partitioning equilibrium with the ferromagnesian minerals surrounding it. If these rim

75
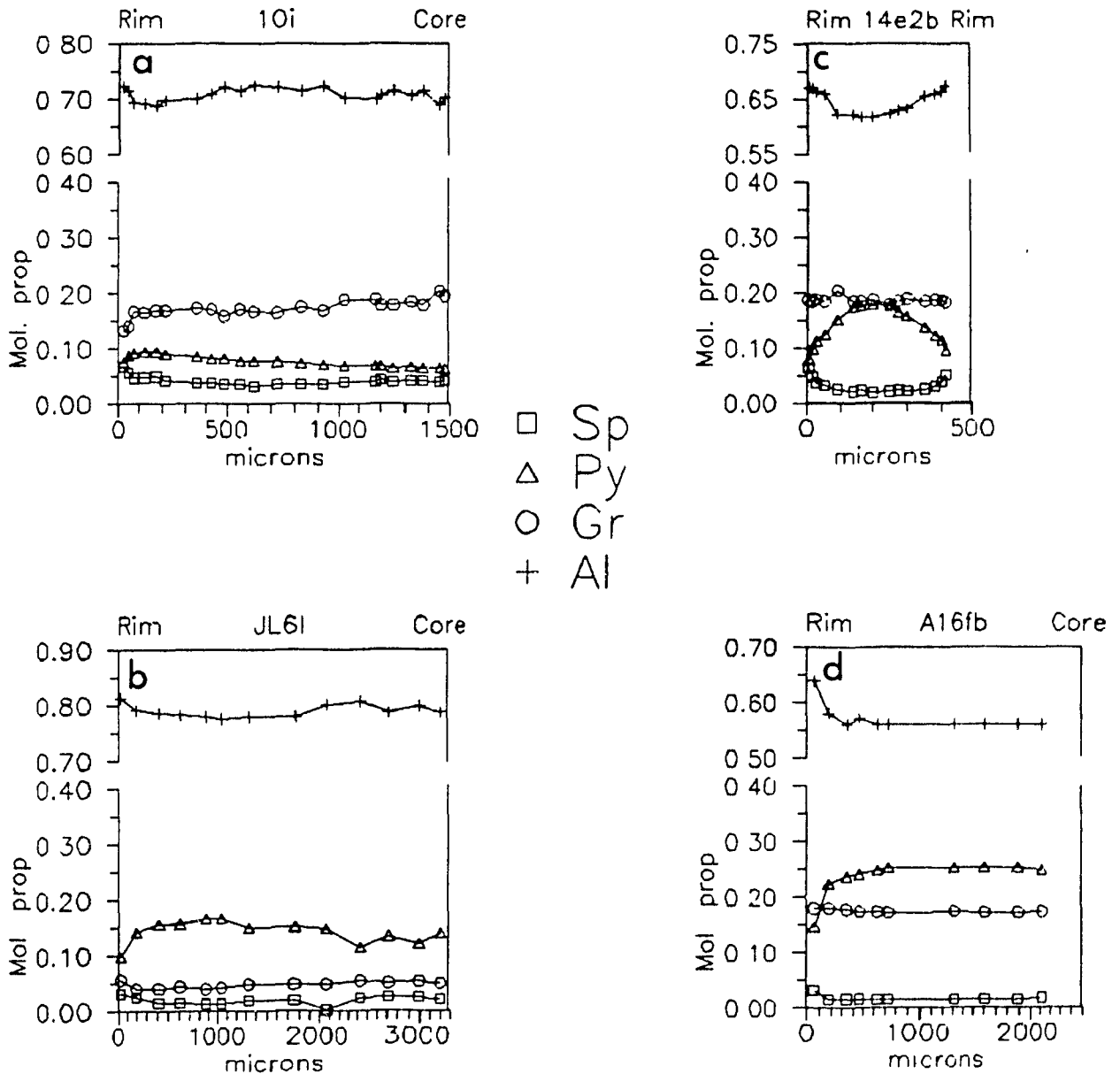
Figure 11. Garnet zoning profiles for GP10i (a), JL6i (b), GP14e2b (c) and A16fb (d). Note rapid changes in composition near rims. X-axis scales have break between almandine and remaining components.

profiles are due to resorption then calculated temperatures correspond to the temperature at which mass transfer becomes so slow that resorption reactions stop (Bohlen, 1987). In either case, the rim temperatures reflect the cessation of any sort of interplay between garnet and the surrounding matrix, and therefore geobarometry results from rim assemblages should represent pressures at this point in the rock's history.

Temperatures calculated from core-matrix pairs, on the other hand, show a much greater variability, especially for garnet-biotite pairs. Core-matrix pressure and temperature results obtained from samples on the SE side of the LTF (see Fig 12) are very low (500-550°C at ≈ 6.5 kbar) and are in conflict with both the presence of sillimanite in the surrounding rocks and with work by Perreault et al. (1987) who estimate temperatures of 700°C for this area. One of these specimens (GP9d) gives the same results for core-matrix and rim-matrix pairs. The garnet in this specimen is highly poikiloblastic, with inclusions of quartz and ilmenite. It is possible that the inclusions in the garnet provided a means for the garnet core to maintain communication with the matrix and maintain equilibrium during retrograde metamorphism. It is also possible that this garnet was not sectioned through its core, and thus results are similar to those for rim pairs. The results from the other two specimens (gp10i and gp26) are more puzzling. Core-matrix results from gp10i average approximately 520°C while rim-rim results average 570°C. Specimen 26A gives core matrix results averaging 560°C while rim-
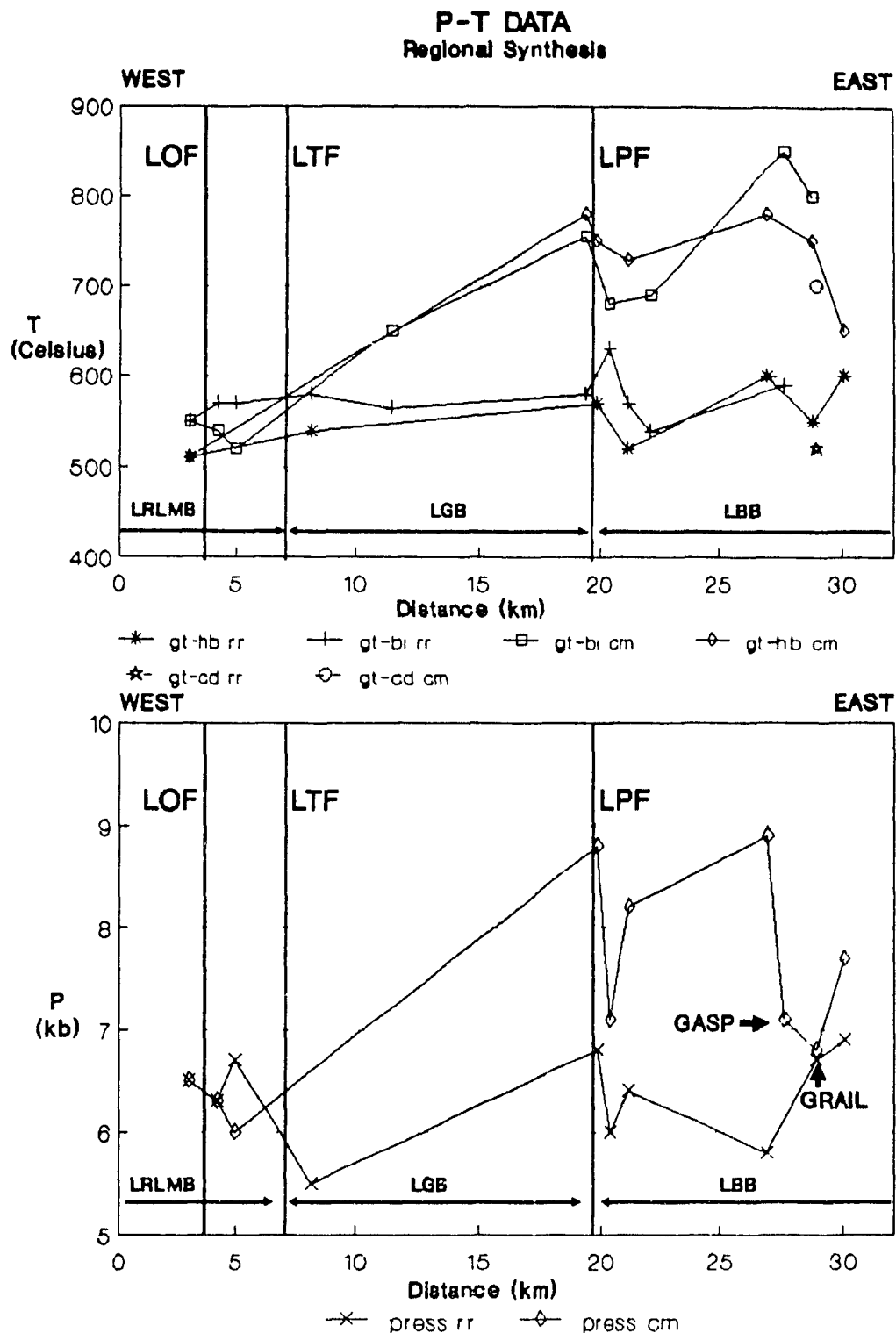
Figure 12. a) Temperature determinations projected onto an east-west line through study area. "rr" refers to results from rims of crystals in contact. "cm" refers to results from cores of isolated crystals. **LOF, LTF** and **LPF** refer to Lac Olmstead , Lac Turcotte and Lac Pingiajjulik faults respectively. b) Pressure determinations plotted on same line as a). All pressures from **GRIPS** barometer unless otherwise specified.

rim results range form 540 to 570°C. Microprobe traverses across garnet from gp10i show irregular and complex zoning (see Fig. 11), although overall the iron content is high in the core and decreases towards the rims, while Mg increases towards the rim of the crystal (except for a small retrograde zone on the edge of the crystal). This sort of zoning pattern is similar in form (but not in magnitude) to those commonly ascribed to the prograde growth of the garnet (Loomis, 1983). The lower results calculated from core-matrix pairs suggest that the core of this garnet has not been homogenized during peak metamorphism, and has maintained the composition it had when it crystallized. The small zone near the edge of the crystal where composition changes rapidly is probably due to retrograde re-equilibration. If so, then calculated rim-rim temperatures correspond to the temperature at which this re-equilibration took place. The other sample in this group (gp26a) has similar modes and mineral compositions and was collected approximately one km to the west of gp10i. It is probable that the results from this specimen represent similar processes.

In order to determine if there are any overall changes in P-T conditions within the study area a plot of temperature and pressure against distance was constructed by projecting the sample locations onto an east-trending line (roughly perpendicular to isograds observed elsewhere in the Trough). The biggest drawback with this presentation (Fig. 12) is the large gap (approximately 8 km) for which there is no information.

Unfortunately the transition from the lower temperatures of the LRLMB and LGB to the higher temperatures of the LBB occurs within this gap. There is some indication of increasing temperature from the results of sample rj13 but the major temperature increase occurs to the east of it. There is some variability in temperatures in the LBB, but most are between 700-800°C. The gt-hb thermometer results are very consistent and suggest that for most of this section peak temperatures were $\approx$ 750°C and fairly uniform.

Calculated peak pressures range from 6.7 to 9.1 kbar with an average of 7.7 $\pm$ 1 kbar for the eastern group of samples. The most probable reason for this variability is the use of the GRIPS barometer on assemblages lacking rutile. As stated earlier the results from these assemblages will be maximum possible pressures (Bohlen and Liotta, 1987). One sample with the full GRIPS assemblage (5W3) gives results considerably lower (7.1 kbar) than those calculated from rutile-free assemblages, and is in good agreement with those calculated using the garnet-sillimanite-plagioclase-quartz (GASP) and GRAIL barometers which give results of 7.0 and 6.7 kbar respectively. This agreement indicates that peak pressures are near 7 kbar, with the higher results being maximum estimates. These results indicate that pressures calculated using the GRIPS with rutile-free assemblages may be up to two kbar greater than the actual pressure. The variability of geobarometry results for core-matrix pairs makes it difficult

to detect the presence or absence of any sort of pressure gradient across the study area.

As with temperatures, pressures calculated from rim pairs are somewhat more consistent (Fig 12b), ranging from 6 to 7 kbar (higher pressures from rutile-free assemblages) and probably represent the pressure conditions at the time when diffusion or reaction processes involving garnet were terminated.

Overall, results from geothermobarometry indicate that peak metamorphic conditions were approximately 750°C at 7-7.5 kbar. The P-T estimates are in good agreement with the presence of sillimanite as the stable aluminosilicate phase (based on Holdaway's (1971) phase relationships). The pressures are also consistent with the bathozone 5 assemblages (Carmichael, 1978) found in the area. These P-T conditions place the study area just below the P-T space occupied by worldwide granulites (England and Thompson, 1984b) (Fig. 13) in accord with the observed mineral assemblages transitional between granulite and amphibolite facies.

The existence of a rock bearing granulite facies assemblages (7e11 : Hb-Plag-Cpx-Gt-Opx) in an otherwise upper amphibolite facies terrain has some implications with regard to metamorphism in the area. If this specimen is a relic from the M_1 event, there must be some reason for why it escaped the retrogression which affected the rocks around it. Alternatively, if it represents an M_2 granulite assemblage it must be somehow different from the rocks around it. Thermometry results (Gt-Hb and Gt-Cpx
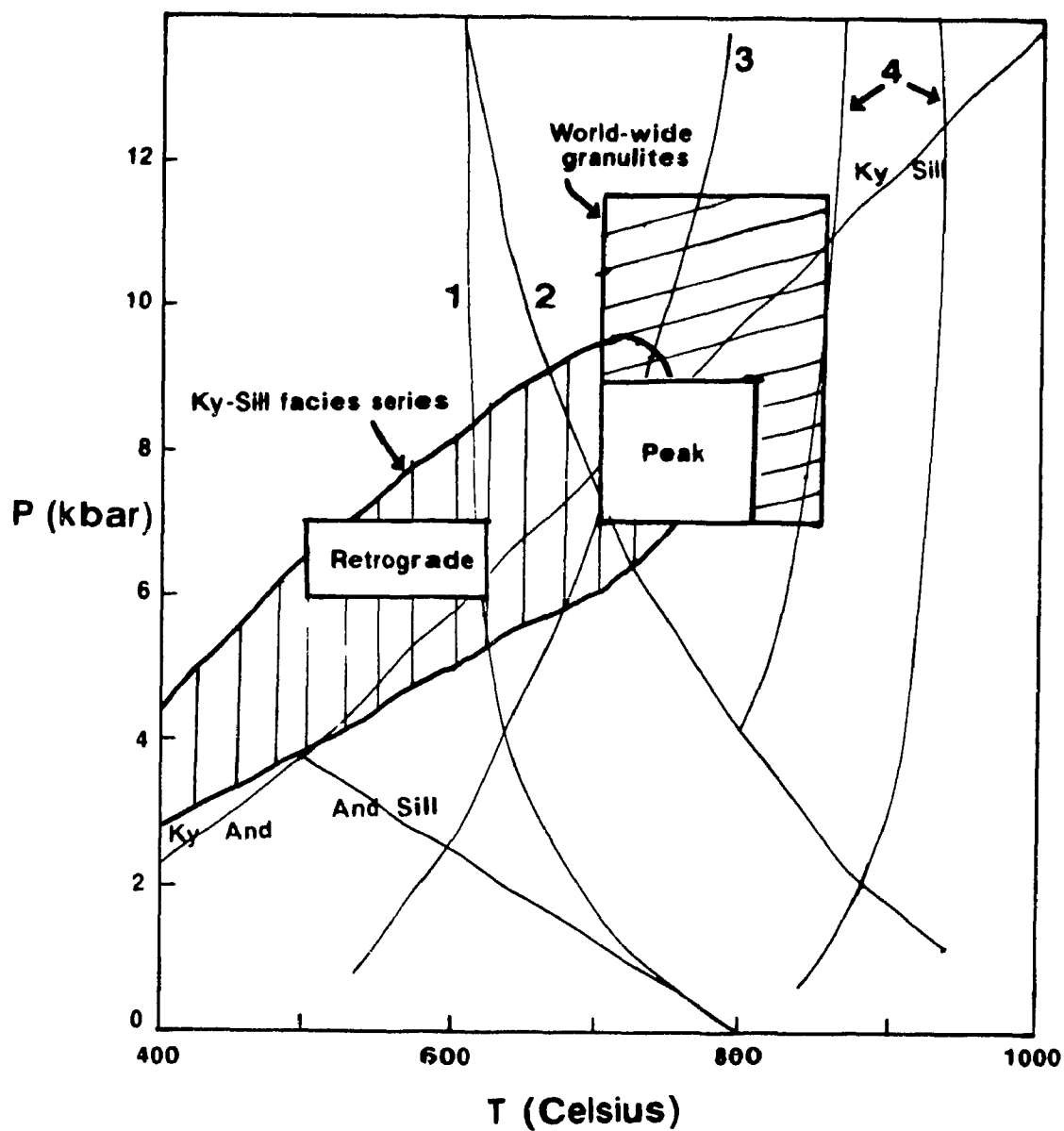
Figure 13. P-T diagram showing aluminosilicate phase relationships, and various melting reactions. 1) Wet melting in pelites. 2) Wet melting in amphibolites. 3) Dry melting in pelites. 4) Dry melting in amphibolites. Boxes labeled "peak" and "retrograde" enclose peak and retrograde results from geothermobarometry (this study). Diagram after England and Thompson, 1984.

82

thermometers) from this specimen indicate peak temperatures of 780°C, which are not significantly higher than results from other specimens in the same area. If temperature and pressure are not factors in the preservation or creation of this assemblage (It is unlikely that this specimen has been subjected to pressures higher than the specimens around it.), then the most probable reason for its presence is reduced P_{H2O}. In most metamorphic terrains which include an amphibolite-granulite transition zone, the change is accompanied by increasing temperature and decreasing P_{H2O} or both, with or without change in pressure (Phillips, 1980; Janardhan et al., 1982; Schreurs, 1984). If P_{H2O} was locally reduced, it could explain preservation of an earlier granulite relic or the development of granulite assemblages in an amphibolite terrain. Local granulite assemblages in amphibolite terrains have been observed elsewhere (Janardhan et al., 1982).

One feature commonly found in high-grade metamorphic terrains, namely partial melting is rare in the study area. Migmatization is only obvious in the "basement" rocks of the Lac Berthet area. Structural evidence from these rocks however(i.e migmatites deformed by D_1 structures), indicates that partial melting occurred before the main metamorphism in the area (i.e. M_2) which was post-tectonic. Migmatites are not observed elsewhere in the study area, but some amphibolites in the LBB and upper LGB have minor quartzofeldspathic "sweats" which may mark the onset of partial melting.

If the geothermobarometry results accurately reflect peak metamorphic conditions, then the lack of migmatites in the area is most puzzling. The rocks are well past conditions of wet and dry pelite melting as determined by Thompson and Tracy (1979) and above the conditions for wet melting in amphibolites (Thompson and England, 1984) but the only evidence for partial melting (except for the Lac Berthet basement rocks) is the presence of quartzofeldspathic sweats in some amphibolites.

One possible explanation for this is that migmatites were simply not recognized. If partial melting occurred before D_1 the subsequent formation of the S_1 foliation could possibly have obscured evidence of migmatization. In view of the fact that migmatites in the Lac Berthet basement (which was deformed by D_1) are so immediately obvious, this does not seem likely. Alternatively it is possible that the melts generated by anatexis were mobile enough to leave the rocks in which they were generated. A possible scenario for this would involve anatexis during the early granulite event, with the melts rising from the rocks in which they were generated. Because the Berthet gneisses are migmatized, this would imply that partial melting occurred prior to the juxtaposition of the gneisses and supracrustal rocks during D_1. The migmatitization of the Berthet gneisses would then occur in response to their being brought into contact with the hotter supracrustals. Although this scenario is possible, there is no evidence for it. The more favoured explanation for the lack of migmatites is that they never formed. Since, as mentioned

above, the temperature conditions for these rocks are above those required for melt generation, there must have been other factors involved. Two variables which are known to displace melting reactions to higher temperatures are water activity and bulk composition. Conditions of $a_{H2O} < 1.0$ have been shown to retard melt generation significantly (Thompson and Algor, 1977; Thompson and Tracy, 1979). A major problem with invoking this factor is that the protoliths of these rocks were sediments and so probably water saturated. The alternative explanation is that the rocks are of an unsuitable bulk composition. Previous studies (Thompson and Algor, 1977; Thompson and Tracy, 1979) have shown that in Ca-rich rocks anatexis occurs at higher temperatures than in pelites. This is a possible explanation for the lack of pelites in the area. The rocks of the area have plagioclase compositions of at least An_{30} and up to An_{50}. The rocks also commonly contain Ca-amphiboles, attesting to their Ca-rich compositions.

Thus, the favoured reason for lack of migmatites in the LBB and LGB is lack of suitable compositions among the rocks of these blocks. The voluminous pegmatites which intrude parts of the area may be an indication that anatexis did occur at depth, and that the melts have risen to the present level of exposure.

If it is assumed that core-matrix thermometer and barometer pairs give P-T conditions corresponding to peak metamorphic conditions (i.e. T_{max} and P_{Tmax} , England and Thompson, 1984) and that rim pairs record P-T conditions during retrograde

85

metamorphism (cf. Bohlen, 1987), then it should be possible to elucidate some portion of the P-T path followed by these rocks during uplift and erosion (i.e. after peak metamorphism).

The biggest assumption in using this method to deduce P-T paths is that results from rim pairs represent a point in P-T space that was actually occupied by the specimen. Whether or not this is true depends on the blocking conditions for the thermometers and barometers used. As mentioned previously the blocking conditions are dependent mainly on diffusion rates in garnet, which are much lower than for most other minerals. If it is assumed that rim temperatures from sections exhibiting retrograde garnet rims and no sign of garnet resorption are those at which diffusion of cations effectively stopped (i.e. the blocking temperature), then barometers should record the pressure at which the rocks cooled through this temperature. Rim pairs should then provide one point on the cooling path of each rock. (Paths from peak to retrograde conditions have been prepared, but in these cases retrograde assemblages rather than rim assemblages have been used (e.g. Allbarede, 1976, Hodges and Royden, 1984)

Rim and core-matrix P-T data for individual rocks are related by fairly uniform positive slopes in P-T space (Fig. 14), close to that of the Ky-Sill phase boundary (Holdaway, 1971). These paths are also roughly parallel to the GRIPS reaction curve. Because these paths are defined by only two points they do not give anyindication of the curvature of the path and any further

86
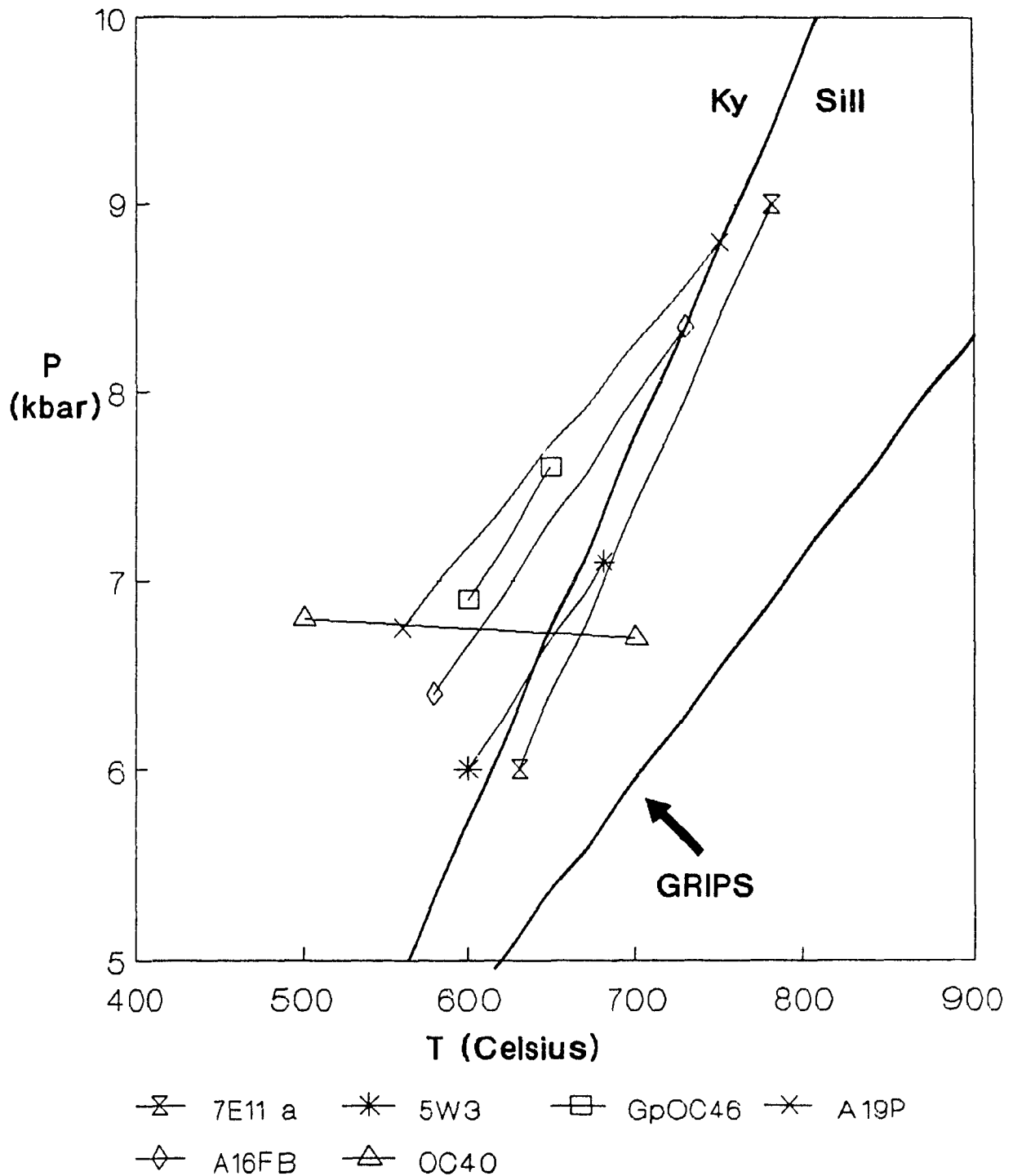
P-t Paths

Figure 14. P-T paths from study area. Line marked GRIPS is reaction slope for GRIPS barometer (Bohlen and Liotta, 1987)

interpretation should be approached with caution. The general form of these P-T paths (*i.e.* decreasing P and T) is, however, roughly similar to those observed and calculated for the uplift and erosion of a tectonically thickened pile (*e.g.* Allbarde, 1976, Hodges and Royden, 1984; England and Thompson, 1984). This is consistent with Ky-Sill facies series metamorphism in the area, which is generally thought to be the result of crustal thickening (England and Thompson, 1984b; Thompson and Ridley, 1987).

5. Geochemistry of the Meta-igneous Rocks

5.1 Introduction

In any investigation of the tectonic history of an area, the nature of the igneous rocks can provide important constraints on its evolution. In some cases petrological and igneous associations can provide important clues to the history of a region (e.g. Pitcher, 1987), but in most cases more information can be derived from the study of whole rock geochemistry of igneous rocks. Because the processes by which igneous rocks are derived differs for each tectonic environment, the chemistry of the resulting rocks often reflects their origin. In many cases the geochemistry of a suite of igneous rocks may allow direct identification of their emplacement environment (e.g. Pearce et al., 1984; Harris et al., 1986; for granitoid rocks; Pearce and Cann, 1973; Pearce, 1975; Pearce et al., 1975; Floyd and Winchester, 1975; Pearce et al.; 1977; Beccaluva et al.; 1979 for basaltic rocks) but even when this is not possible the geochemical characteristics may still provide some clues as to their origin.

For this study whole rock analyses for major and trace elements were obtained using X-ray fluorescence (XRF) for 8 amphibolites ("metabasalts") from the Lac à Foin area and 38 gabbroic to granitoid rocks from the Lac Gabriel complex. This chapter is concerned with the geochemistry of these rocks and its implications with respect to their origin.

89

5.2 Amphibolites

5.2.1 Igneous Affinity

Due to the obliteration of primary features by high-grade metamorphism, care must be taken to ensure that the amphibolites used for geochemistry are actually igneous in origin. It has been shown that mixtures of calcareous and pelitic rock can mimic the chemistry and therefore the mineralogy of basaltic rocks (Leake, 1964). One of the amphibolite units sampled displayed deformed pillow structures (Bosdachin, 1986) which provide evidence of its igneous extrusive origin. The other units sampled provide no such evidence. The most useful way to distinguish between para and ortho-amphibolites is by using trends defined by high field strength elements (Leake, 1964) such as Zr, Y, Nb and Ti which remain relatively immobile during metamorphism (Pearce and Cann, 1973; Floyd and Winchester, 1975). Although para-amphibolites may mimic ortho-amphibolite geochemistry, the trends defined by the immobile elements may allow discrimination between the two (Leake, 1964). When plotted on these diagrams, the data show trends like those of igneous rocks. On the basis of these trends and the presence of pillow structures in one unit, it is assumed that these amphibolites are igneous in origin.

Although the effect of metamorphism and alteration on the chemistry of these rocks has not been rigorously assessed, the presence of minor calcite in some of the specimens indicates some mobility of calcium. Sills and Tarney (1984) have shown that

90

metamorphism usually works to decrease SiO_2 concentration and increase the concentration of K_2O, Rb, Na_2O, BaO, Sr and CaO.

Using the classification scheme of Irvine and Baragar, (1971) these rocks are tholeiitic basalts. (Fig. 15. Note: Even though diagrams used in this classification are based on Na_2O and K_2O, enrichment in these oxides during metamorphism would not alter this classification. Because these rocks presently plot in the tholeiitic fields, enrichment in K_2O and Na_2O could only have moved them closer to the field boundaries. A decrease in SiO_2 concentration would have a similar effect (for Fig. 15b)). When plotted on an alkaline-tholeiitic discrimination based on more immobile elements (TiO_2 vs Y/Nb, Winchester and Floyd, 1975) the samples also plot well within the tholeiitic field (Fig. 16a).

These rocks are very similar in major element chemistry to the Hellancourt Volcanics (HV) farther to the west, which are low-K tholeiitic basalts (Boone, 1987; see Fig. 16b). The Hellancourt volcanics are chemically transitional between P-type MORB and continental tholeiite using both Zr/Nb ratios and elemental abundances of K, Rb, Sr and Ba (Boone, 1987). The metabasalts of the study area have Zr/Nb ratios (9-10) which are slightly higher than those of the Hellancourt Volcanics (6-8) but still intermediate between the Zr/Nb ratios of P-type MORB and continental tholeiite. Abundances of K, Rb, and Sr are also slightly higher than those of the HV (0.5 wt%, 200 ppm and 217 ppm respectively versus 0.3 wt%, 180 ppm and 160 ppm), but these values may be of little significance due to the high grade
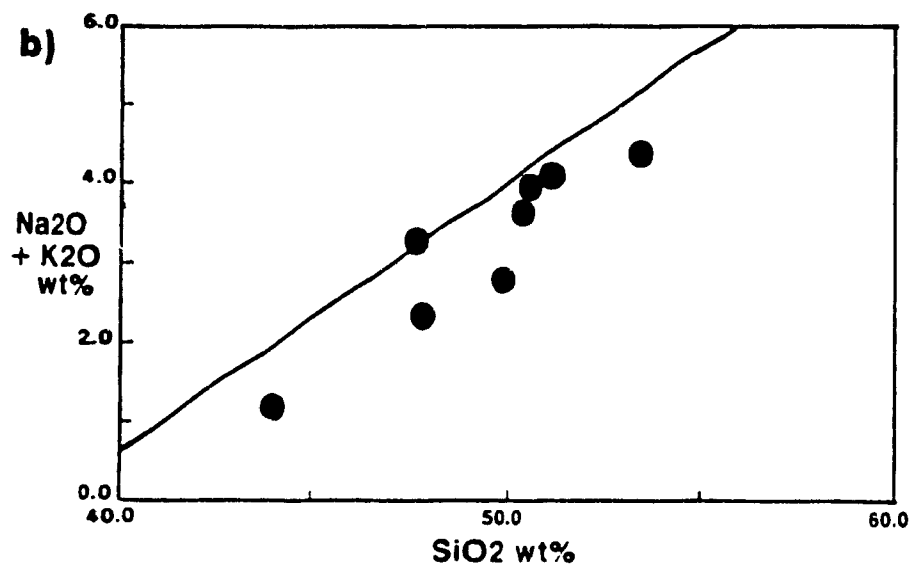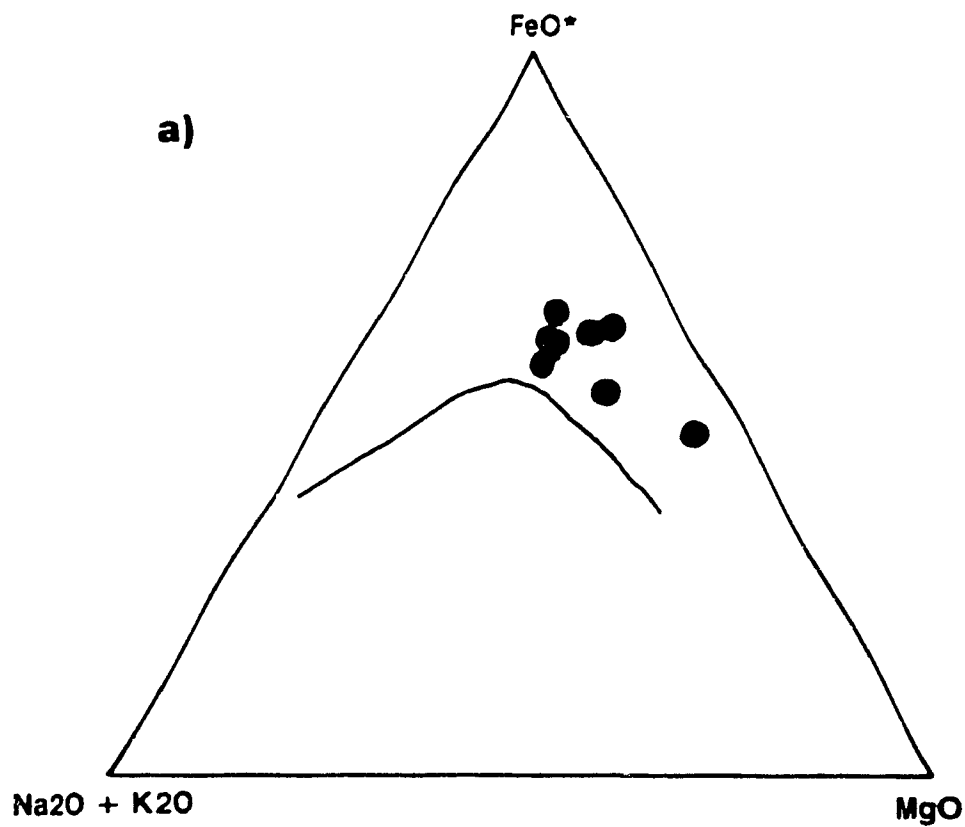
Figure 15. a) AFM and **b)** total alkali versus silica diagrams for Lac a Foin amphibolites. Lines dividing calc-alkaline and tholeiitic fields from Irvine and Baragar, 1972.
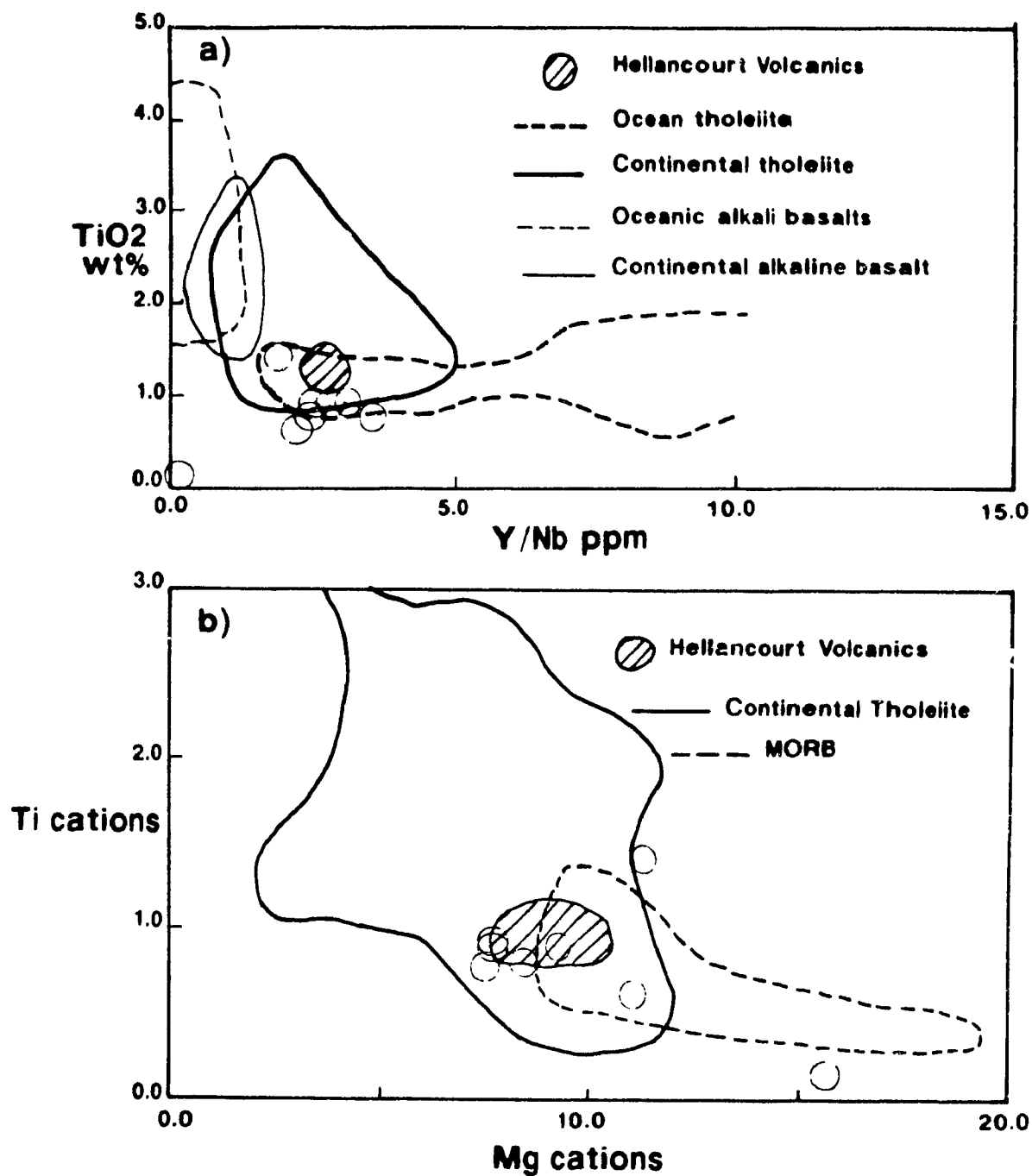
Figure 16. a) TiO_2 versus Y/Nb diagram for Lac a Foin amphibolites. Basalt fields from Floyd and Winchester (1976). b) Ti versus Mg (in cation percent) diagram for Lac a Foin amphibolite, after Boone (1987).

metamorphism undergone by these samples (cf. Sills and Tarney, 1984). Overall these samples are sufficiently similar to the Hellancourt volcanics that they may well be correlative to them. In this case they are geochemically transitional between P-type MORB and continental tholeiites. However, given the degree of their metamorphism, their tectonic environment should be interpreted with caution. Suffice it to say that these rocks were probably emplaced in an area of thinned or absent continental crust.

Although there have been a number of schemes proposed for the tectonic discrimination of basalt emplacement environment, the highly metamorphosed nature and lack of certainty as to the origins of these samples make the use of such schemes questionable. The ages of these rocks also must be considered, as most of these discrimination diagrams were derived using Cenozoic basalts (e.g. Pearce and Cann, 1973; Pearce et al., 1977; Beccaluva et al., 1979).

5.3 Lac Gabriel Complex

5.3.1 Geochemistry

Samples from the Lac Gabriel complex show a wide range in SiO_2 content, (40-73 wt. %) with the majority of the granitoids containing less than 60 weight percent silica. Harker plots for various elements (Fig. 17) show smooth trends, especially for total iron, CaO and TiO_2, with more scatter in plots of MgO and Al_2O_3. These diagrams also show considerable overlap in the
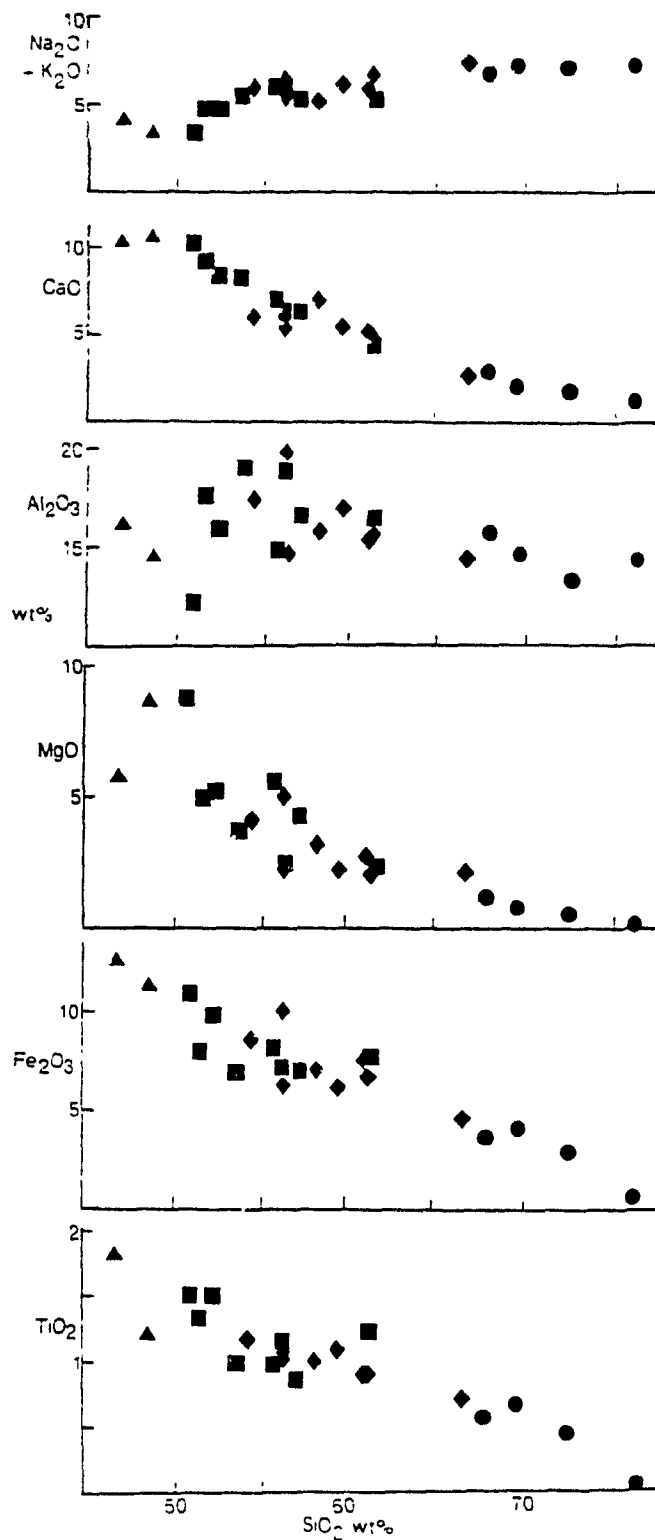
Figure 17. Major element Harker plots for granitoids of the Lac Gabriel complex. Triangles: diorite; Squares: tonalite; Diamonds: granodiorite; Circles: granite.

silica content of the tonalites and granodiorites. These features suggest derivation of the granitoids from a common source, but trace elements provide no conclusive evidence for this. On Y/Zr plots (Fig. 18) there is a poorly defined trend connecting the hornblende gabbros to the granodiorites and granites, but other trace element plots (Rb/Sr, Rb/Zr, see Fig. 18) show a large degree of scatter and no observable trends. Most of the rocks of this complex are slightly peraluminous. The samples are also calc-alkaline, having a Peacock index of 59 and showing a good calc-alkaline trend on AFM and Na_2O-K_2O-CaO diagrams (Fig. 19). The Harker plots also show calc-alkaline trends, with MgO, CaO, TiO_2 and total iron decreasing and Na_2O and K_2O increasing with increasing silica content (cf. Atherton and Sanderson, 1987).

5.3.2 Tectonic Affinity of the Lac Gabriel Complex

Various studies have shown that the characteristics of granitoid intrusives are closely related to the tectonic environment of their emplacement. Most of these studies have used both physical and chemical characteristics, (e.g. White and Chappell, 1974; Pitcher, 1983) but purely geochemical parameters have also been used (Pearce et al., 1984; Harris et al., 1986).

On the tectonic discrimination diagram of Pearce et al. (1984) the granitoids all fall within the field of volcanic arc granites (Fig. 20). A problem with this mode of discrimination is its incapacity to distinguish volcanic arc granitoids from

96
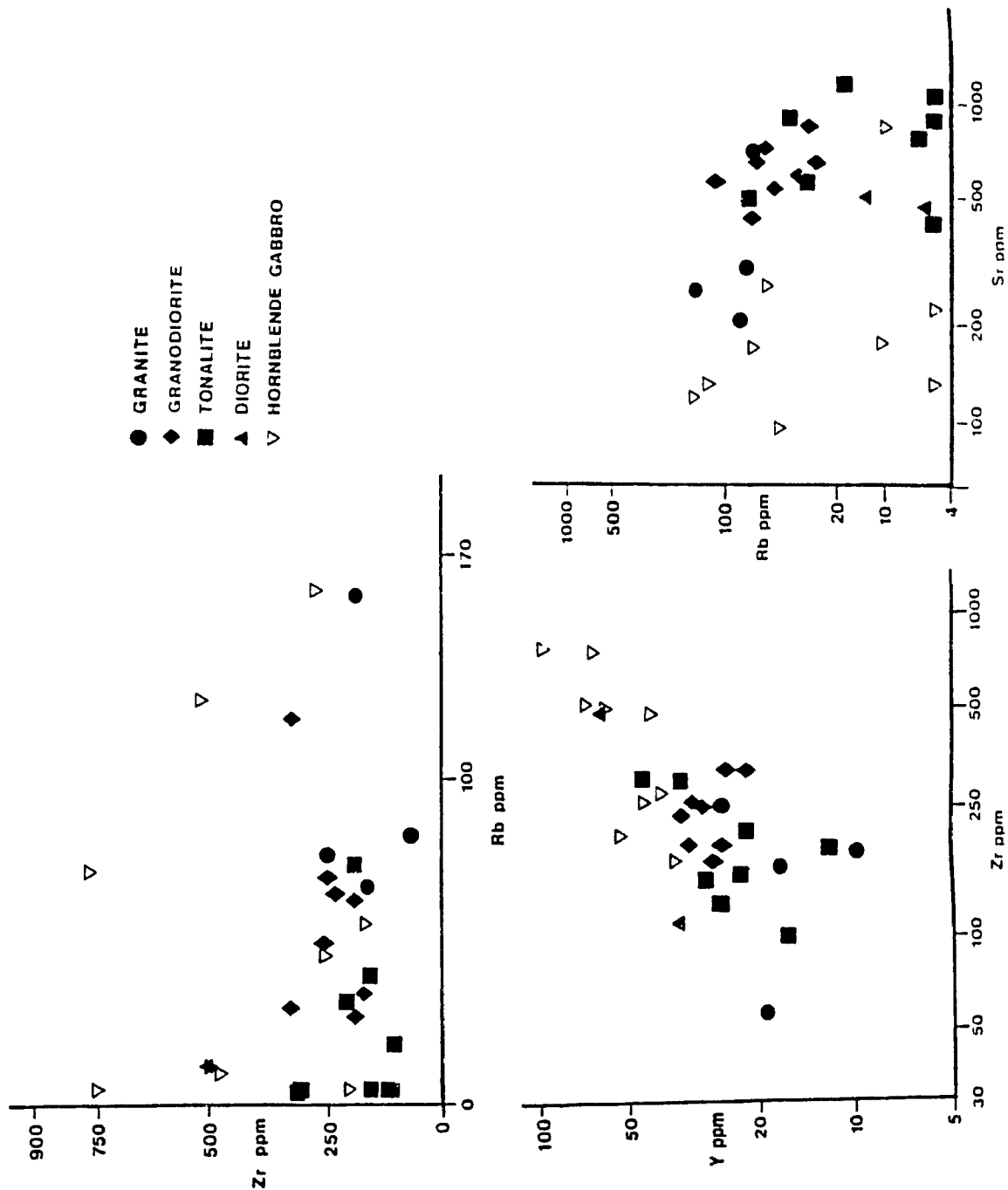
Figure 18. Rb-Sr, Rb-Zr and Y-Zr variation for phases in the Lac Gabriel complex.
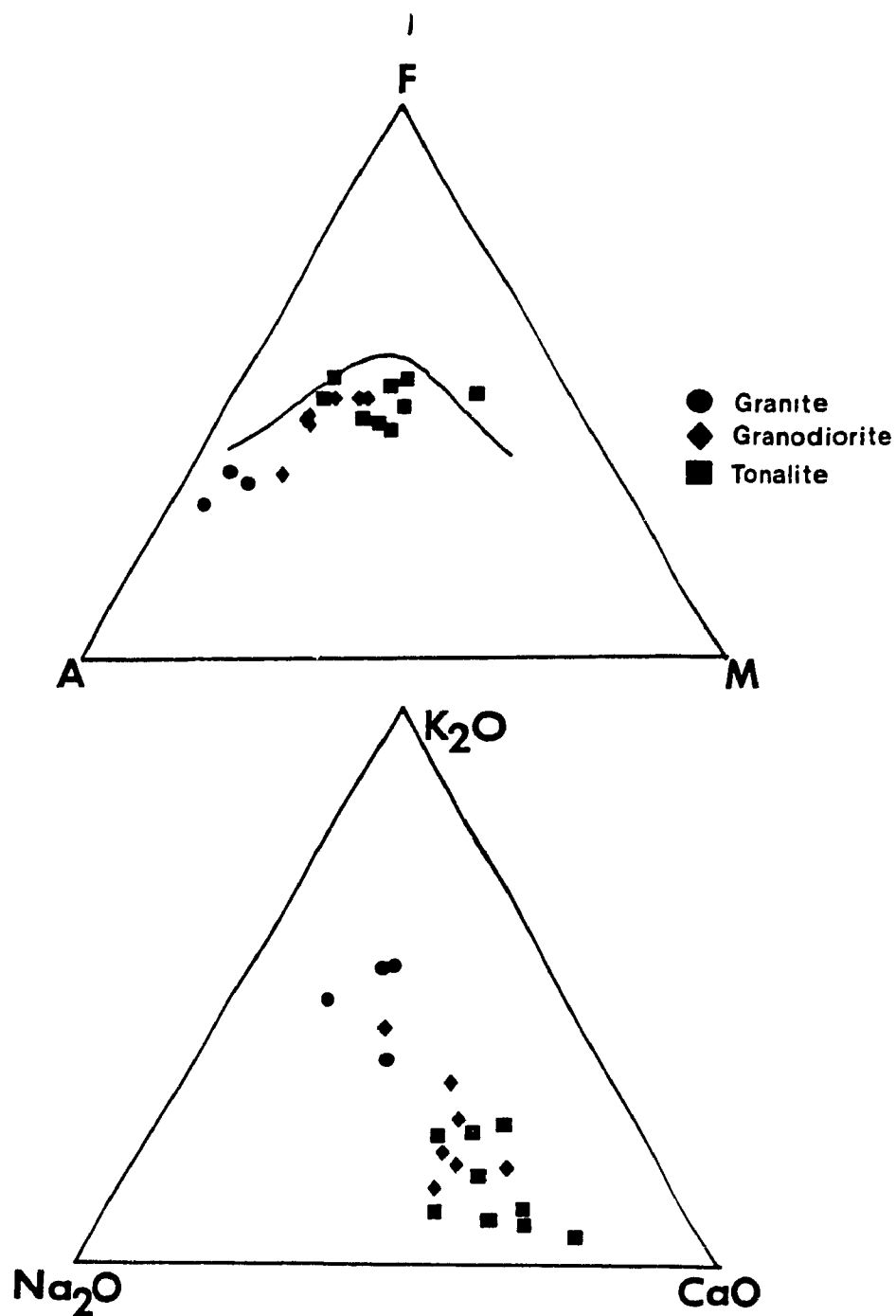
Figure 19. Granitoids from the Lac Gabriel Complex plotted on **AFM** and Na_2O-K_2O-CaO diagrams. Line separating tholeiitic and calc - alkaline compositions from Irvine and Baragar (1971).
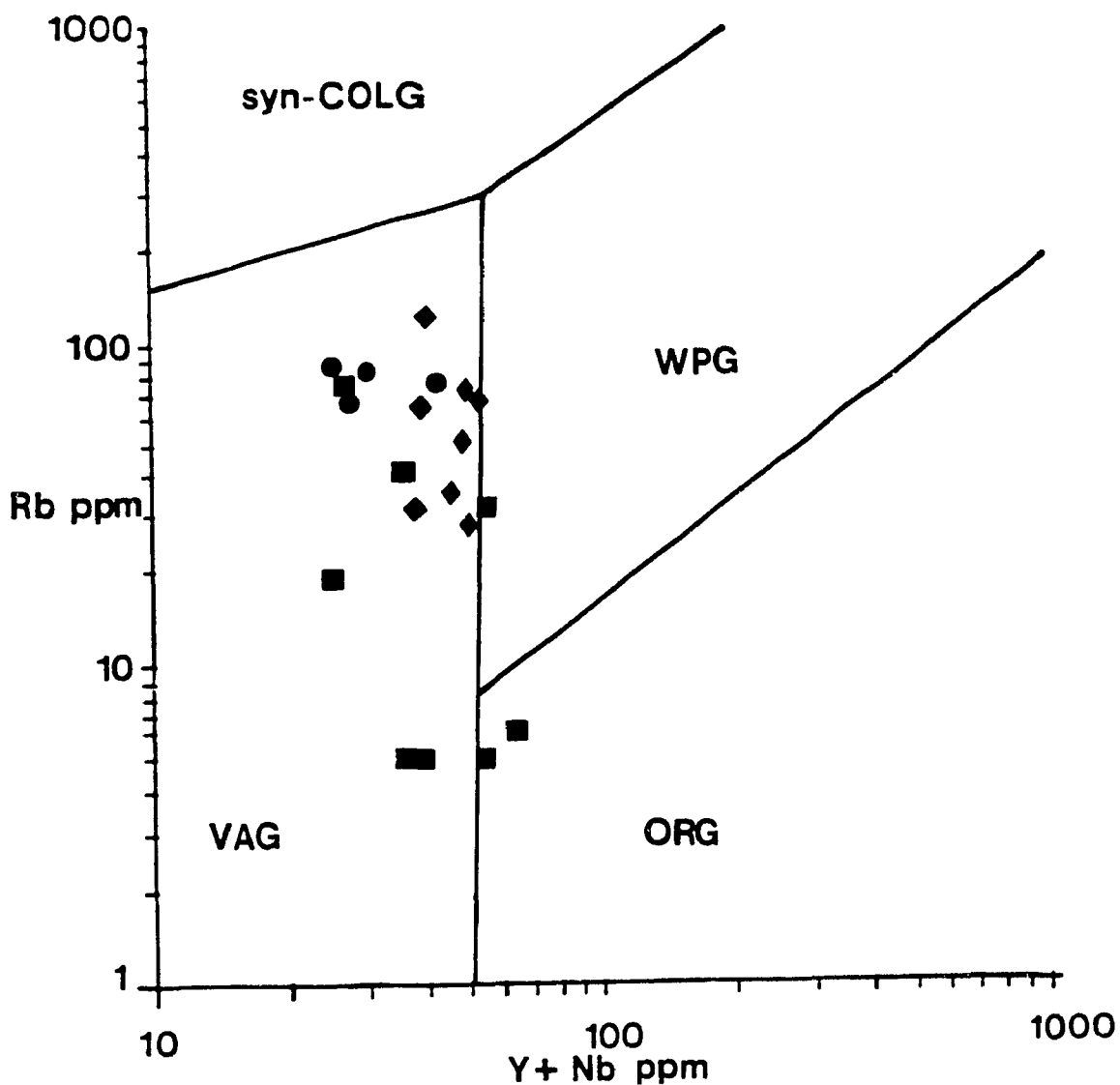
Figure 20. Granitoids from the Lac Gabriel complex plotted on a Rb /(Y + Nb) discrimination plot (Pearce et al., 1984). Symbols as for Fig. 17. VAG: volcanic arc granitoids; syn – COLG: syn – collisional granitoids; WPG: within plate granitoids; ORG: ocean ridge granitoids.

post-collision granitoids, which may share many of the same characteristics (Pitcher, 1983). However, other features of the granitoids, such as a wide range in composition and SiO_2 content, the dominance of hornblende over biotite as a mafic component, the common association with magnetite and the presence of mafic xenoliths and mafic intrusives are more typical of "Cordilleran" I-type granitoids characteristic of continental arc terrains, than of "Caledonian" I-types, which are characteristic of post-orogenic uplift (Pitcher, 1983). One feature of "Cordilleran" I-type granitoids absent here is their common association with large amounts of andesite and dacite. A likely explanation for this is that deep erosion, as evidenced by the high metamorphic grades, has removed a formerly associated volcanic pile.

Chapter 6. DISCUSSION AND CONCLUSIONS

6.1 Introduction

The synthesis of data presented earlier in this work allows the formulation of an overall picture of processes which led to the formation of the eastern margin of the Labrador Trough as it is presently observed. In this chapter the implications of these data are discussed and they are integrated into a geological history for the area. This history is then used to provide some constraints on tectonic models for the area.

6.2 Summary and Discussion

6.2.1 Lithological Associations

This section deals with the lithological associations of the study area and their implications for depositional environments. Correlations between the study area and other parts of the Labrador Trough Orogen are also discussed.

The predominance of pelitic and semipelitic rocks in the Lac Rachael-Lac Murrray Block indicates that the block preserves sediments deposited in a deep-water, low energy environment. The basaltic and gabbroic amphibolites in the block indicate that this basin was subjected to episodic basaltic volcanism and attendant intrusion. The base of the sequence, which contains several marble units and a metaconglomerate with Archean(?)

gneiss clasts   indicates that deposition of the early parts of the sequence took place in shallow water on or near continental crust. The metaquartzite unit at the top of the sequence suggests a late (if younging is to the east) shallowing-up episode.

Work by Boone (1987) and Boone and Hynes (in press) has provided some evidence that sediments in this block may have been deposited on thinned continental crust. As mentioned previously the Hellancourt volcanics of the Labrador Trough s.s. have petrochemical characteristics intermediate between continental tholeiite and MORB (Boone, 1987) which is compatible with eruption on thinned crust. When palinspastically restored to their pre-deformation position, these volcanics are located to the east of the gneiss- cored antiforms of the LRLMB. The presence of volcanics and deep -water sediments is consistent with a continental rise origin for the block.

In contrast, the eastern two blocks consist of thick sequences of immature clastic metasediments and possible pyroclastics. Although the Lac Gabriel and Lac Berthet blocks each have distinctive lithological features, their depositional environments appear to have been fairly similar, and they are tentatively considered correlative.

The lithological features of these two blocks, such as quartz-rich and arkosic sediments, epiclastic amphibolites and possible pyroclastics, are compatible with deposition in a slope-shelf environment on a continental margin. The

predominance of gneissic metasandstones and arkosic rocks favours a continental sedimentary source (Dickinson, 1980) but whether these metasediments were deposited on continental crust is uncertain. If the gneissic nappe in the northern section of the Lac Berthet block is Archean, it may represent their overthrust basement.

Although there has been no development of a formal stratigraphy for the area, parts of it may be correlated to other rock units in the Trough and northern Quebec and Labrador. The most obvious similarity is found between the rocks of the LRLMB and a belt of schistose metasediments and metavolcanics found in the hinterland of the Central Labrador Trough. The belt is known as the Laporte schists or the Laporte "Group" (Dimroth et al., 1971; Taylor, 1979; Wardle and Bailey, 1981). The rocks of the belt have been interpreted as the metamorphosed equivalents of a deep basinal shale-greywacke sequence which was subjected to episodic shallowing. These rocks have been correlated with the upper parts of the Knob Lake Group of the Kaniapiskau Supergroup.

Work in the western parts of the LRLMB at the latitude of the study area (Moorhead and Hynes, 1986) has shown that the rocks of the area are similar to those of the Labrador Trough s.s to the west and are probably correlative with parts of the Kaniapiskau Supergroup. These correlations and suggestions that volcanics of the Hellancourt formation may have originated a considerable distance to the east of their present location (Boone and Hynes, in press) indicate that the rocks of the LRLMB, and the Laporte

"Group" in general, may be distal equivalents of the Trough supercrustal succession, which were deposited on a continental rise.

The rocks of the LGB and LBB on the other hand, exhibit no obvious similarities to rocks of the Kaniapiskau Supergroup. Although the overall lithologies of the blocks have some similarities to those of the Lake Harbour Group of northern Labrador and southern Baffin Island (i.e. mainly paragneiss, metasandstone and amphibolite; Taylor, 1979), there is not enough evidence to make a correlation.

6.2.2 Structural Geology

Although, as shown in Chapter 3, the study area has been polydeformed, it is in general structurally simple. The following paragraphs provide a brief summary of the major structural features.

The main structural element over the entire area is a well defined foliation formed during the first phase of deformation. Two distinct styles of later folds deform this foliation and are assumed to represent two later events (D_2 and D_3). The second phase of deformation produced a spaced crenulation in some rocks of the LRLMB.

The area is cut by three major faults. The earliest is the Lac Turcotte Fault which has been assigned to D_1. The Lac Pingiajjulik Fault has features suggesting that it was active syn-to-post D_2 and pre-D_3. The Lac Olmstead Fault was determined

104

to be syn to post-metamorphic.

The overall structural features of the study area suggest a history of major compressional shortening during the Labrador Trough Orogeny. The presence of a major S_1 foliation and the accompanying emplacement of basement above the supracrustal rocks indicate that D_1 was accompanied by major shortening. If, as postulated by Perreault et al. (1987), M_2 was the result of extensive overthrusting during D_3, then D_3 was also a major shortening event. Wardle et al. (1987) suggest that deformation in the central zone of the Labrador Trough Orogen (which includes the study area) was controlled by transpression. Some evidence for strike slip motion has been observed on the LOF, but elsewhere no evidence is observed. It is possible that transpression controlled deformation in the region, but this has not been demonstrated in the study area.

One of the interesting features of the study area is the heterogeneous imprint of D_3 deformation. As mentioned in Chapter 3, D_3 is the major deformation event in the Labrador Trough s.s. In the study area however, D_3 was the least intense deformation (in terms of folding and production of foliation). There are several possible explanations for this relative lack of intensity. The most probable reason is that by the time of D_3 deformation the rocks of the area had become sufficiently hardened (through incresaed crystallinity) to resist major deformation, and simply transmitted the stress to the west. A second mechanism may also have been in effect. If the D_3 event

was restricted to upper levels of the crust, then the rocks of the study area (which were at deeper crustal levels than those in the west) would have escaped major deformation.

6.2.3 Metamorphism

As discussed above (Chapter 4) parts of the area were affected by two metamorphic events, one at 1830 and one at 1790 Ma. Evidence for the early metamorphism (M_1) has been found only in the Lac Gabriel and Lac Berthet blocks, mainly in the form of relict Opx-bearing assemblages and garnet zoning profiles (Perreault et al., 1988). Metamorphic grades for this event reached granulite facies in the LBB and upper amphibolite facies in the LGB. The assemblages of this event were extensively overprinted during M_2, which occurred simultaneously in all three blocks of the study area (Perreault et al., 1988).

Because M_1 was so thoroughly overprinted by M_2, little is known about pressure and temperature conditions during this event. P and T conditions during M_2 can, however, be estimated using geothermobarometry. Using a variety of calibrations for several assemblages, pressure and temperature conditions have been estimated for peak metamorphism, and in some case for subsequent retrograde re-equilibration. Retrograde assemblages give similar results across the area, regardless of the geothermometer/geobarometer used. Temperatures range from 520 to 600°C. Pressures are somewhat more erratic, but for the most part are restricted to between 6 and 7 kbar. Peak metamorphic

conditions (at least in the study area, see Chapter 4) are more variable. Core-matrix results for the LRIMB are between 520 and 550°C and 6 and 6.5 kbar, but these are not thought to represent peak conditions (see Chapter 4). P-T data are sparse for the LGB, but there seems to be an increase from 650 to 750°C from the center of the block to its eastern limit. No reliable pressure results are available for this block. Core-matrix results for Gt-Bi pairs in the LBB range from 680 to 850°C, while Gt-Hb results are more consistent at approximately 750°C. Pressures for this block are quite variable, but rutile bearing assemblages give GRIPS pressures of 7 kbar, in good agreement with garnet-aluminosilicate-plagioclase-quartz and GRAIL results of 6.3 and 7.0 kbar respectively.

The P-T paths constructed from geothermometry results are relatively uniform in slope, and are roughly parallel to the Ky-Sill phase boundary (Holdaway, 1971). The paths are similar to those calculated and observed for the uplift and erosion of a tectonically thickened pile (e.g. Allbarede, 1976, Hodges and Royden, 1984; England and Thompson, 1984).

6.2.4 Geological History

The relative timing features and events described above can be used to outline the geological history of the study area, with available isotopic dating providing some control on the timing of events (see Chapters 2,4 and 5 for sources of dates). This history is depicted graphically in Figure 21.

Geological History

Deformation Event	Faults	Intrusions	Metamorphism
D1	LTF		
		LGC ca. 1840	
D2	LGC Fault		M1 Metamorphism ca. 1830
	LPF		
D3			
		Pegmatites	M2 Metamorphism ca. 1790
	LOF	1775	
		Diabase ca. 1200	

all dates Ma Bp.
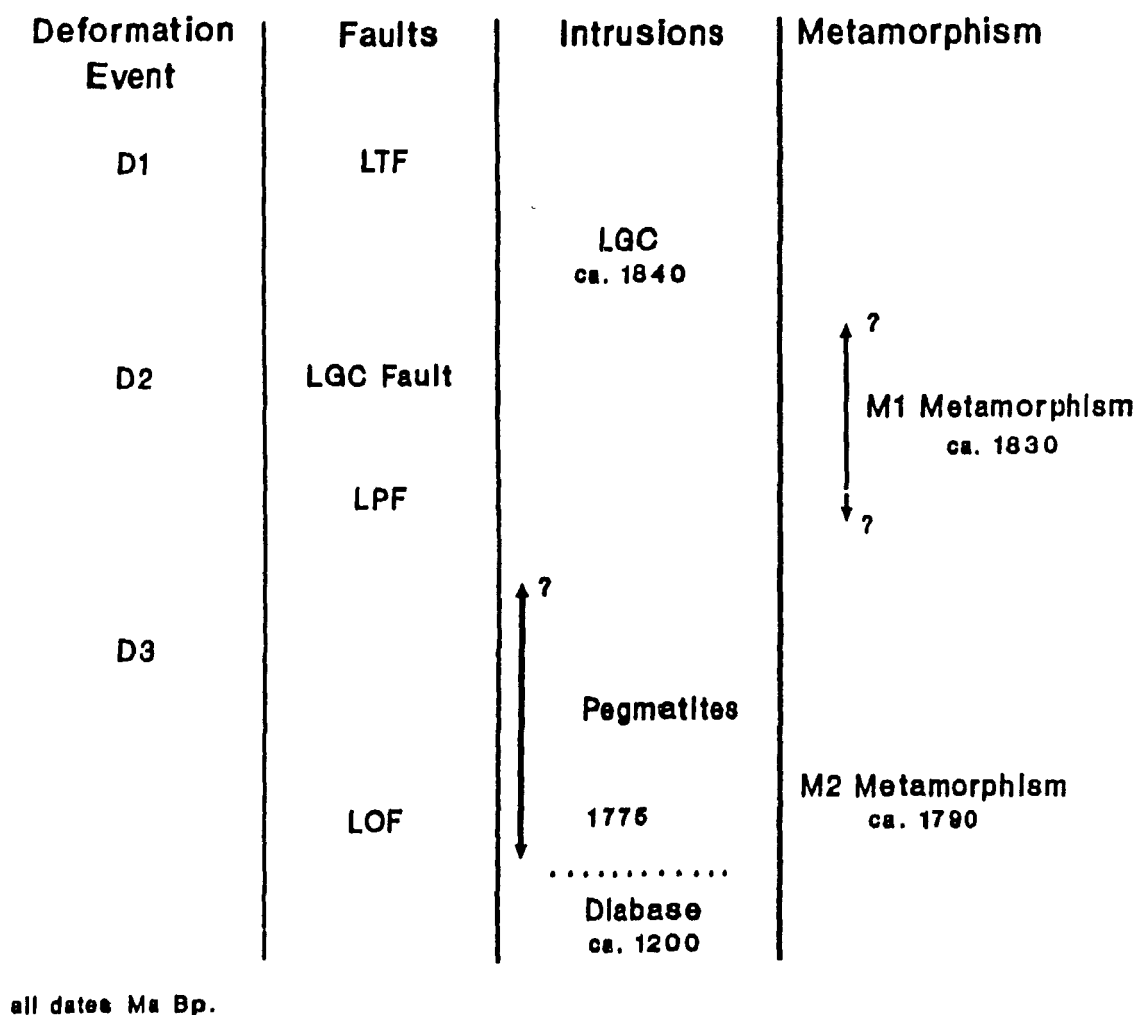
Figure 21. Graphical representation of geological history of study area.

108

After the deposition of the supracrustal rocks, the first recognized event in the area was the D_1 deformation, during which 1) the main foliation was produced, 2) basement was placed above cover in the LBB and 3) movement occurred on the Lac Turcotte Fault. The next event which occurred was the intrusion of the Lac Gabriel complex and associated intrusive rocks at about 1845 to 1840 Ma. As related in Chapter 2, field evidence indicates that the mafic intrusives were emplaced prior to the granodioritic and tonalitic rocks.

At about 1830 to 1833 Ma, peak conditions of the M_1 metamorphism were reached in the LBB and LGB. D_2 occurred at some time after M_1 with attendant shearing of the southern edge of the LGC. Motion on the LPF occurred during or after D_2. The restriction of granulite facies assemblages to the east side of this fault suggests that their presence is somehow associated with this fault.

The next event was D_3 deformation which had a variable effect on various parts of the study area. Deformed pegmatite veins in the area indicate that they were intruded before D_3 in the LBB and LGB.

Peak M_2 metamorphic conditions in all three blocks were reached at some point after D_3 (ca. 1790). Pegmatite intrusion continued for at least 15 m.y. after this (until 1775 Ma).

Dextral strike-slip faulting on the LOF occurred after peak metamorphism, but before the rocks had time to cool significantly. The final event in the area was the intrusion of

a series of Neohelikian diabase dykes and sills.

6.2.5 Interpretation

Although the data presented above and in the previous chapters do not imply any specific tectonic environment for the study area, they do provide some constraints which must be taken into account in any proposed model.

There are several features of the history which are of major importance to an interpretation of tectonic environment. These are 1) the early LTF which juxtaposed blocks of highly contrasting lithology, 2) the presence of a suite of syntectonic calc-alkaline, Cordilleran "I"-type granitoids with volcanic arc granitoid affinities (see Chapter 5) and 3) syn and post-tectonic metamorphic events.

The origin of the granitoids is critical to any interpretation. If they are mantle derived, the LBB and LGB may represent a subduction-related arc terrain. If this is the case, then questions of when subduction occurred and what was subducted arise. The presence of the D_1 LTF which juxtaposes rocks of highly different origin suggests some possibilities.

A Proterozoic suture has long been postulated somewhere in the hinterland of the Labrador Trough (cf. Gibb and Walcott, 1971; Dewey and Burke, 1973.) The presence of an early fault separating contrasting rock types would appear to fill the requirements of such a suture. The timing of the fault is also suitable. The strong S_1 found throughout the area would require a

major deformation event to produce it. If the LTF represents the suture of such a collision then its timing is also consistent with the appearance of arc-related plutonic rocks after D_1 and before D_2. The presence of the granitoids would indicate that subduction with attendant plutonism occurred sometime after collision. The presence of a suture zone on this fault would imply east directed subduction of the LRLMB which, as suggested earlier, may have been deposited on thin continental crust.

Although at first glance this may be appear to be a satisfactory interpretation for the area, there are some problems. The first is the size of the igneous complex, which is quite small in comparison with arcs developed above more modern subduction zones. This is not a major problem, since it is possible that greater volumes of granitoid rocks exist at depth, or that these complexes represent the eroded roots of a much larger complex.

A more serious problem with this interpretation is the location of the plutonic rocks with respect to the LTF. In more recent examples of subduction-related magmatism, the arc is generally located 100 to 200 km from the arc trench (Dickinson, 1971, 1975). In this area, however, the distance between the postulated suture and the magmatic rocks is between 5 and 10 kilometers. It is possible that these rocks are only a small part of the complex. Recent work (van der Leeden et al., 1987) has shown that the Central Labrador Batholith approximately 100 km to the east consists of calc-alkaline "I" type granitoids with

111

volcanic arc granitoid affinities. The size of this batholith and its distance from the postulated suture are more like those for modern arc complexes.

An alternative explanation for the presence of the LGC is suggested by the close temporal and spatial relationships between it and the LTF (See Figs. 4 and 21). If the LTF reflects large scale westward thrusting, the rocks on the lower plate of the thrust may have experienced significant temperature increases as geotherms re-equilibrated to new, deeper conditions. Thermal modeling by England and Thompson (1986) has shown that under some conditions, overthrusting may raise temperatures in the lower plate enough to promote melting of amphibolitic rock, giving rise to calc-alkaline "I"-type magmas. If this process occurred in response to thrusting on the LTF then the subsequently generated magmas may have risen into the upper plate of the thrust.

This model is also attractive in that it may explain the M_1 metamorphism in the LGB and LBB. If these rocks were brought up along the LPF, the sudden, virtually isothermal pressure drop may have been responsible for the metamorphic event.

The main problem with this model is the VAG affinity of the magmatic rocks in the LGC, which would suggest some mantle component. Pearce et al. (1984) however, suggest that there may be some difficulties in applying this type of tectonic discrimination scheme to Precambrian rocks.

Although it is not possible to chose between these models, they have some points in common. The first is that the rocks of

the LRLMB, which show affinities to those of the LT, were juxtaposed with the rocks of the LGB and LBB early in the history of the area. Whether the Lac Gabriel and Lac Berthet Blocks represent exotic blocks (i.e. the LTF is a suture) or are simply an uplifted portion of the eastern margin of the Labrador Trough is uncertain. The second common feature of the models is that intrusion of the igneous complexes occurred in response to motion on the LTF. As suggested above the melting may be the result of magmatism above a subduction zone or simply due to thermal re-equilibration in response to overthrusting.

A final part of this discussion is more regional in scope and deals with the suitabiltiy of published models for the development of the Labrador Trough Orogen in light of data from the study area and the Labrador segment in general. As reviewed in Chapter 1 there are three main types of model for the development of the orogen. Early models invoked basement remobilization in a Himalayan-type continental collision (Dewey and Burke, 1973; Kearey, 1976). In 1981 Dimroth (1981) presented a model in which subsidence of an ensialic basin and subsequent A-type subduction were the result of lithospheric delamination. The last types of model are those in which the Labrador Trough Orogen is envisioned as analogous to an Andean-type continental margin (Thomas and Kearey, 1980; van der Leeden et al., in press)

The model presented by Dimroth has several deficiencies, not with respect to the study area, but in terms of the entire Labrador Segment. First, this model does not explain the

eastward-directed thrusting and deformation observed at the Nain-Churchill boundary (Morgan, 1975). The model also does not explain the presence of the 500 km long early Proterozoic batholith observed in the central parts of the orogen (Taylor, 1979; van der Leeden et al., in press), the apparent absence of which was one of the reasons for Dimroth's objection to a plate tectonic origin for the Trough. One of the main reasons for the problems with this model is that it is based mainly on the rocks of the Labrador Trough s.s., rather than on the hinterland itself which has the potential to provide more information on the post-depositional stages of the orogen.

Models which invoke plate tectonic processes, on the other hand, are more successful in explaining features of the orogen. Modern tectonic processes involving continents have two stages: 1) an initial stage entailing subduction of oceanic crust beneath a continent (e.g. Peruvian Andes) and docking of island arcs with continental crust and 2) a terminal stage in which all oceanic crust has been subducted and continents on either side of the former ocean basin collide. A first-stage model can explain such features as the calc-alkaline "I"-type Central Labrador batholith and has been proposed by Thomas and Kearey (1980) and van der Leeden et al. (in press). It is obvious, however that the Labrador Trough Orogeny has advanced to its terminal stage, since it is flanked on either side by stable cratons (i.e Superior and Nain Provinces). A modern example of a terminal continental collision is the Himalayan orogen, which has many

similarities to the Labrador Trough orogen. The Himalayan orogen is the result of a terminal collision between the Indian and Asian continents after the subduction of the intervening oceanic crust (Tethys) and at least one island arc continent collision in the western Himalayas (i.e. Kohistan arc, Coward et al., 1986) During the subduction of the intervening oceanic crust the leading edge of the Asian plate is believed to have resembled an Andean type margin (Allegre et al., 1984).

On the largest scale, the orogens are similar in that both contain a highly deformed and metamorphosed core flanked on either side by stable cratons. There are similarities on a smaller scale as well. The Labrador segment has a distinct asymmetry, with distinct fault bounded lithotectonic domains occurring parallel to the borders of the orogen. Almost all of these domains have rough analogs with different portions of the Himalayan orogen. Moving from west to east these zones are: 1) a low grade autochthonous zone, equivalent to the miogeoclinal portion of the Trough. 2) a foreland fold and thrust belt. 3) A zone of reworked basement and supracrustals analogous to the LRIMB, 4) A metamorphosed imbricate zone possibly analogous to the Lac Gabriel and Lac Berthet blocks and 5) A long line of calc-alkaline, "I"-type batholiths (e.g. the Kohistan, Ladakh and Gangdise batholiths (Searle et al., 1987)) which are believed to have origins on an Andean type margin and are mainly post tectonic (Coward et al., 1987). These are analogous to the rocks of the Central Labrador batholith, which are also late tectonic,

calc-alkaline "I"-types (van der Leeden et al., in press).

Another similarity between the Himalayan orogen and the Labrador segment is also observed. A late tectonic Barrovian metamorphism is observed south of the Indus or Southern suture with grade increasing to the north (or towards the suture) (Le Fort, 1986, Coward et al., 1986) This metamorphism is believed to be due to overthrusting (Le Fort, 1986). This is analogous to the late Barrovian event described by Perreault et al., (1987), which is also believed to be the result of overthrusting.

There are some features of the Himalayan orogen which have no analogs in the Labrador Segment. The most notable is the absence of ophiolite sequences and high-pressure metamorphic rocks. Ophiolites occur throughout the length of the Himalayan orogen, but are generally restricted to the hanging walls of the Indus and Southern sutures (cf. Allegre et al., 1984; Coward et al., 1987). Blueschists and other high-pressure metamorphic rocks are found immediately south of the Indus suture in central India (Le Fort, 1986) and the Southern suture in Pakistan (Coward et al., 1987) Another common feature which is absent in the Labrador Segment is bodies of post-collisional leucocratic granitoids, which are widespread south of the Indus suture (Le Fort, 1986). No analogs are known for any of these features in the Labrador Segment. The erosion of some 20 to 30 km of overlying rock (based on paleopressures for the LBB and assuming an average rock density of 2700 Kg m^{-3}) may explain why some of these features are absent (e.g. high-level leucocratic granites) but does not

116

explain the lack of ophiolites, which in most published cross-sections extend to considerable depth. Modeling by Hynes (1982, 1987) predicts that in Proterozoic orogens, blueschist metamorphic rocks and ophiolite complexes should be rare, but ophiolites have been described in the early Proterozoic Cape Smith Belt (Scott et al., 1988; St-Onge et al., 1988) and in Proterozoic rocks in Norway. The lack of blueschist facies rocks could be explained by the age of the orogen. Work by England and Richardson (1977) has shown that age is a major factor in the preservation of blueschists. These authors suggest that thermal relaxation and erosion increase temperatures within blueschist terrains and tend to convert them to greenschist and amphibolite facies rocks. Modeling by these authors shows that for any reasonable range of parameters the probability of preserving blueschist facies rocks goes to zero within 500 million years.

The problem with comparing the features of two orogenies is that in all likelihood no orogeny has ever proceeded in the same manner as another, and therefore there are bound to be differences. The above discussion shows that the Labrador Segment has some similarities with the Himalayan orogen and that it (the Himalayan Orogeny) is probably the best modern analog for Hudsonian tectonism in the Labrador Trough Orogeny.

6.3 Conclusions

The structural and metamorphic features of the three blocks

117

which make up the study area are the result of the early Proterozoic Hudsonian Orogeny. The rocks of the LRLMB are correlative to those of the Laporte "Group" and are believed to represent distal equivalents of the Kaniapiskau Supergroup which were deposited on a continental rise. The rocks of the LBB and LGB are lithologically distinct from those of the LRLMB, but are considered to be correlative with each other. These two blocks are considered to be the result of deposition on a continental slope/shelf environment, with a continental sediment source.

The structural geology of the three blocks is similar, all showing the effect of three deformation episodes. The early event produced the main foliation throughout the area and rare rootless intrafolial folds. The second event produced common mesoscopic and macroscopic tight-to-open folds with a rare axial planar cleavage, while D_3 produced macroscopic upright folds. The heterogeneous imprint and relative lack of intensity of D_3 (compared with the Labrador Trough s.s.) are believed to be the result of the more crystalline nature of the rocks of the study area during D_3. In general deformation in the area involved major shortening and probable southwest transport.

The LBB and LGB show evidence for an early metamorphic event of granulite and upper amphibolite facies. A later event which occurred simultaneously throughout the region overprinted much of the early event. Geothermobarometric studies indicate that peak metamorphic conditions for the second event were approximately 750 °C and 7 kbar, slightly below granulite facies,

although minor granulite facies assemblages have been observed. The lack of migmatization in the area is believed to be the result of Ca-rich bulk rock compositions. P-T paths prepared from geothermobarometric results have forms similar to those predicted for tectonic crustal thickening.

Geochemical and petrological studies of the amphibolites of the Lac à Foin area and the granitoids of the LGC have provided information about their origin. The LGC rocks are calc-alkaline, Cordilleran "I"-type granitoids, with volcanic arc granitoid affinities on trace element discrimination plots. The amphibolites are believed to represent metamorphosed basalts and are geochemically quite similar to the Hellancourt Volcanics of the Labrador Trough, which are low-K tholeiites transitional between P-MORB and continental tholeiites.

The juxtaposition of the LRLMB with the other blocks occurred early in the orogeny along the LTF. The temporal and spatial relationships between the juxtaposition and intrusion of the LGC suggest some sort of causal relationship between them. Possible models are either subduction magmatism related to subduction (i.e. LGB is a magmatic arc), or simply magmatism in response to overthrusting along the LTF. The lack of correlation between the rocks of the LBB and LGB and the LRLMB (and the Labrador Trough s.s.) suggest that they may be exotic blocks transported along the LTF. Alternatively, they could simply be an uplifted portion of the eastern margin of the Labrador Trough.

Comparison of the Labrador Segment with modern orogenies

119

suggests that the Himalayan orogeny is probably the best modern analog for the Hudsonian orogeny in this region, although small differences do exist.

6.4 Suggestions for Further Work

Of any projects proposed for the area, the most important in terms of overall geology would be more detailed mapping of the areas east of the Koksoak River. Although all of this area is mapped at 1:250,000 (Taylor, 1979) more detailed mapping would provide much needed information on the structure and lithology of the area and possibly allow the development of a much more complete tectonic interpretation for the area.

Also important for further study is a more detailed examination of the syntectonic intrusives of the area. Such a study should deal with petrological and geochemical aspects of various phases of the three complexes with the specific aim of determining where and how they were generated. (The high metamorphic grades of the area could make this very difficult).

A final area where further work would be beneficial are the "basement" gneisses of the Lac Berthet block. The most important work would be isotopic dating of these rocks to verify their assumed Archean age. A more detailed study of the structural geology of the contact between these rocks and the supracrustals would also be beneficial in determining the mechanism by which they have been placed above supracrustal rocks.

120

References

Ahmedali, T. 1983. XRF procedures circular # 1. Department of Geological Sciences, McGill University.

Allbarede, F. 1976. Thermal models of post-tectonic decompression as exemplified by the Haut-Allier granulites (Massif Central, France). Bulletin de la Societé de Geologié Francais. 17, pp. 1023-1032.

Allegre, C. J. and 34 others, 1984. Structure and evolution of the Himalaya-Tibet orogenic belt. Nature, 307, pp. 17-22.

Anderson, D. E. and Olimpio, J. C., 1977. Progressive homogenization of metamorphic garnets, South Morar, Scotland. Canadian Mineralogist, 15, pp. 205-216.

Atherton, M. P., Sanderson, L. M. 1987. The Cordillera Blanca Batholith: A study of granite intrusion and the relation of crustal thickening to peraluminosity. Geologische Rundschau, 76, pp. 213-232.

Baragar, W. R. A. and Scoates, R. F. J., 1981. The Circum Superior Belt: a Proterozoic plate margin? In Precambrian Plate Tectonics, Edited by A. Kröner. Elsevier, Amsterdam,

pp. 297-230.

Beccaluva, L., Ohnenstetter, D. and Ohnenstetter, M. 1979. Geochemical discrimination between ocean-floor and island-arc tholeiites -- application to some ophiolites. Canadian Journal of Earth Sciences, 16, pp. 1874-1882.

Bergeron, R. 1957. Région de Brochant-de Bonnard, Nouveau Québec. Ministère de Mines Québec, Rapport Préliminaire, 348.

Bohlen, S.R. 1987. Pressure-Temperature-time paths and a tectonic model for the evolution of granulite. Journal of Geology, 95 , pp. 617-632.

Bohlen, S. R. and Liotta, J. J., 1987. A barometer for garnet amphibolites and garnet granulites. Journal of Petrology, 27, pp. 1025-1043.

Bohlen, S. R., Wall, V. J. and Boettcher, A. L., 1983. Geobarometry in Granulites. In Kinetics and equilibria in mineral reactions. Edited by S. K. Saxena. Advances in Geochemistry, 3 , pp 141-171.

Boone, E. 1987. Petrology and tectonic implications of the Hellancourt volcanics, Northern Labrador Trough, Quebec. M.Sc. thesis, McGill University, Montreal, Quebec.

_____ and Hynes, A. 1989. A structural cross section of the Northern Labrador Trough, New Quebec. In Geological Association of Canada Special Volume on the Trans-Hudson Orogen. Edited By J. F. Lewry and M. R. Stauffer. (In press)

Bosdachin, R. 1986. Structural deformation and metamorphism of the Lac à Foin metasediments, Fort Chimo, Quebec. B.Sc thesis, McGill University, 20 pages + figures.

Carmichael, D. M. 1978. Metamorphic bathozones and bathograds: a measure of the depth of post-metamorphic uplift and erosion on the regional scale. American Journal of Science, 278, pp. 769-797.

Chappell, B. W. 1978. Granitoids from the Moonbi District, New England Batholith, Eastern Australia. Journal of the Geological Society of Australia, 25, pp. 267-283.

Chipera, S. J. and Perkins, D. III 1988. Evaluation of biotite-garnet thermometers: Application to the English River Subprovince, Ontario. Contibuticns to Mineralogy and Petrology, 98, pp. 40-48.

Coward, M. P., Windley, B. F., Broughton, R. D., Luff, I. W., Petterson, M. G., Pudsey, C. J., Rex, D. C., Asif kahn, M.

1986. Collision tectonics in NW Himalayas. In Collision Tectonics, Edited by M. P. Coward and A. C. Ries. Geological Society Special Publication, no. 19, 203-219.

_____, Butler, R. W. H, Asif Kahn, M., Knipe, R. J., 1987. The tectonic history of Kohistan and its implication for Himalayan structure. Journal of the Geological Society of London, , pp. 377-391.

Currie, K. L., 1974. A note on the calibration of the garnet-cordierite geothermometer. Contributions to Mineralogy and Petrology, 44, pp. 35-49.

Dahl, P. S. 1979. Comparative geothermometry based on major-element and oxygen isotope compositions in Precambrian metamorphic rocks from southwestern Montana. American Mineralogist. 64, pp. 1280-1293.

Dewey, J. F. and Burke, K. C., 1973. Tibetan, Variscan and Precambrian basement reactivation: products of continental collision. Journal of Geology, 81, pp. 683-692.

Dickinson, W. R. 1971. Plate tectonic models of geosynclines. Earth and Planetary Science Letters, 10, pp 165-174.

_____, 1975. Potash-depth (K-h) relations in continental

margin and intra-oceanic magmatic arcs. Geology, **3**, pp 53-56.

_____ 1980. Plate tectonics and key petrological associations. <u>In</u> The Continental crust and its mineral deposits. <u>Edited by</u> D. W. Strangway. Geological Association of Canada, special paper 25, pp. 341-360.

Dimroth, E., 1970. The evolution of the Labrador Geosyncline. Geological Society of America Bulletin, **81**, pp. 2717-2742.

_____, 1971. The evolution of the central segment of the Labrador Geosyncline, Part II: the ophiolite sequence. N. Jh. Palont. Abh., **137** , pp 209-248.

_____, 1972. The Labrador Geosyncline revisited. American Journal of Science, **272**, pp. 487-506.

_____ 1978. Labrador Trough area (54°30' - 56°30'). Ministere des Richesses Naturelles, Quebec. Rapport Geologique 193, 346 p.

_____ 1981. Labrador Geosyncline: a type example of early Proterozoic cratonic reactivation. <u>In</u> Precambrian Plate Tectonics. <u>Edited by</u> A. Kröner. Elsevier, Amsterdam, pp. 331-352.

_____, Baragar, W. R. A., Bergeron, P. and Jackson, G. D., 1970. The Filling of the Labrador Trough. In Basins and Geosynclines of the Canadian Shield, Edited by A. J. Baer. Geological Survey of Canada, Paper 70-40, pp. 45-142.

Dimroth, E. and Dressler, B. 1978. Metamorphism of the Labrador Trough. In Metamorphism in the Canadian Shield, Geological Survey of Canada, paper 78-10, pp. 215- 236.

Dymek, R. F., 1983. Titanium, aluminum and interlayer cation substitutions in biotite from high-grade gneisses, West Greenland. American Mineralogist, 68, pp. 880-899.

England, P. C. and Richardson, S. W. 1977. The influence of erosion on the mineral facies of rocks from different metamorphic environments. Journal of the Geological Society of London, 134, pp. 201-213.

_____ and Thompson, A. 1984. Pressure-temperature - time paths of regional metamorphism I. Heat transfer during the evolution of regions of thickened continental crust. Journal of Petrology, 25, pp. 894-928.

_____ 1986. Some thermal and tectonic models for crustal melting in continental collision zones. In. Collision tectonics. Edited by M. P. Coward and A. C. Ries.

Geological Society Special Publication No. 19, pp. 83-94.

Ellis, D. J. and Green, D. H., 1979. An experimental study of the effect of Ca upon garnet-clinopyrcxene Fe-Mg exchange equilibria. Contributions to Mineralogy and Petrology, 71, pp. 13-22.

Essene, E. J., 1982. Geologic thermometry and barometry. In characterization of metamorphism through mineral equilibria. Edited by J. M. Ferry, Reviews in Mineralogy, 10, Mineralogical society of America, Washington, D. C. pp. 153-206.

Ferry, J. M. and Spear, F. S., 1978. An experimental calibration of partitioning of Fe and Mg between biotite and garnet. Contributions to Mineralogy and Petrology, 66, pp. 113-117.

Floyd, P. A. and Winchester, J. A. 1975. Magma type and tectonic setting discrimination using immobile elements. Earth and Planetary Science Letters, 27, pp. 211-218.

Frarey, M. J. and Duffell, S. 1964. Revised stratigraphic nomenclature for the central part of the Labrador Trough. Geological Survey of Canada, paper 64-25, 13 p.

Fraser, A. A., Heywood, W. W. and Mazurki, M. N., 1978.

Metamorphic map of the Canadian Shield. Geological Society of Canada, Map No. 1475A.

Ganguly, J. and Saxena, S. K. 1984. Mixing properties of aluminosilicate garnets: constraints from natural and experimental data and applications to geothermometry and geobarometry. American Mineralogist, 69, pp. 88-97.

Gélinas, L. 1958. Thevenet Lake area, (east half) New Quebec. Quebec Department of Mines, Preliminary report 363, 8 p.

_____ 1959. Region du Lac Gabriel (partie est), et la region de Fort Chimo (partie ouest), Nouveau Quebec. Ministere des Mines, Quebec, Rapport preliminaire 407.

_____ 1960. Region du Fort Chimo (partie est), Nouveau Quebec. Ministere des Mines, Quebec. Rapport preliminaire 418, 5 p.

_____ 1965. Geologie de la region de Fort Chimo et des Lacs Gabriel et Thevenet, Nouveau Quebec. D.Sc. thesis, Universite Laval, Quebec, 212 p.

Ghent, E. D., 1976. Plagioclase, garnet, Al_2SiO_5, quartz: a potential geothermometer-geobarometer. American Mineralogist. 61, pp. 710-714.

Gibb, R. A., 1983. A model for suturing of Superior and Churchill plates: an example of double indentation tectonics. Geology, 11, pp. 413-417.

Gibb, R. A. and Wolcott, R. I., 1971. A Precambrian suture in the Canadian Shield. Earth and Planetary Science Letters, 10, pp. 417-422.

Glikson, A. Y. 1980. Precambrian sial-sima relations: evidence for earth expansion. Tectonophysics, 63, pp. 193-234.

Goulet, N., Gariepy, L., Mareschal, J.-C. and Machado, N. 1987. Structure, geochronology, gravity and tectonics of the Northern Labrador Trough. Geological Association of Canada and Mineralogical Association of Canada, Joint Annual Meeting, Program with Abstracts, p. 48.

Graham, C. M. and Powell, R. 1984. A garnet-hornblende geothermometer: calibration, testing and application to the Pelona schist, Southern California. Journal of Metamorphic Geology, 2, pp. 1-13

Grant, J. R. and Weiblen, P. W. 1971. Retrograde zoning in garnet near the second sillimanite isograd. American Journal of Science, 270, pp. 281-296.

Harris, N. B. W., Pearce, J. A. and Tindle, A. G. 1986.
Geochemical characteristics of collision-zone magmatism.
In Collision tectonics. Edited by M. P. Coward and J. A.
Ries. Geological Society special publication no. 19, pp.
67-81.

Hine, R., Williams, I. S., Chappell, B. W., and White, A. J. R.
1978. Contrasts between I-type and S-type granitoids of the
Kosciusko Batholith. Journal of the Geological Society of
Australia, 25, pp. 235-247.

Hodges, K. V. and Spear, F. S. 1982. Geothermometry,
geobarometry and the Al_2SiO_5 triple point at Mt. Moosilauke,
New Hampshire. American Mineralogist, 67, pp. 1118-1134.

_____ and Royden, L. 1984. Geologic thermobarometry of
retrograded metamorphic rocks: an indication of the uplift
trajectory of a portion of the northern Scandinavian
Caledonides. Journal of Geophysical Research, 89, pp. 7077-
7090.

_____ and McKenna, C. V. 1987. Realistic propagation of
uncertainties in geologic thermobarometry. American
Mineralogist, 72, pp. 671-680.

Hoffman, P. F. 1980. Wopmay Orogen: a Wilson cycle of early Proterozoic age in the northwest of the Canadian Shield. In The Continental crust and its mineral deposits. Edited by D. W. Strangway. Geological Association of Canada, special paper 25, pp. 523-549.

_____ 1981. Autopsy of Athapuscau Aulocogen: a failed arm affected by three collisions. In Proterozoic basins of Canada. Edited by F. H. A. Campbell. Geological Survey of Canada, paper 81-10, pp. 97-102.

_____ 1987. Early Proterozoic foredeeps, foredeep magmatism and Superior-type iron-formations of the Canadian Shield. In Proterozoic Lithospheric Evolution, Edited by A. Kröner. American Geophysical Union, Geodynamics series, 17, pp. 85-98.

_____, 1988. United Plates of America, the birth of a craton: early Proterozoic assembly and growth of Laurentia. Annual Review of Earth and Planetary Sciences, 16, pp.543-603.

Holdaway, M. J. 1971. Stability of andalusite and the aluminum silicate phase diagram. American Journal of Science, 271, pp. 97-131

_____ and Lee, S. M. 1977. Fe-Mg cordierite stability

in high-grade pelitic rocks based on experimental, theoretical and natural observations. Contributions to Mineralogy and Petrology. 63 pp.175-198

Hynes, A. 1978. Early recumbent folds in the northeastern part of the northern Labrador Trough. Canadian Journal of Earth Sciences, 15, pp. 245-252.

_____, 1982. Stability of the oceanic tectosphere - a model for early Proterozoic intracratonic orogeny. Earth and Planetary Science Letters, 61, pp. 333-345.

_____, 1987. Back-arc spreading in the Proterozoic a theoretical approach. Precambrian Research, 36, pp. 189-199.

_____ and Francis, D. M. 1982. A transect of the early Proterozoic Cape Smith Fold Belt, New Quebec. Tectonophysics, 88, pp. 23-59.

Indares, A. and Martignole, J. 1985. Biotite-Garnet geothermometry in the granulite facies: influence of Ti and Al in biotite. American Mineralogist, 70, pp. 272-278.

Irvine, T. N. and Baragar, W. R. A. 1971. A guide to the chemical classification of common volcanic rocks. Canadian Journal of Earth Sciences, 8, pp. 523-548.

Jackson, G. D. and Taylor, F. C., 1972. Correlation of major Aphebian rock units in the Canadian Shield. Canadian Journal of Earth Sciences, 9, pp. 1650-1669.

_____ and Morgan, W. L., 1978. Precambrian metamorphism on Baffin and Bylot Islands. In Metamophism in the Canadian Shield, Edited by J. A. Fraser and W. W. Haywood. GSC paper 78-10, pp. 249-267.

Janardhan, A. S., Newton, R. C. and Essene, E.J. 1982. The transformation of amphibolite facies gneiss to charnockite gneiss in Southern Karnataka and Northern Tamil Nadu, India. Contributions to Mineralogy and Petrology, 79, pp. 130-149.

Kearey, P., 1976. A regional structural model of the Labrador Trough, Quebec from gravity studies, and its relevance to continental collision in the Precambrian. Earth and Planetary Science Letters, 28, pp. 371-378.

Koziol, A. M. and Newton, R. C. 1988. Redetermination of anorthite breakdown and improvement of the plagioclase-garnet-aluminosilicate-quartz barometer. American Mineralogist, 73, pp. 216-224.

Kröner, A. 1981. Precambrian plate tectonics. (editor).

Elsevier, Amsterdam, 781 p.

Lasaga, A. C., Richardson, S. M. and Holland, H. C., 1977. Mathematics of cation diffusion and exchange between silicate minerals during retrograde metamorphism. In Energetics of geological processes, Edited by S. K. Saxena and S. Bhattacharji. Springer-Verlag, Berlin, pp. 353-388.

Leake, B. E. 1964. The chemical distinction between ortho and para-amphibolites. Journal of Petrology, 5, pp. 238-254

Le Fort, P. 1986. Metamorphism and magamatism during the Himalayan collision. In Collision Tectonics, Edited by M. P. Coward and A. C. Ries. Geological Society Special Publication, no. 19. pp. 159-172.

LeGallais, C. J. and Lavoie, S. 1982. Basinal evolution of the lower Proterozoic Kaniapiskau Supergroup, Central Labrador Miogeocline (Trough), Quebec. Bulletin of Canadian Petroleum Geology, 30, pp. 150-166.

Lewry, J. F., 1981. Lower Proterozoic arc-microcontinent collisional tectonics in the western Churchill Province. Nature, 294, pp.69-72.

_____ and Sibbald, T. I. I. 1980. Thermotectonic evolution

of the Churchill Province in northern Saskatchewan. Tectonophysics, 68, pp. 45-82.

_____, Stauffer, M. R. and Fumerton, S. 1981. A Cordilleran type batholith belt in the Churchill Province in northern Saskatchewan. Precambrian Research, 14, pp. 277-313.

_____, Sibbald, T. I. I. and Schledwitz, D. C. P. 1985. Variation in the character of Archean rocks in the western Churchill Province and its significance. In Evolution of Archean supercrustal sequences. Edited by L. D. Ayres, P. C. Thurston, K. D. Card and W. Webber. Geological Association of Canada, special paper 28, pp. 239-261.

Loomis, T. P. 1983. Compositional zoning of crystals: a record of growth and reaction history. In Kinetics and Equilibria in Mineral Reactions, Edited by S. K. Saxena, Advances in Geochemistry, 3, pp. 1-60.

Lucas, S. B. and St. Onge, M. R. 1987. Structural and thermal history of a 1.9 Ga thrust-fold belt: Cape Smith Belt, Northern Quebec. Geological Association of Canada-Mineralogical Association of Canada, Joint Annual Meeting, Program with Abstracts, 12, p. 68.

Machado, N., Goulet, N. a..d Gariepy, C. 1987. Evolution of the northern Labrador Trough basement: evidence from U-Pb geochronology. Geological Association of Canada and Mineralogical Association of Canada, Joint Annual Meeting, Program with Abstracts, p. 69.

_____, Perreault, S. and Hynes, A. 1988. Timing of continental collision in the northern Labrador Trough, Quebec: Evidence from U-Pb geochronology. Geological Association of Canada and Mineralogical Association of Canada, Joint Annual Meeting, Program with Abstracts, 13, P. 76.

Martignole, J. and Sisi, J. C. 1981. Cordierite-garnet-H_2O equilibria: a geological thermometer, barometer and water fugacity indicator. Contributions to Mineralogy and Petrology, 77 pp. 38-46

Moorhead, J. and Hynes, A. 1986. Structure and metamorphism of the eastern flank of the Renia gneiss dome. Geological Association of Canada and Mineralogical Association of Canada, Joint Annual Meeting, Program with Abstracts, 11, p. 103.

Morgan, W. C., 1975. Geology of the Precambrian Ramah Group and basement rocks in the Nachvak Fiord - Saglek Fiord area, North Labrador. Geological Society of Canada, Paper 74-54. 42

p.

Newton, R. C., Charlu, T. V., Kleppa, O. J. 1980. Thermochemistry of high structural state plagioclase. Geochemica et Cosmochemica Acta, **44**, pp. 933-941

_____. and Haselton, H. T., Jr., 1981. Thermodynamics of the garnet-plagioclase-Al$_2$SiO$_5$ geobarometer. <u>In</u> Thermodynamics of Minerals and Melts, <u>Edited by</u>: R. C. Newton, A. Navrotsky and B. J. Wood. Springer-Verlag, New York, pp. 129-145.

Pearce, J. A. 1975. Basalt geochemistry used to investigate past tectonic environments on Cyprus. Tectonophysics, **25**, pp. 41-67

_____ and Cann, J. R. 1973. Tectonic setting of basic volcanic rocks using trace element analyses. Earth and Planetary Science Letters, **19**, pp. 290-300.

_____ and Norry, M. J. 1979. Petrogenetic implications of Ti, Zr, Y and Nb variations in volcanic rocks. Contributions to Mineralogy and Petrology, **69**, pp. 33-47.

_____, Harris N. B. W., and Tindle, A. G. 1984. Trace element discrimination diagrams for the tectonic interpretation of granitic rocks. Journal of Petrology,

25, pp 956-983.

Pearce, T. H., Gorman, B. E. and Birkett, T.C. 1975. The TiO_2-K_2O-P_2O_5 diagram, a method of discriminating between oceanic and non-oceanic basalts. Earth and Planetary Science Letters, 24, pp. 419-426.

_____ 1977. The relationship between major element chemistry and tectonic environment of basic and intermediate volcanic rocks. Earth and Planetary Science Letters, 36, pp. 121-132.

Perchuk, L. L. and Lavrent'eva, I. V. 1983. Experimental investigation of exchange equilibria in the system cordierite-garnet-biotite. In Kinetics and Equilibria in Mineral Reactions, Edited by S. K. Saxena, Advances in Geochemistry 3 pp. .xxx

Perkins, D. III, and Newton, R. C., 1981. Charnockite geobarometers based on co-existing garnet-pyroxene-quartz. Nature, 292, pp. 144-146.

_____ and Chipera, S. J. 1985. Garnet- orthopyroxene-plagioclase-quartz barometry: refinement and application to the English River subprovince and the Minnesota River valley. Contributions to Mineralogy and Petrology, 89, pp. 69-80

Perreault, S., Hynes, A. and Moorhead, J. 1987. Metamorphism of the eastern flank of the Labrador Trough, Ungava, Northern Quebec. Geological Association of Canada and Mineralogical Association of Canada, Joint Annual Meeting, Program with Abstracts, 12, p. 80.

_____, Machado, N. and Hynes, A. 1988. Timing$$$ in the NE segment of the Labrador Trough, Kuujjuaq, Northern Quebec. Geological Association of Canada and Mineralogical Association of Canada, Joint Annual Meeting, Program with Abstracts, 13, p. 97.

Phillips, N. G. 1980. Water activity changes across an amphibolite-granulite facies transition, Broken Hill, Australia . Contributions to Mineralogy and Petrology, 75, pp. 377-386.

Pigage, L. C. 1982. Linear regression analysis of sillimanite forming reactions at Azure Lake, B.C.. Canadian Mineralogist 20, pp.349-378.

Piper, J. D. A. 1976. Paleomagnetic evidence for a Proterozoic supercontinent. Philosophical transactions of the Royal Society of London, 280, pp. 469-490.

_____ 1982. The Precambrian paleomagnetic record: the case for a Proterozoic supercontinent. Earth and Planetary Science Letters, 59, pp. 61-89.

Pitcher, W. S. 1983. Granite type and tectonic environment. In Mountain building processes. Edited by K. J. Hsu. Academic Press, London, pp. 19-40.

Poirer, G., Perreault. S., and Hynes A. In Press. The Nature of the eastern boundary of the Labrador Trough near Kuujjuaq, Quebec. To be published in a forthcoming Geological Association of Canada special volume.

Powell, R. 1985. Regression diagnostics and robust regression in geothermometer/geobarometer calibration: The garnet/clinopyroxene geothermometer revisited. Journal of Metamorphic Geology, 3, pp. 231-249.

Pownceby, M. I., Wall, V. J. and O'Neil H. St. C. 1987. Fe-Mn partitioning between garnet and ilmenite, experimental calibration and application. Contributions to Mineralogy and Petrology, 97 pp. 116-126.

Raase, P. 1974. Al and Ti contents of hornblende: Indicators of pressure and temperature of regional metamorphism. Contributions to Mineralogy and Petrology, 45, pp. 231-236.

_____, Raith, M., Ackermand, D. and Lal, R. K. 1986. Progressive metamorphism of mafic rocks fron greenschist to granulite facies in the Dharwar Craton of South India. Journal of Geology, **94**, pp. 261-282.

Ramsay, J. G. 1967. Folding and fracturing in rocks. MacGraw-Hill Book Company, 568 p.

_____ 1980. Shear zone geometry: a review. Journal of Structural Geology, **2**, pp. 83-99.

Sauve, P. and Bergeron, R. 1965. Gerido Lake-Thevenet Lake area, New Quebec. Geological Report no. 104, Quecec Dept. of Natural Resources 110 p.

Saxena, S. K., 1979. Garnet-clinopyroxene geothermometer. Contributions to Mineralogy and Petrology, **70**, pp. 229- 235.

Schreurs, J. 1984. The amphibolite-granulite transition in West Uuisma, SW Finland: A Fluid inclusion study. Journal of Metamorphic Geology, **2**, pp. 327-341.

Scott, D. J., St-Onge, M. R., Lucas, S. B. and Helmsteadt, H. 1988. Oceanic crust preserved in the ca. 1.9 Ga Cape Smith Fold-Thrust Belt, Northern Quebec. Program with Abstracts,

Geological Association of Canada, 13, pp. 110.

Searle, M. P., Windley, B. F., Coward, M. P., Cooper, D. J. W., Rex, A. J., Tingdong, Li, Xuchang, Xiao, Jan M. Q., Thakur, V. C. and Kumar, S. 1987. The closing of Tethys and the tectonics of the Himalaya. G. S. A. Bulletin, 98, pp. 678-701.

Sills, J. D. and Tarney, J. 1984. Petrogenesis and tectonic significance of amphibolites interlayered with metasedimentary gneisses in the Ivrea Zone, Southern Alps, Northwest Italy. Tectonophysics, 107, pp. 187-206.

Simpson, C. and Schmidt, S. M. 1983. Evaluation of criteria to deduce the sense of movement in sheared rocks. Geological Society of America Bulletin, 94, pp. 1281-1288.

Stauffer, M. R. 1984. Manikewan: an early Proterozoic ocean in central Canada, its igneous history and orogenic closure, Precambrian Research, 25, pp. 257-281.

Stephenson, N. C. N., Hensel, H. D. 1979. Intergrown calcic and Fe-Mg amphiboles from the Wongwibinda Complex, N.S.W., Australia. Canadian Mineralogist, 17, pp. 11-23.

Stockwell, C. H. 1963. Third report on structural provinces, orogenies and time classification of rocks of the Canadian

Precambrian Shield. Geological Survey of Canada, Paper
63-17, pp. 125-131.

St-Onge, M. R., Lucas, S. B., Scott, D. J., Begin, N. J.,
Helmsteadt, H. and Carmichael, D. 1988. Thin-skinned
imbrication and subsequent thick-skinned folding of rift fill,
transitional crust and ophiolite suites in the 1.9 Ga Cape
Smith Belt, northern Quebec. Current Research, Part C,
Geological Survey of Canada. Paper 88-1c, pp. 1-18.

Taylor, F. C., 1968. Operation Torngat, Quebec, Newfoundland -
Labrador. Geological Survey of Canada, Report of Activities,
Pt. A, Paper 68-1.

_____, 1969. Reconnaissance geology of part of the
Precambrian Shield, northeastern Quebec and northern
Labrador. Geological Survey of Canada, Paper 68-43.

_____, 1970. Reconnaissance geology of part of the
Precambrian Shield, northeastern Quebec and northern
Labrador, Part 2. Geological Survey of Canada, Paper 70- 24

_____, 1974. Reconnaissance geology of part of the
Precambrian Shield, northern Quebec and Northwest
Territories. Geological Survey of Canada, Paper 74-21.

_____, 1979. Reconnaissance geology of a part of the Precambrian Shield, Northeastern Quebec, Northern Labrador and Northwest Territories. Geological Survey of Canada, Memoir 393, 99 p.

_____, and Skinner, R. 1963. Fort Chimo, New Quebec. Geological Survey of Canada, Paper 63-47, 4 p.

Thomas, M. D. and Kearey, P., 1980. Gravity anomalies, block faulting, and Andean type tectonism in the eastern Churchill Province. Nature, 283, pp. 61-63.

_____, and Gibb, R. A., 1985. Proterozoic plate subduction and collision: processes for reactivation of Archean crust in the Churchill Proince. In Evolution of Archean Supracrustal Sequences, Edited by L. D. Ayres, P. C. Thurston and W. Weber Geological Association of Canada Special paper # 28.

Thompson, A. B. 1976. Mineral reactions in pelitic rocks: II, Calculation of some P-T-x(Fe-Mg) phase relations. American Journal of Science, 276, pp. 425-454

_____ and Algor, J. R. 1977. Model systems for anatexis of pelitic rocks. I: Theory of melting reactions in the system $KAlO_2-NaAlO_2-Al_2O_3-SiO_2-H_2O$. Contributions to Mineralogy and Petrology, 63, pp. 247-269 .

_____ and Tracy, R. J. 1979. Model systems for anatexis of pelitic rocks. II: Facies series melting and reactions in the system CaO-KAlO$_2$-NaAlO$_2$-Al$_2$O$_3$-SiO$_2$-H$_2$O. Contributions to Mineralogy and Petrology, **70**, pp. 429-438

_____ and England, P. C 1984. Pressure-temperature-time of paths of regional metamorphism. II: Their inference and interpretation using mineral assemblages in metamorphic rocks. Journal of Petrology, **25**, pp. 929-955.

_____ and Ridley, J. R. 1987. Pressure-temperature-time (P-T-t) histories of orogenic belts. Philosophical Transactions of the Royal Society of London, **321**, pp. 27-45

Tracy, R. J. 1982. Compositional zoning and inclusions in metamorphic minerals. In Characterization of metamorphism through mineral equilibria. Edited by J. M. Ferry, Reviews in Mineralogy, 10, Mineralogical society of America, Washington, D. C. pp. 355-397

Trzcienski, W. E. 1977. Garnet zoning - Product of a continuous reaction. Canadian Mineralogist, **15**, pp. 250-256.

Turner, F. J. 1981. Metamorphic Petrology: Mineralogical, field and tectonic aspects, 2nd edition. McGraw-Hill Book Company,

524 p.

van der Leeden, J. R., Belanger, M., Danis, D., Girard, R. and Martelain, J. (in press) Lithotectonic domains in the high-grade terrains east of the Labrador Trough, Quebec. Submitted to GAC special volume on the Trans-Hudson Orogen

Van Schmus, W. R., Bickford, J. F., Lewry, J. F. and MacDonald, R. 1987. U-Pb geochronology in the Trans-Hudsonian orogeny, northern Saskatchewan, Canada. Canadian Journal of Earth Sciences, 24, pp. 407-424.

Vernon, R. H. 1976. Metamorphic processes: reactions and microstructures. Allen and Unwin Ltd., London. 247p.

Vernon, R. H. and Flood, R. H. 1977. Interpretation of assemblages containing fibrolitic sillimanite. Contributions to Mineralogy and Petrology, 59, pp. 227- 235.

Vielzeuf, D. and Holloway, J. R. 1988. Experimental determination of fluid-absent melting relations in the pelitic system. Contributions to Mineralogy and Petrology, 98, pp. 257-276

Wardle, R. J. and Bailey, D. G. 1981. Early Proterozoic sequences in Labrador. In Proterozoic basins of Canada. Edited by F. H. A. Campbell. Geological Survey of Canada,

paper 81-10, pp. 331-359.

_____, Ryan, B. A. and Nunn G. A. 1987. Labrador segment of the Trans-Hudson Orogen: Crustal development through oblique convergence and collision. Geological Association of Canada and Mineralogical Association of Canada, Joint Annual Meeting, Program with Abstracts, p. 99.

White, A. J. R., Chappell, B. W. and Cleary, J. R. 1974. Geologic setting and emplacement of some Australian Paleozoic batholiths and implications for intrusive mechanisms. Pacific Geology, 8, pp. 159-171.

White, A. J. R. and Chappell, B. W. 1977. Ultrametamorphism and granitoid gneiss. Tectonophysics, 43, pp. 7-22.

Williams, H., Turner, F. J. and Gilbert, C. M. 1954. Petrography, an introduction to the study of rocks in thin-section. W. H. Freeman and Co., San Francisco. 406 p.

Woodsworth, G. J. 1977. Homogenization of zoned garnets from pelitic schists. Canadian Mineralogist, 15, pp. 230-242

Yardley, B. W. D. 1977. An empirical study of diffusion in garnet. Canadian Mineralogist, 15, pp. 793-800.

<u>Plate 1.</u>

a) Typical physiography of study area. Photo looking north towards Lac à Foin.

b) Calc Silicate layers defining foliation in marble (LRLMB).

c) Calc-silicate layers delineating F_2 folds in marble (LRLMB). Long dimension of notebook is 19 cm.

d) Texture interpreted as recrystallized graded bedding in gneissic metasandstone (LGB). Match case is approximately 6 cm high.

e) Hornblende-biotite paragneiss showing contact between rusty (bottom) and clean (top) units (LGB). Long dimension of photo is approximately 0.75 m.

f) Garnet porphyroblasts in epiclastic amphibolite unit (LBB).

<u>Plate 2.</u>

a) S_1 foliation in pelite (LRLMB) defined by preferred orientation of biotite and muscovite. Long dimension of photograph is 7.4 mm, crossed polars.

b) S_1 foliation in amphibolite (LRLMB) defined by long dimensions of hornblende, biotite and garnet (center). Note trails of opaques in garnet oriented parallel to foliation. Long dimension of photo is 3.1 mm. Plane polarized light.

c) Isoclinal F_1 fold in iron-formation near Lac à Foin (LGB).

d) F_1-F_2 mushroom-type interference pattern, Lac à Foin (LGB).

e) Tight F_2 folds in basement gneiss near Lac Berthet (LBB). Hammer is approximately one meter long.

f) F_2 fold in semipelite schist, Lac Murray area. White object at bottom of photo is notebook (approximately 12 cm wide).
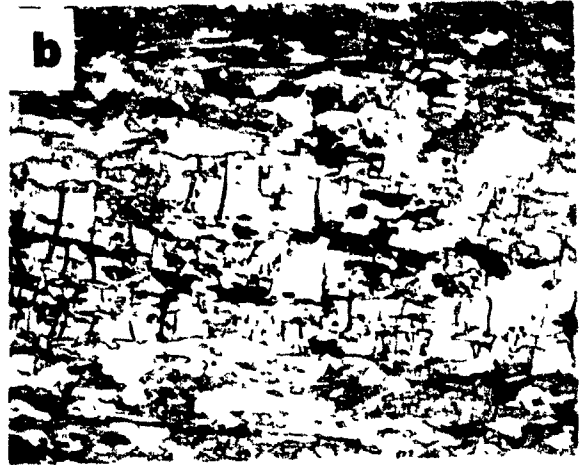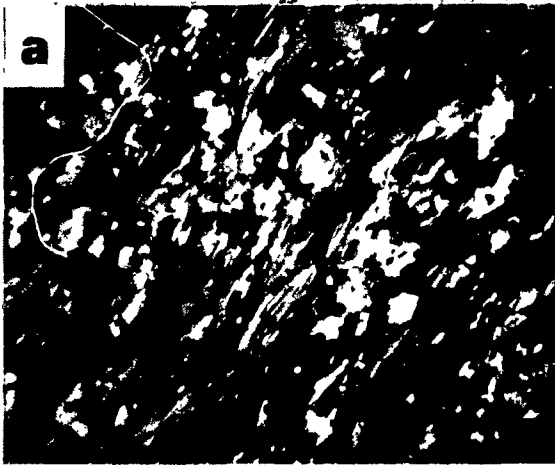
<u>Plate 3.</u>

a) F_2 fold in amphibolite unit (LRLMB). White object in center of photo is notebook (12 x 19 cm).

b) Surface expression of D_2 crenulation in semipelite schist (LRLMB). Arrow on notebook points east.

c) Crenulation in closure of F_2 fold in amphibolite (LRLMB).

d) Microphotograph of small biotite flakes oriented parallel to axial plane of small F_2 fold in semipelitic schist (LRLMB). Long dimension of photo is 7.4 mm. Plane polarized light.

e) F_2-F_3 interference pattern in hornblende-biotite gneiss (LGB). F_2 axis is parallel to long axis of basin. Hammer is approximately one meter long.

f) F_2-F_3 dome and basin interference patterns defined by calc-silicate layers in marble (LRLMB).Structure to right of hammer is a dome, structure to left of hammer is a basin. Hammer is approximately one meter long.
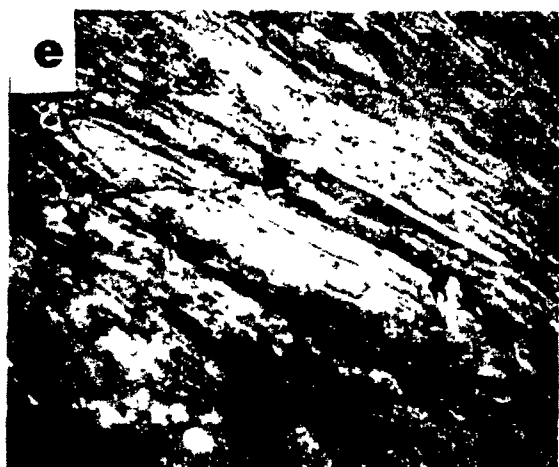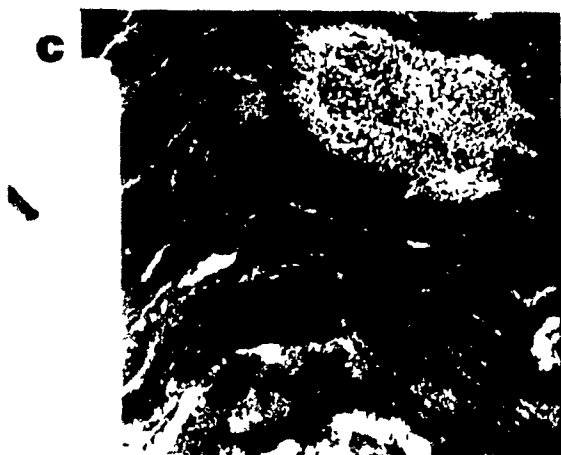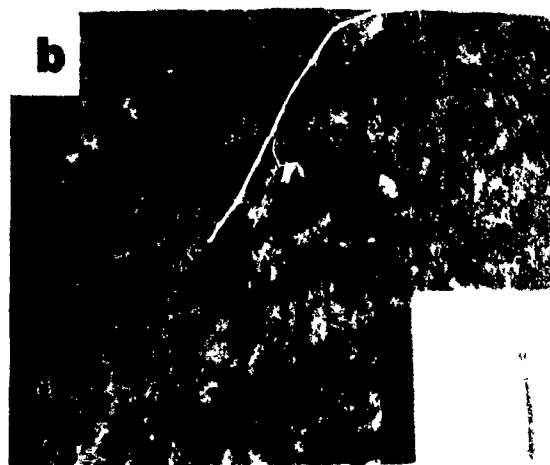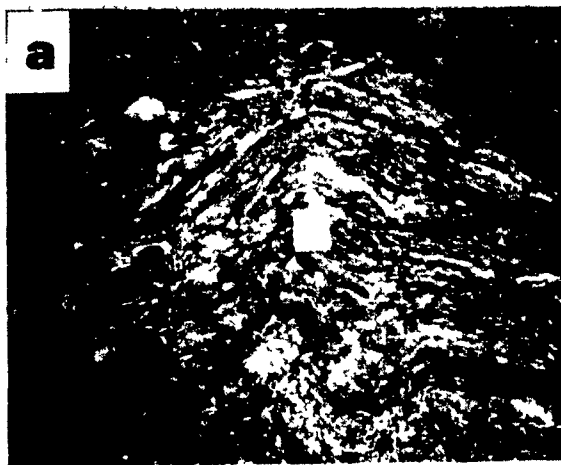
Plate 4.

a) Planar structures (quartz veins) reoriented into parallelism with minor shear zone on LOF.

b) Zone of grain size reduction associated with minor shear zone on LOF.

c) Garnet-cored sillimanite nodule in pelitic schist (LRLMB).

d) Microphotograph of garnet-cored sillimanite nodule. Base of photograph is 7.4 mm. Plane polarized light.

e) Fine lamellae of hornblende (dark bands) in cummingtonite. Base of photo is 0.8 mm wide. Plane polarized light.

f) Patchy hornblende (dark) and cummingtonite (light) intergrowth. Note indistinct grain boundaries between the two amphiboles. Base of photo is 0.8 mm wide. Plane polarized light.

g) Stably coexisting cummingtonite (light) and hornblende (dark). Base of photo is 0.8 mm wide. Plane polarized light.

h) Cummingtonite rimmed by poikiloblastic hornblende. White mineral is plagioclase. Base of photo is 0.8 mm wide. Plane polarized light.
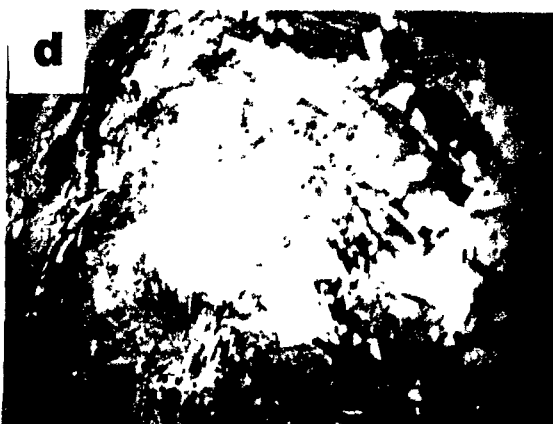
Appendix 1.

Whole Rock geochemistry

Whole rock analyses of rocks from the Lac Gabriel Complex. All analyses were carried on a Philips PW 1400 XRF unit. Major elements + BaO, Cr_2O_3, Ni and V were analysed using fused beads prepared from ignited samples. Raw data was corrected using an alpha - technique (Ahmedali, 1983). Detection limits are 0.01 wt% for major elements, 15 ppm for Cr_2O_3 and 10 ppm for V, Ni and BaO. Analytic precision for these elements (one standard deviation in wt%) were calculated from 20 replicate analyses and are as follows: Si - 0.05, AL - 0.03, Cr - 0.001, Fe - 0.01, Mn-0.001, Mg - 0.058, Ca - 0.01, Na - 0.06, K - 0.001, P - 0.004. Analytical precision for Ti, Ba and V is estimated to be 5%. Nb, Zr, Y, Sr, Rb, Pb, Th, and U were analysed using pressed powder pellets. Raw data corrected using a Rh Kb Compton scatter procedure. Detection limits for these elements is 5 ppm. Analytical precision is estimated to be 5%.

				Lac Gabriel Complex				
				Hornblende	Gabbros			
	A24H2	A27G	A2N	A25E2	JL18X1	A25E1	J20F1	A24H1	A3K2
SiO_2	38.92	39.50	40.23	40.86	40.76	41.14	41.56	44.22	44.98
TiO_2	2.60	2.74	2.83	1.88	2.33	1.76	2.18	2.05	1.47
Al_2O_3	14.76	13.65	14.95	14.39	14.33	12.37	12.57	17.64	13.78
Fe_2O_3	20.16	19.87	19.76	16.76	18.05	17.28	18.03	15.18	15.51
MnO	0.24	0.24	0.29	0.24	0.22	0.29	0.19	0.18	0.21
MgO	8.44	8.28	6.22	12.44	9.14	11.49	9.90	6.02	9.36
CaO	11.67	10.60	12.85	7.53	9.12	11.22	11.91	9.83	9.88
Na_2O	1.58	1.02	1.20	0.71	0.86	1.10	1.24	2.71	1.50
K_2O	1.14	2.80	1.19	4.39	3.62	1.96	1.49	1.16	2.36
P_2O_5	0.72	0.75	1.00	0.60	0.81	0.59	0.82	0.56	0.85
L.O.I.	0.53	0.76	0.44	0.93	0.95	0.67	0.62	0.43	0.63
TOTAL	100.88	100.38	101.01	101.00	100.39	100.07	100.65	100.10	100.79

Trace elements (ppm)

	A24H2	A27G	A2N	A25E2	JL18X1	A25E1	J20F1	A24H1	A3K2
Ni	74	54	<10	181	111	166	104	49	158
Cr_2O_3	279	267	41	730	401	802	416	201	570
V	388	392	382	354	331	315	375	304	253
Y	67	96	55	41	71	46	62	44	37
Zr	751	771	201	274	519	257	502	486	168
Nb	17	43	16	15	26	15	18	13	17
Rb	<5	72	<5	159	125	46	11	10	56
Sr	225	170	131	119	131	95	176	848	264
BaO	460	1060	300	1190	1280	440	480	680	650
Pb	<5	10	<5	<5	13	5	<5	<5	<5
Th	33	66	<5	23	41	16	<5	7	<5
U	<5	<5	9	<5	<5	6	7	9	6

	Diorite		Tonalite						
	A27F	A27C	J20F3	A26LL	A24D2	A24A1	A3K1	J20EC3	A26A
SiO_2	46.87	48.52	50.86	51.61	52.37	53.61	56.25	56.34	57.28
TiO_2	1.81	1.19	1.52	1.33	1.51	0.99	1.10	1.02	0.85
Al_2O_3	16.15	14.46	12.24	17.71	15.93	19.07	18.96	14.86	16.67
Fe_2O_3	13.85	12.48	12.07	8.88	10.89	7.71	7.99	11.12	7.80
MnO	0.19	0.16	0.09	0.12	0.14	0.10	0.09	0.08	0.13
MgO	5.73	8.57	8.69	4.96	5.09	3.65	2.32	5.00	4.30
CaO	10.27	10.52	10.17	9.28	8.38	8.27	6.34	5.43	6.46
Na_2O	2.58	2.59	2.63	3.73	3.32	4.32	4.80	2.80	3.42
K_2O	1.33	0.66	0.63	0.98	1.26	1.05	1.12	2.60	1.88
P_2O_5	0.56	0.35	0.19	0.49	0.36	0.48	0.43	0.34	0.40
L.O.I.	0.62	0.53	0.71	0.65	0.86	1.06	0.44	0.51	0.83
TOTAL	99.96	100.03	99.80	99.74	100.11	100.31	99.84	100.10	100.02

Trace elements (ppm)

Ni	41	56	92	56	33	28	10	77	53
Cr_2O_3	198	450	788	229	141	125	60	391	224
V	288	266	235	173	224	138	133	177	142
Y	58	34	29	35	46	26	16	12	23
Zr	485	108	148	305	301	124	99	188	154
Nb	29	13	9	18	19	11	9	14	13
Rb	12	<5	<5	<5	6	<5	19	74	40
Sr	506	475	415	888	774	1043	1153	495	899
BaO	420	200	160	340	580	520	550	1300	790
Pb	<5	<5	<5	<5	<5	<5	7	<5	<5
Th	27	<5	<5	<5	<5	<5	<5	<5	<5
U	12	14	13	14	12	15	15	7	7

	Tonalite	Granodiorite							
	SP8690	JL18L	J28C1	A25I	A26X1	A24O	A25A	A24L	A27A
SiO_2	61.47	54.34	55.76	56.33	58.36	59.68	61.11	61.29	66.66
TiO_2	1.20	1.16	0.97	1.06	0.99	1.08	0.88	0.88	0.69
Al_2O_3	16.24	17.45	14.86	19.84	15.79	17.00	15.39	15.73	14.47
Fe_2O_3	8.53	9.52	9.03	6.93	8.07	6.93	8.28	7.45	5.12
MnO	0.12	0.12	0.13	0.09	0.11	0.10	0.14	0.12	0.10
MgO	2.24	4.05	5.57	2.17	3.18	2.14	2.70	2.10	2.05
CaO	4.11	5.98	7.12	6.12	7.00	5.51	5.12	4.92	2.69
Na_2O	3.09	3.72	2.76	4.57	2.93	3.76	2.98	2.94	3.08
K_2O	2.25	2.12	3.28	1.72	2.12	2.34	2.82	3.71	4.24
P_2O_5	0.42	0.45	0.42	0.41	0.31	0.47	0.26	0.26	0.29
L.O.I.	0.52	0.67	0.59	0.65	0.88	0.59	0.44	0.32	0.36
TOTAL	100.49	99.58	99.62	99.89	99.74	99.60	100.12	99.70	99.77

<div align="center">Trace elements (ppm)</div>

Ni	<10	38	84	11	31	<10	13	<10	12
Cr_2O_3	29	154	353	39	124	58	66	100	86
V	137	184	161	114	157	133	139	134	378
Y	33	35	26	28	32	30	22	30	22
Zr	210	233	189	324	189	169	256	250	323
Nb	23	18	13	13	17	17	16	19	18
Rb	32	65	63	50	27	34	50	70	119
Sr	570	655	710	848	650	582	533	434	562
BaO	1530	830	1160	520	1220	910	1630	1330	1440
Pb	10	8	38	<5	<5	23	<5	12	8
Th	<5	7	10	<5	<5	<5	<5	17	10
U	11	12	11	10	7	7	6	6	6

Lac Gabriel Complex (cont.)			

	Granites			
	J22D2	J21C	J28G2	SP86334
SiO_2	67.80	69.56	72.48	76.15
TiO_2	0.56	0.66	0.44	0.04
Al_2O_3	15.75	14.67	13.41	14.38
Fe_2O_3*	4.09	4.58	3.38	0.64
MnO	0.05	0.04	0.05	0.08
MgO	1.21	0.77	0.55	0.08
CaO	2.?1	2.06	1.90	1.30
Na_2O	3.23	2.21	2.31	3.18
K_2O	3.54	5.01	4.86	4.02
P_2O_5	0.24	0.23	0.10	0.01
L.O.I.	0.51	0.25	0.27	0.15
TOTAL	99.89	100.04	99.75	100.03

Trace elements (ppm)

	J22D2	J21C	J28G2	SP86334
Ni	10	10	10	10
Cr_2O_3	53	54	15	15
V	68	46	19	10
Y	17	10	26	19
Zr	162	181	250	57
Nb	10	15	16	11
Rb	67	157	77	83
Sr	70.5	254	302	205
BaO	1420	1350	980	950
Pb	8	19	7	26
Th	<5	8	13	<5
U	10	<5	6	<5

	Q5	QA1	QH10B	QV5	R4	R3	ZM1	ZM4
				Lac a Foin Amphibolites				
SiO_2	43.95	47.89	50.39	53.44	50.63	49.89	51.25	47.62
TiO_2	0.22	1.99	1.31	1.12	1.13	1.26	1.25	0.88
Al_2O_3	15.66	12.75	15.11	15.15	14.99	14.11	14.68	15.83
Fe_2O_3	10.87	16.92	16.26	12.83	14.56	14.73	14.69	12.85
MnO	0.16	0.23	0.23	0.17	0.20	0.20	0.21	0.21
MgO	10.95	8.05	5.54	5.40	5.97	6.60	5.53	7.95
CaO	13.43	10.44	8.09	7.69	7.80	9.78	7.72	10.91
Na_2O	1.05	2.00	2.99	3.05	3.67	2.45	3.83	2.88
K_2O	0.15	0.31	0.65	1.36	0.29	0.35	0.28	0.39
P_2O_5	0.01	0.17	0.12	0.18	0.07	0.11	0.09	0.05
L.O.I	3.75	0.49	0.80	0.93	0.67	0.67	0.65	---
TOTAL	100.23	101.28	101.50	101.32	100.01	100.15	100.18	99.57

Trace elements (ppm)

	Q5	QA1	QH10B	QV5	R4	R3	ZM1	ZM4
Cr_2O_3	292	382	178	68	204	338	160	746
NiO_2	41	95	37	24	40	71	26	143
Nb	8	14	10	9	10	10	9	9
Zr	40	125	108	122	98	98	91	85
Y	1	27	31	32	24	25	24	20
Sr	85	71	203	282	265	216	290	193
Rb	18	19	33	58	19	18	19	18
Pb	10	16	15	17	14	18	16	17
Th	3	7	4	9	4	6	3	3
U	14	15	14	16	15	15	16	15

Appendix 2. Mineral Analyses

	GP9d		GP10i			26A		Q2D		Jl10n			A19p	
	r	c	r(bi)	r(pl)	c	r	c	r	m	r(hb)	r(bi)	c	r	c
SiO_2	37.55	37.51	37.42	37.42	37.51	37.80	37.96	37.32	36.84	37.14	36.57	37.25	38.35	38.43
TiO_2	0.03	0.03	0.04	0.05	0.08	0.02	0.01	---	0.11	0.13	0.09	0.06	0.06	0.05
Al_2O_3	21.29	21.12	20.79	20.89	20.99	20.79	20.88	20.81	20.53	20.68	20.57	21.03	20.86	21.05
FeO	30.67	30.79	31.63	32.03	31.69	32.15	30.75	30.39	24.35	29.64	29.23	28.71	29.18	28.00
MnO	3.30	3.04	2.32	2.56	1.83	2.64	2.45	3.98	10.04	2.08	3.40	1.49	1.90	0.71
MgO	2.39	2.62	2.29	2.26	1.71	2.76	2.83	2.34	1.60	3.26	2.74	4.44	2.84	5.36
CaO	5.68	5.40	5.30	4.70	6.79	4.26	4.68	4.31	5.85	6.77	6.72	6.69	6.54	6.84
TOTAL	100.92	100.51	99.79	99.91	100.60	100.40	99.57	99.16	99.32	99.70	99.32	99.68	100.85	100.44

Stoichiometry on the basis of 8 cations

	r	c	r(bi)	r(pl)	c	r	c	r	m	r(hb)	r(bi)	c	r	c
Si	2.981	2.988	3.010	3.011	2.995	3.022	3.049	3.023	2.988	2.963	2.941	2.946	3.032	2.996
Ti	0.002	0.002	0.003	0.003	0.005	0.001	0.001	---	0.007	0.008	0.005	0.004	0.004	0.003
Al_{IV}	---	0.012	0.005	0.007	0.015	---	---	---	0.012	0.037	0.059	0.054	---	0.004
Al_{VI}	1.971	1.968	1.964	1.972	1.959	1.962	1.974	1.985	1.948	1.906	1.888	1.905	1.942	1.929
Fe	2.036	2.051	2.127	2.155	2.116	2.169	2.065	2.059	1.652	1.977	1.966	1.899	2.003	1.825
Mn	0.222	0.205	0.158	0.174	0.124	0.182	0.167	0.273	0.690	0.140	0.232	0.100	0.127	0.047
Mg	0.283	0.311	0.274	0.271	0.204	0.340	0.339	0.282	0.193	0.388	0.328	0.524	0.334	0.623
Ca	0.483	0.461	0.457	0.405	0.581	0.323	0.403	0.375	0.508	0.578	0.579	0.567	0.555	0.571
X_{al}	0.673	0.677	0.705	0.717	0.700	0.720	0.694	0.689	0.543	0.641	0.633	0.615	0.633	0.595
X_{sp}	0.073	0.068	0.052	0.058	0.041	0.060	0.056	0.091	0.227	0.046	0.075	0.032	0.042	0.015
X_{py}	0.094	0.103	0.091	0.090	0.067	0.113	0.114	0.094	0.063	0.126	0.106	0.170	0.111	0.203
X_{gr}	0.160	0.152	0.152	0.135	0.192	0.107	0.136	0.125	0.167	0.188	0.186	0.183	0.184	0.186

Abbreviations used in tables

m : matrix grain
r : rim of garnet crystal
i : inclusion in garnet
i(rim), i(core) : rim and core of inclusion in garnet crystal
cr : core of grain on garnet rim
c : core of garnet crystal
r(bi), r(hb) : garnet rim in contact with biotite and hornblende
nd : not determined
--- : not detected

	GARNET (continued)												
	5V3		A16fb		7E11			6ER27		14e2b		0C46	
	r	c	r	c	r(di)	r(hb)	c	r	c	r	c	r	c
SiO$_2$	37.59	37.47	38.12	39.09	38.06	37.89	37.69	38.09	39.57	37.70	38.56	37.60	37.42
TiO$_2$	0.04	0.06	0.09	0.19	0.07	0.06	0.09	0.05	0.05	0.10	0.07	0.04	0.01
Al$_2$O$_3$	20.89	21.21	21.02	21.22	20.53	20.61	20.69	20.85	21.64	20.38	20.44	20.42	20.06
FeO	30.93	30.37	29.68	26.79	29.76	30.40	28.46	35.63	28.45	30.72	29.29	32.24	33.46
MnO	0.83	0.70	1.39	0.83	1.19	1.24	1.12	1.07	0.53	2.83	0.89	1.22	1.02
MgO	4.40	5.54	3.76	6.69	3.86	3.96	5.12	4.13	9.61	2.03	4.70	2.04	2.18
CaO	4.62	3.99	6.42	6.44	6.85	6.38	6.60	0.99	1.07	6.70	6.94	6.32	5.83
TOTAL	99.52	99.34	100.48	99.91	100.33	100.74	99.77	100.80	100.94	100.46	100.89	99.89	99.98

Stoichiometry on the basis of 8 cations

	r	c	r	c	r(di)	r(hb)	c	r	c	r	c	r	c
Si	3.007	2.967	3.006	3.001	3.006	2.991	2.968	3.029	3.019	3.013	3.013	3.023	3.012
Ti	0.002	0.004	0.005	0.011	0.004	0.001	0.005	0.003	0.003	0.006	0.004	0.003	---
Al$_{IV}$	---	0.033	---	---	---	0.009	0.032	---	---	---	---	---	---
Al$_{VI}$	1.968	1.944	1.952	1.918	1.908	1.902	1.886	1.952	1.945	1.918	1.880	1.933	1.901
Fe	2.045	2.011	1.957	1.720	1.965	2.007	1.874	2.369	1.816	2.053	1.914	2.168	2.252
Mn	0.056	0.047	0.093	0.054	0.080	0.083	0.075	0.072	0.035	0.192	0.059	0.083	0.069
Mg	0.525	0.654	0.442	0.765	0.455	0.466	0.601	0.489	1.093	0.242	0.547	0.244	0.261
Ca	0.396	0.338	0.542	0.530	0.579	0.539	0.577	0.084	0.088	0.574	0.581	0.544	0.503
X_{al}	0.677	0.659	0.645	0.560	0.638	0.648	0.603	0.786	0.599	0.671	0.617	0.713	0.730
X_{sp}	0.019	0.015	0.031	0.018	0.026	0.027	0.024	0.024	0.011	0.063	0.019	0.027	0.022
X_{py}	0.174	0.214	0.146	0.249	0.148	0.151	0.194	0.162	0.361	0.079	0.177	0.080	0.085
X_{gr}	0.131	0.111	0.179	0.173	0.188	0.174	0.179	0.028	0.029	0.187	0.187	0.179	0.163

	GP9d	GP10i			26A	02D		J110n		A19p		5L3		16Fb	
	r	r	i	m	r	r	i	r	m	r	m	r	l	r	m
SiO_2	46.84	46.92	58.01	54.82	45.63	60.78	54.67	56.84	58.56	50.53	57.95	59.48	60.77	58.19	58.46
TiO_2	---	---	0.01	0.01	---	---	---	---	---	---	---	0.01	---	0.00	---
Al_2O_3	34.18	26.41	28.11	17.10	33.19	24.39	28.97	26.87	26.29	31.70	26.07	26.03	24.88	27.01	25.86
FeO	0.15	0.19	0.17	0.12	0.14	0.21	0.24	0.26	0.25	0.42	0.08	0.26	0.19	0.10	0.12
MnO	---	---	0.03	---	---	0.01	0.03	0.05	---	0.03	---	0.03	---	0.06	0.02
CaO	17.39	17.16	8.27	10.60	18.19	6.28	11.63	9.52	8.77	14.39	8.49	7.58	6.92	8.88	8.55
Na_2O	1.53	1.55	6.56	5.47	1.10	7.85	5.12	6.04	6.73	3.37	6.69	6.88	7.02	6.33	6.39
K_2O	0.14	0.06	0.10	0.05	0.01	0.06	0.07	0.05	0.09	0.08	0.17	0.06	0.36	0.10	0.13
TOTAL	100.23	99.20	99.65	99.12	98.26	99.58	100.74	99.64	100.69	100.51	99.45	100.31	100.15	100.67	99.53

Cations on the basis of 32 oxygen

	GP9d	GP10i			26A	02D		J110n		A19p		5L3		16Fb	
	r	r	i	m	r	r	i	r	m	r	m	r	l	r	m
Si	8.593	8.679	10.414	9.456	8.558	10.847	9.814	10.245	10.423	9.176	10.433	10.572	10.795	10.345	10.497
Ti	---	---	0.004	0.001	---	---	---	---	---	---	---	0.001	---	---	---
AL	7.383	7.275	5.590	6.019	7.330	5.125	6.123	5.703	5.510	6.778	5.526	5.446	5.204	5.654	5.468
Fe	0.023	0.026	0.024	0.018	0.021	---	0.036	0.040	0.037	0.063	0.012	0.038	0.028	0.015	0.018
Mn	---	---	0.003	---	---	0.002	0.005	0.007	---	0.004	---	0.004	---	0.009	0.005
Ca	3.418	3.405	1.591	2.063	3.655	1.200	2.238	1.839	1.672	2.800	1.638	1.443	1.317	1.691	1.645
Na	0.543	0.566	2.285	1.927	0.401	2.716	1.781	2.111	2.321	1.187	2.334	2.369	2.418	2.182	2.225
K	0.034	0.013	0.022	0.011	0.003	0.013	0.017	0.011	0.021	0.018	0.040	0.014	0.082	0.024	0.030
X_{or}	0.008	0.003	0.005	0.002	0.001	0.017	0.004	0.003	0.005	0.004	0.010	0.004	0.021	0.006	0.008
X_{ab}	0.135	0.139	0.566	0.483	0.098	0.671	0.437	0.527	0.573	0.291	0.580	0.613	0.629	0.556	0.567
X_{an}	0.865	0.857	0.408	0.516	0.901	0.306	0.559	0.470	0.422	0.704	0.410	0.348	0.350	0.438	0.425

	PLAGIOCLASE (continued)							
	JI6I		7E11	6Er27		14E2b	OC46	
	i	r	m	r	m	r	r	m
SiO$_2$	58.99	60.58	57.99	60.75	61.02	57.84	61.04	61.57
TiO$_2$	0.04	0.01	---	0.01	---	---	0.03	0.02
Al$_2$O$_3$	25.74	24.93	26.57	24.78	24.80	26.37	24.25	25.58
FeO	0.55	0.69	0.04	0.18	0.14	---	0.09	0.25
MnO	---	0.05	---	0.02	---	0.02	0.03	---
CaO	6.10	3.99	7.95	6.96	6.94	8.44	6.53	7.15
Na$_2$O	8.08	9.21	7.70	7.33	7.56	6.65	7.69	7.40
K$_2$O	0.07	0.06	0.17	0.06	0.06	0.21	0.08	0.09
TOTAL	99.57	99.51	100.43	100.09	100.52	99.61	99.75	102.09

Cations on the basis of 32 oxygen

Si	10.579	10.807	10.361	10.794	10.799	10.348	10.876	10.735
Ti	0.005	0.01	---	0.001	---	---	0.004	0.003
Al	5.436	5.237	5.590	5.185	5.169	5.587	5.086	5.252
Fe	0.082	0.103	0.007	0.027	0.021	---	0.014	0.036
Mn	---	0.007	---	0.003	---	0.001	0.004	---
Ca	1.173	0.763	1.522	1.325	1.316	1.636	1.246	1.336
Na	2.810	3.184	2.669	2.525	2.594	2.318	2.657	2.500
K	0.016	0.013	0.040	0.013	0.013	0.048	0.018	0.021
X$_{or}$	0.004	0.003	0.009	0.003	0.003	0.012	0.005	0.005
X$_{ab}$	0.689	0.773	0.630	0.649	0.658	0.579	0.674	0.641
X$_{an}$	0.307	0.224	0.361	0.348	0.339	0.409	0.321	0.353

	GP9d	GP10i		26A		Q2D		J110n			5W3			A16fb
	r	r	m	r	m	r	c	i	r	m	i	r	m	i
SiO_2	37.16	34.73	35.74	36.21	37.01	36.33	36.22	35.96	35.73	36.77	37.38	37.13	37.97	37.46
TiO_2	2.40	3.88	2.21	2.00	2.11	2.32	1.94	2.60	2.56	2.58	4.41	4.51	4.69	2.27
Al_2O_3	17.07	17.80	18.75	16.36	17.11	15.89	15.47	15.99	15.60	15.58	14.85	14.82	14.54	18.51
FeO	19.46	20.88	20.45	20.24	17.87	21.05	22.43	22.54	23.22	23.14	17.74	17.76	18.14	15.06
MnO	0.07	0.14	0.07	0.06	0.03	0.07	0.10	0.23	0.22	0.28	0.01	0.06	0.03	0.02
MgO	10.73	9.26	9.25	11.50	12.09	9.66	10.16	9.31	8.90	9.08	12.03	12.33	11.88	13.53
CaO	0.42	0.02	0.01	0.08	0.03	0.05	0.62	0.04	0.07	0.04	---	---	0.01	0.06
Na_2O	0.14	0.10	0.11	0.09	0.11	0.17	0.14	0.16	0.15	0.12	0.05	0.07	0.04	0.11
K_2O	8.62	9.53	9.35	8.73	9.65	9.08	9.13	9.62	9.69	9.24	9.70	9.73	9.86	9.06
F	nd	nd	nd	0.36	0.09	0.53	0.23	1.32	0.67	0.77	0.47	0.28	0.33	nd
TOTAL	96.08	96.34	95.94	95.70	96.10	95.15	96.47	97.76	96.81	97.61	96.64	96.69	96.49	100.00

Stoichiometry on the basis of 22 oxygen

Si	5.579	5.293	5.423	5.519	5.549	5.616	5.558	5.519	5.529	5.612	5.607	5.564	5.573	5.502
Al_{IV}	2.421	2.707	2.577	2.481	2.451	2.384	2.442	2.481	2.471	2.388	2.393	2.436	2.447	2.498
Al_{VI}	0.600	0.491	0.777	0.458	0.572	0.511	0.357	0.411	0.374	0.415	0.292	0.182	0.199	0.706
Ti	0.271	0.455	0.252	0.229	0.238	0.270	0.224	0.300	0.297	0.296	0.498	0.509	0.493	0.251
Fe	2.444	2.661	2.595	2.580	2.241	2.721	2.879	2.893	3.006	2.954	2.225	2.226	2.287	1.850
Mn	0.009	0.018	0.009	0.007	0.004	0.009	0.014	0.030	0.029	0.036	0.001	0.001	0.004	2.962
Mg	2.402	2.104	2.092	2.632	2.702	2.226	2.325	2.129	2.053	2.065	2.690	2.775	2.669	0.002
Na	0.041	0.030	0.032	0.025	0.032	0.051	0.041	0.047	0.046	0.036	0.015	0.019	0.011	0.031
Ca	0.067	0.003	0.002	0.008	0.004	0.008	0.102	0.007	0.012	0.006	---	---	0.002	0.009
K	1.652	1.856	1.812	1.697	1.846	1.791	1.787	1.883	1.913	1.798	1.855	1.861	1.898	1.698

	BIOTITE (cont)		
	6ER27		14e2b
	r	m	m
SiO_2	36.66	36.98	35.91
TiO_2	2.22	2.40	2.57
Al_2O_3	18.28	18.24	16.09
FeO	18.52	17.73	23.17
MnO	0.02	---	0.09
MgO	11.13	11.17	8.53
CaO	---	0.02	0.10
Na_2O	0.31	0.25	0.07
K_2O	9.22	8.95	9.81
F	0.09	0.27	nd
TOTAL	96.15	96.03	96.34

Stoichiometry on the
basis of 22 oxygen

Si	5.475	5.524	5.535
Al_{IV}	2.520	2.476	2.465
Al_{VI}	0.711	0.735	0.458
Ti	0.250	0.270	0.298
Fe	2.315	2.215	2.987
Mn	0.002	---	0.012
Mg	2.481	2.488	1.960
Na	0.041	0.072	0.020
Ca	---	0.004	0.017
K	1.756	1.706	1.928

	HORNBLENDE														
	GP9d		Q2d		JL10N			A19P		A16fB		7E11			
	r	m	r	cr	r	m	cr	r	m	r	m	i(rim)	i(core)	r	m
SiO_2	42.99	43.41	41.94	41.81	40.92	43.63	46.68	44.50	45.42	45.10	46.02	40.88	41.07	40.86	40.56
TiO_2	0.63	0.22	0.54	0.67	0.35	0.48	0.43	0.42	0.42	0.76	0.79	2.10	2.92	2.83	2.69
Al_2O_3	14.29	15.70	12.62	12.37	15.01	12.03	9.62	12.09	11.22	11.44	10.70	13.36	12.75	13.11	12.25
FeO	17.14	17.27	21.16	21.47	20.86	19.98	20.10	18.52	18.34	16.16	16.66	17.04	18.17	20 90	20.65
MnO	0.13	0.18	0.26	0.31	0.50	.30	0.41	0.13	0.19	0.15	0.10	0.07	0.07	0.20	0.10
MgO	7.91	7.59	7.18	7.35	6.04	7.25	8.65	9.10	9.46	10.45	10.79	10.34	9.20	7.82	8.08
CaO	11.34	11.15	10.56	10.24	11.48	11.48	11.38	11.49	11.47	11.35	11.45	11.07	10.92	11.05	11.20
Na_2O	1.07	1.16	1.60	1.66	1.41	1.29	1.06	1.10	0.67	1.07	0.84	2.27	2.25	2.52	2.36
K_2O	0.65	---	0.41	0.39	1.24	1.03	0.75	0.84	---	0.59	0.50	0.99	1.00	0.85	0.92
F	nd	nd	0.50	---	0.30	0.20	---	0.12	---	nd	nd	0.12	---	0.38	0.08
TOTAL	96.12	96.62	96.79	96.28	98.11	97.69	99.07	98.31	97.20	97.07	97.86	98.25	98.38	100.66	98.89

Stoichiometry based on 15 cations + Na_A + K

	r	m	r	cr	r	m	cr	r	m	r	m	i(rim)	i(core)	r	m
Si	6.459	6.417	6.351	6.315	6.204	6.660	6.866	6.556	6.668	6.635	6.697	6.044	6.177	6.054	6.102
Al_{IV}	1.541	1.583	1.649	1.685	1.796	1.400	1.134	1.444	1.332	1.365	1.303	1.956	1.883	1.946	1.898
Al_{VI}	0.989	1.153	0.604	0.516	0.886	0.744	0.533	0.656	0.609	0.619	0.532	0.372	0.354	0.343	0.273
Ti	0.071	0.025	0.062	0.076	0.040	0.055	0.048	0.046	0.046	0.084	0.087	0.233	0.327	0 316	0.304
Fe	2.153	2.128	2.080	2.712	2.645	2.528	2.473	2.283	2.253	1.998	2.027	2.107	2.264	2.589	2.598
Mn	0.016	0.022	0.033	0.040	0.064	0.039	0.051	0.016	0.024	0.019	0.013	0.009	0.009	0.025	0.012
Mg	1.771	1.672	1.621	1.655	1.365	1.634	1 895	1.999	2.071	2.290	2.342	2.279	2.042	1.727	1.813
Ca	1.826	1.765	1.714	1.657	1.864	1.851	1.793	1.814	1.805	1.790	1.786	1.754	1.743	1.775	1.806
Na_{M4}	0.174	0.235	0.286	0.343	0.136	0.139	0.207	0.186	0.192	0.210	0.214	0.246	0.260	0.255	0.194
Na_A	0.137	0.099	0.183	0.142	0.280	0.240	0.094	0.128	---	0.095	0.022	0.405	0.390	0.500	0.494
K	0.124	---	0.080	0.076	0.239	0.199	0.141	0.158	---	0.110	0.094	0.186	0.189	0.160	0.177
F					0.248	0.163	---	0.096	---			0.096	---	0.302	0.064

	HORNBLENDE (cont.)						
	14E2b			OC46			
	r	cr	m	r	cr	m	m
SiO_2	44.26	44.08	44.56	41.47	41.60	41.59	41.76
TiO_2	3.55	0.88	0.74	0.65	0.88	0.97	0.90
Al_2O_3	12.62	12.54	12.15	13.45	12.94	12.50	12.99
FeO	18.95	19.18	19.44	23.26	23.85	23.05	22.96
MnO	0.16	0.23	0.25	0.17	0.17	0.09	0.14
MgO	7.33	7.41	7.66	5.73	6.11	6.08	6.28
CaO	10.68	11.10	10.87	10.37	10.54	10.78	11.14
Na_2O	1.28	1.46	1.28	1.62	1.49	1.61	1.68
K_2O	0.51	0.62	1.40	0.49	0.47	0.51	0.59
F	nd	nd	nd	nd	nd	nd	nd
TOTAL	99.35	97.50	98.35	97.21	98.05	97.19	98.44

Stoichiometry based on 15 cations + Na_A + K

Si	6.485	6.601	6.634	6.272	6.236	6.326	6.282
Al_{IV}	1.515	1.399	1.366	1.728	1.764	1.674	1.718
Al_{VI}	0.655	0.814	0.765	0.670	0.524	0.567	0.584
Ti	0.342	0.099	0.082	0.074	0.099	0.111	0.102
Fe	2.322	2.403	2.420	2.942	2.990	2.931	2.888
Mn	0.020	0.029	0.032	0.021	0.022	0.011	0.018
Mg	1.601	1.654	1.700	1.293	1.365	1.379	1.407
Ca	1.671	1.782	1.734	1.680	1.694	1.756	1.796
Na_{M4}	0.323	0.218	0.266	0.320	0.306	0.244	0.204
Na_A	0.041	0.205	0.103	0.154	0.126	0.233	0.284
K	00.00	0.095	0.118	0.095	0.090	0.100	0.113
F							

	GP9d	GP10i	26A	02D		A19p	5L3	A16Fb			7E11	0C40	0C46
	r	i	r	l	m	r	r	m	r	l	r	r	r
SiO_2	0.01	0.08	0.01	0.05	0.01	0.03	0.02	---	0.02	---	0.05	---	0.04
TiO_2	52.92	51.89	52.33	48.45	49.99	51.20	51.98	52.44	52.93	51.90	51.36	53.44	51.20
Al_2O_3	0.01	0.08	---	0.01	---	---	---	---	---	---	---	---	---
FeO	44.97	45.59	46.56	48.24	48.19	46.84	47.86	46.58	46.12	45.98	48.43	45.34	47.77
MnO	0.67	0.29	0.68	1.68	1.25	0.57	0.23	0.81	0.43	0.33	0.49	0.16	0.39
MgO	0.24	0.13	0.31	0.43	---	0.45	0.20	0.10	---	0.91	0.04	0.53	0.14
CaO	---	---	---	0.17	0.03	0.02	0.04	---	---	---	---	---	---
TOTAL	98.81	98.15	99.91	99.06	100.11	99.12	100.39	99.92	99.50	99.11	100.37	99.47	99.58

Cations on the basis of three oxygen

	GP9d	GP10i	26A	02D		A19p	5L3	A16Fb			7E11	0C40	0C46
Si	---	0.002	0.001	0.001	---	0.001	0.001	---	---	---	0.001	---	0.001
Ti	1.001	1.000	0.994	0.946	0.952	0.984	0.987	0.997	1.007	0.991	0.979	1.011	0.985
Al	---	0.002	---	---	---	---	---	---	---	---	---	---	---
Fe	0.955	0.978	0.984	1.047	1.020	1.001	1.011	0.985	0.976	0.976	1.027	0.954	1.009
Mn	0.014	0.006	0.015	0.037	0.027	0.012	0.005	0.017	0.009	0.007	0.011	0.003	0.009
Mg	0.009	0.005	0.012	0.016	---	0.017	0.008	0.004	---	0.034	0.002	0.020	0.005
Ca	---	---	---	0.005	0.001	---	---	---	---	---	---	---	---
X_{ilm}	0.976	0.988	0.974	0.951	0.974	0.971	0.988	0.979	0.992	0.959	0.988	0.976	0.986

CORDIERITE			
	OC40		
	m	r	r
SiO_2	49.54	48.90	48.94
Al_2O_3	32.93	33.32	33.81
FeO	5.16	5.10	4.71
MnO	0.02	0.03	0.02
MgO	10.35	10.37	10.10
CaO	0.01	0.02	0.04
Na_2O	0.23	0.24	0.17
TOTAL	98.23	98.02	97.80

Cations on the basis of 18 oxygen

Si	5.030	4.980	4.981
Al_{IV}	0.970	1.020	1.019
Al_{VI}	2.967	2.975	3.032
Fe	0.438	0.434	0.401
Mn	---	0.003	0.002
Mg	1.566	1.574	1.532
Ca	0.002	0.002	0.005
Na	0.045	0.048	0.034
X_{mg}	0.976	0.988	0.974

CUMMINGTONITE			
	5V3		
	r	m(rim)	m(core)
SiO_2	53.99	54.33	54.63
TiO_2	0.03	0.02	0.04
Al_2O_3	0.61	0.39	0.38
FeO	22.31	24.47	24.60
MnO	0.16	0.20	0.19
MgO	19.04	17.19	17.57
CaO	0.83	0.86	0.71
Na_2O	0.02	0.01	0.04
TOTAL	97.14	97.56	98.15

Stoichiometry based on
15 cations + Na_A + K

Si	7.875	7.984	7.966
Al_{IV}	0.106	0.016	0.034
Fe^{3+}	0.002	---	---
Al_{VI}	---	0.051	0.031
Ti	0.003	0.002	0.004
Fe^{2+}	2.577	3.007	2.994
Fe^{3+}	0.124	---	0.006
Mn	0.020	0.035	0.023
Mg	4.140	3.776	3.819
Ca	0.130	0.136	0.111
Na_A	0.006	0.003	0.004

<u>Appendix 3</u> Sample Location Key

East of Lac Berthet

1	1Fe9
2	1Fe6
3	1Fe5
4	1Fe4
5	1Fe3
6	1Fe2
7	1Fe1
8	2Fe3
9	2Fe5 ts
10	2Fe6
11	2Fe7
12	Oc48
13	1e1
14	13e15
15	12e13
16	Oc46 ps
17	14e4
18	12e6
19	Oc32
20	Oc43
21	6e21
22	Oc29 ts
23	12e3
24	Oc30 ps
25	6e7
26	Oc17
27	14e2 ps
28	12e1
29	8e3 ps
30	8e4
31	9e1
32	9e9
33	9e15
34	Oc40 ps
35	Oc10
36	Oc11
37	Oc12
38	6e1
39	Oc26
40	Oc25 ps
41	5e9
42	Oc24
43	6eR27 ps
44	7e9
45	7e11 ps
46	7e8
47	7e1
48	7e2
49	7e5
50	7e7

West of Lac Berthet

51	6w1
52	6w6
53	6w7
54	6w8
55	6w9
56	6w14
57	2w8
58	2w9
59	A17m
60	A17g
61	A17d
62	1w11 ts
63	A16e
64	4w15 ps
65	1w8
66	4w12
67	1w5
68	4w8
69	4w3
70	4w6
71	A17a
72	A16f ps
73	A18f

West of Lac Berthet, North of Lac Pingiajulik

74	A18l
75	A19v
76	A15q
77	A19r
78	A19q
79	A19p ps
80	A19o
81	A15n
82	A20f

83	A20j
84	A20b ps
85	A10t
86	A15k
87	A15j
88	A15i
89	A15h
90	A19d
91	A70
92	A7j ps
93	A7g
94	A7f
95	A10d ts
96	A10e
97	A10f
98	A10g ps
99	A10i
100	A10m
101	A10n
102	A10o
103	A20n
104	A7b ts
105	A9h ts
106	A9i
107	A9j
108	A9l
109	A9m
110	A9v ts
111	A9w ts
112	A9x ts
113	A8j
114	A8k
115	A8m ts
116	A8n
117	A13e
118	A13e ts
119	A13f
120	A13h
121	A13i
122	A13k
123	A11i ts
124	A11g
125	A11f
126	A11e
127	A14a
128	A11l

129	A11v
130	J115j ts
131	J115g ts
132	J114d

West Of Lac Pingiajjulik

133	A14p ts
134	A14o
135	A14m ts
136	A14e ps
137	A14f ts
138	A14j ts
139	A14k ts
140	J18i
141	J18h ts
142	J18g
143	J18m ps
144	J19c
145	J19d ts
146	J18f ts
147	J15i ts
148	J18b
149	J114i
150	J115f
151	J115b
152	J115d
153	J114g ts
154	J17q
155	J17m
156	J15k
156b	J116f
157	J18l
158	J111j
159	J111i
160	J111h
161	J111g ts
162	J111d
163	J19h
164	J19i ts
165	J116c
166	J17i
167	J17g
168	J16i ps
169	J17g ts

170 J16f **ts**
171 J16l
172 J15a
173 J110b **ps**
174 JL5b
175 J112b
176 J112c
177 J112h
178 J110n **ps**
179 J110m
180 J110k **ts**
181 J110j
182 J110i
183 J110f
184 J113c
185 J113h
186 J120k
187 J120n
188 J120p
189 J120q
190 J120t
191 J120i
192 J120g **ts**
193 J120d
194 J117d
195 J117g
196 J117r
197 J117k
198 J117i
199 J120b
200 J120aa
201 J120ee
202 J120gg

**South of Lac
Pingiajjulik**

203 J119a
204 J118e
205 J118k **ts**
206 J119d
207 J119e
208 J119f
209 J120mm
210 J119r **ts**
211 J119q
212 J119n
213 J118l **ts,g**
214 J118u
215 J118r
216 J118s
217 A3k **ts,g**

218 A3n **ts**
219 A3q
220 A3u
221 A3v

**East of Lac
Pingiajjulik**

222 J125d
223 JL25c
224 J125g **ts**
225 J127a
225b J125l
226 J131i **ps**
227 A6a **ts**
228 A6b
229 A6d
230 J131c
231 J131d
232 J131f
233 J127x
234 J129a
235 J127f
236 J127g
237 J127h
238 J127i
239 J126b
240 J128c
241 J127q
242 J128f
243 J128d
244 J128b
245 J129h **ts**
246 J129k
247 J129m
248 J128k
249 J128u **ts**
250 J128q
251 J130g
252 J130h
253 A2m **g**
254 A2o
256 A4y
257 A3a
258 A4o

**North of Lac
à Foin**

259 J29c
260 J29e **ts**
261 J29f **ts**

262 J29g
263 J21j
264 J13k
265 J13j
266 J29b
267 J15a
268 J21d
269 J21f
270 J13d **ts**
271 J20c
272 J15d **ts**
273 J15c **ts**
274 J30b
275 J15f
276 J15g
277 J20a **ts**
278 J11g **ts**
279 J11c
280 J11a **ts**
281 J20b
282 J16c
283 J22b
284 J12a
285 J27a
286 J22i
287 J20c **ts**
288 J22d **ts,g**
289 J16e
290 J16f **ts**
291 J27b
292 J20f **g**
293 J20e **ts,g**
294 J20g **ts**
295 J27g
296 J28b **ts**
297 A23e **ts**
298 J28i **ts**
299 J28h
300 J28g **ts**
301 J28c **g**
302 A23f
303 J28e
304 A24a **g**
305 A24c **ts**
306 A24d **g**
307 A24h **g**
308 A24i **ts**
309 A24j
310 A24l **g**
311 A25a **g**
312 A25c
313 A25d **ts**

314 A27a **g**
315 A27b **g**
316 A26k **g**
317 A26h
318 A26g
319 A26f
320 J28d **ts**
321 A26ll **ts,g**
322 A23b **ts**
323 A23a
324 Qv6 **ts**
325 Qv5 **ts,g**
326 Q5 **ts,g**
327 Q2 **ps**
328 A26e
329 A26d
330 A24m **ts**
331 A25e **ts,g**
332 A25f **ts**
333 A25g
334 A25h
335 A26gg
336 A26ee
337 A26a **g**
338 Rg9 **ts**
339 A25i **g**
340 Rd15 **ts**
341 R13 **ts**
342 R14 **ts**
343 Rv5
344 Rg9 **ts**
345 Rg8 **ts**
346 A25o
347 A25m
348 A25j

**Lac à Foin
Area**

349 Qb6 **ts**
350 Qa6 **ts**
350a Rd2 **ts**
350b Qa1 **ts,g**
351 Re6 **ts**
352 Re13 **ts**
353 Qh10 **ts,g**
354 R3 **ts,g**
355 Zp5c **ts**
356 Zm1 **ts,g**
357 Zm3 **ts**
358 Zm4 **ts,g**
359 Rj13 **ts**

360	Zo2	ts	408	19a ts
361	Rj12	**ps**	409	21h
362	Zm6	ts	410	21q
363	Zo4	ts	411	24e
364	Zo10	ts	412	12b
365	R4	g,ts	413	12d ts

414 12f ts

Lac Murray 415 19d ts
Area 416 5d

417 9a ts

366	22p		418	9b
367	22m	ts	419	23b ts
368	22c		420	9d **ps**
369	22k		421	9f
370	22f		422	9g
371	22e	ts	423	23c
372	17c	ts	424	9k **ps**
373	8k	ts	425	23e
374	16o	ts	426	19f ts
375	16n	ts	427	19g ts
376	25f	ts	428	20b
377	25e		429	19h ts
378	6e		430	20c ts
379	25c	**ps**	431	20d
380	16h		432	24j
381	25a	ts	433	24k ts
382	25b		434	12i
383	16g		435	5j ts
384	16c	ts		
385	18c	ts		
386	17d	ts		
387	22c	ts		
388	22x			
389	24b	ts		
390	24a	ts		
391	22ac	ts		
392	17h			
393	21d	ts		
394	10i	**ps**		
395	10e	ts		
396	10d			
397	10a	ts		
398	26d			
399	26a	**ps**		
400	6a			
401	8l	ts		
402	5b			
403	25i	ts		
404	6e	ts		
405	6f			
406	6g			
407	6h	ts		

National Library
of Canada

Bibliothèque nationale
du Canada

Canadian Theses Service

Service des thèses canadiennes

NOTICE

AVIS

THE QUALITY OF THIS MICROFICHE
IS HEAVILY DEPENDENT UPON THE
QUALITY OF THE THESIS SUBMITTED
FOR MICROFILMING.

LA QUALITE DE CETTE MICROFICHE
DEPEND GRANDEMENT DE LA QUALITE DE LA
THESE SOUMISE AU MICROFILMAGE.

UNFORTUNATELY THE COLOURED
ILLUSTRATIONS OF THIS THESIS
CAN ONLY YIELD DIFFERENT TONES
OF GREY.

MALHEUREUSEMENT, LES DIFFERENTES
ILLUSTRATIONS EN COULEURS DE CETTE
THESE NE PEUVENT DONNER QUE DES
TEINTES DE GRIS.

Location of Study Area

Map showing the location of the study area near Kuujjuaq, with Baffin Island, Ungava Bay, Labrador, Hudson Bay, and Schefferville labeled.

LAC BERTHET

8
9 10 11

2 3 4 5 6 7
1

68° 20

15

16

12

13

58°30

14

N

Location of Study Area

LAC BERTHET

70

Schefferville

58° 2

69°
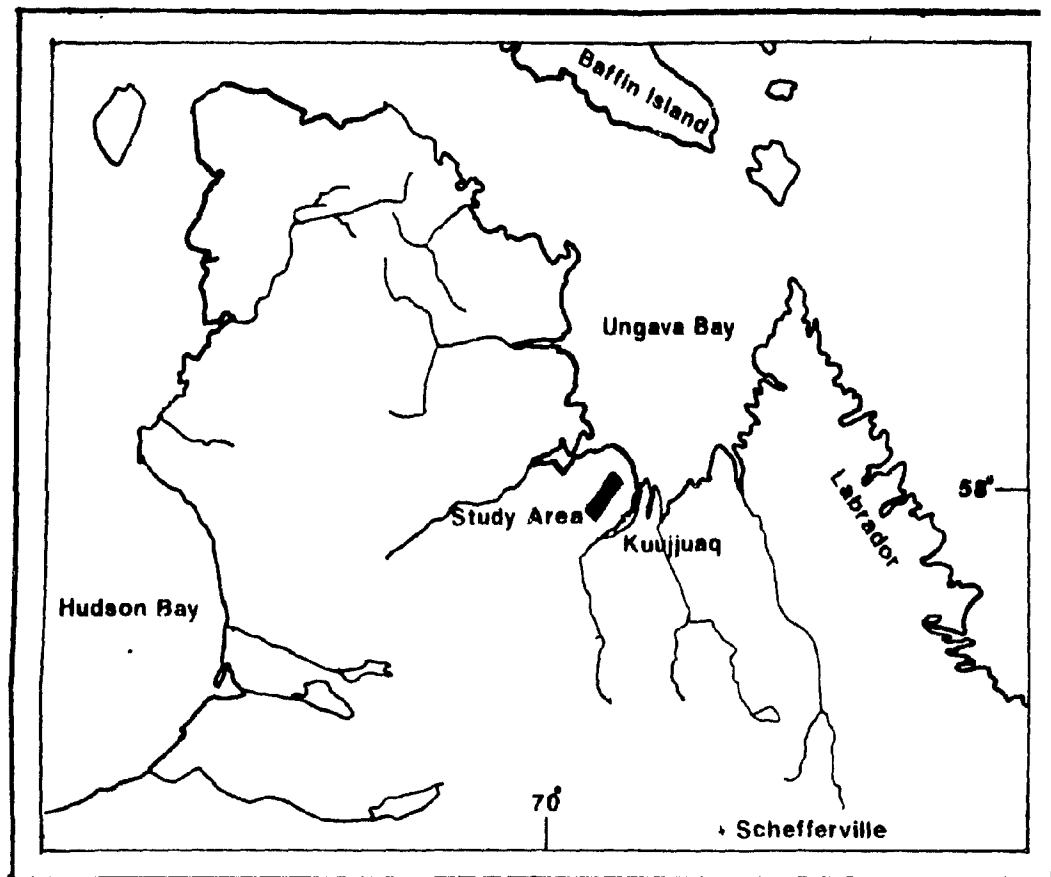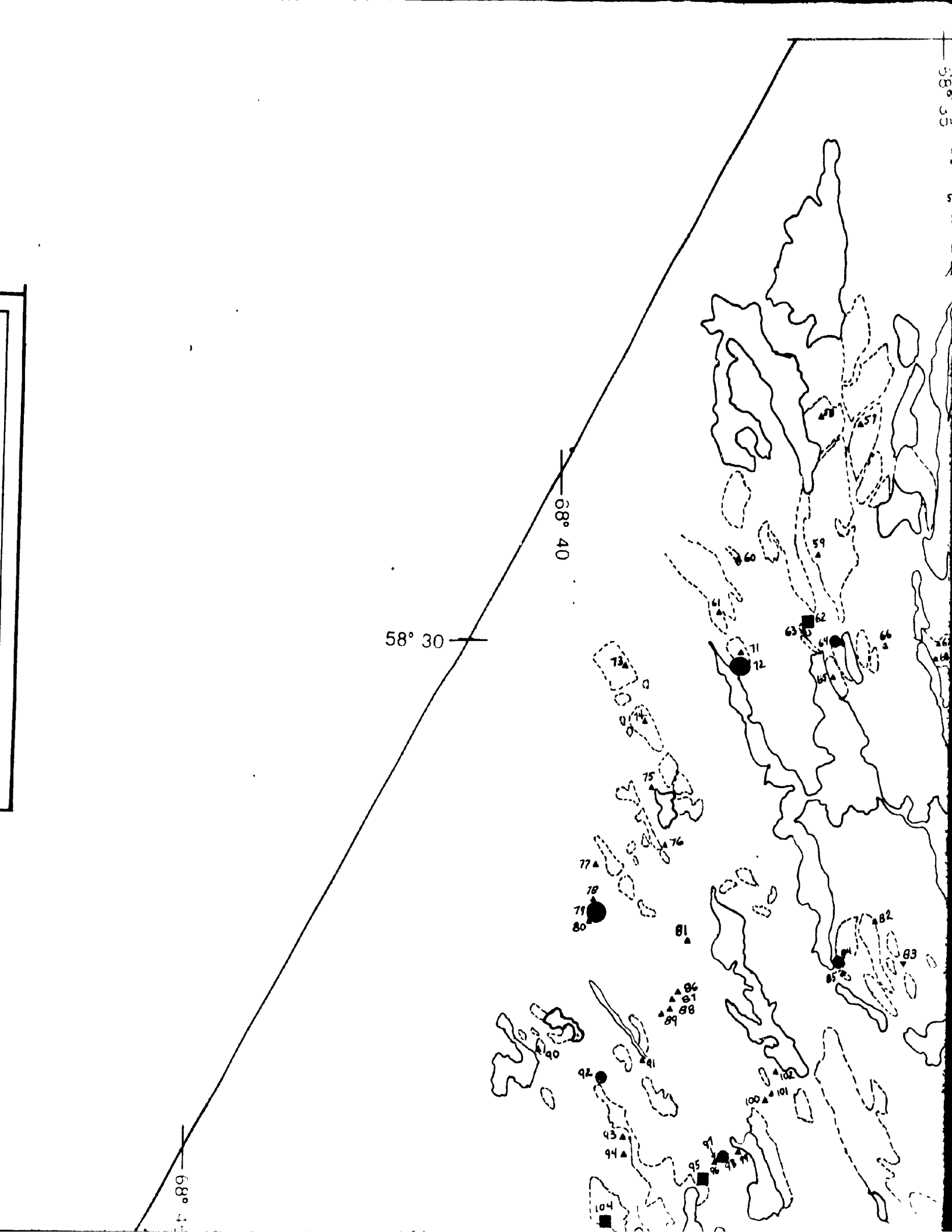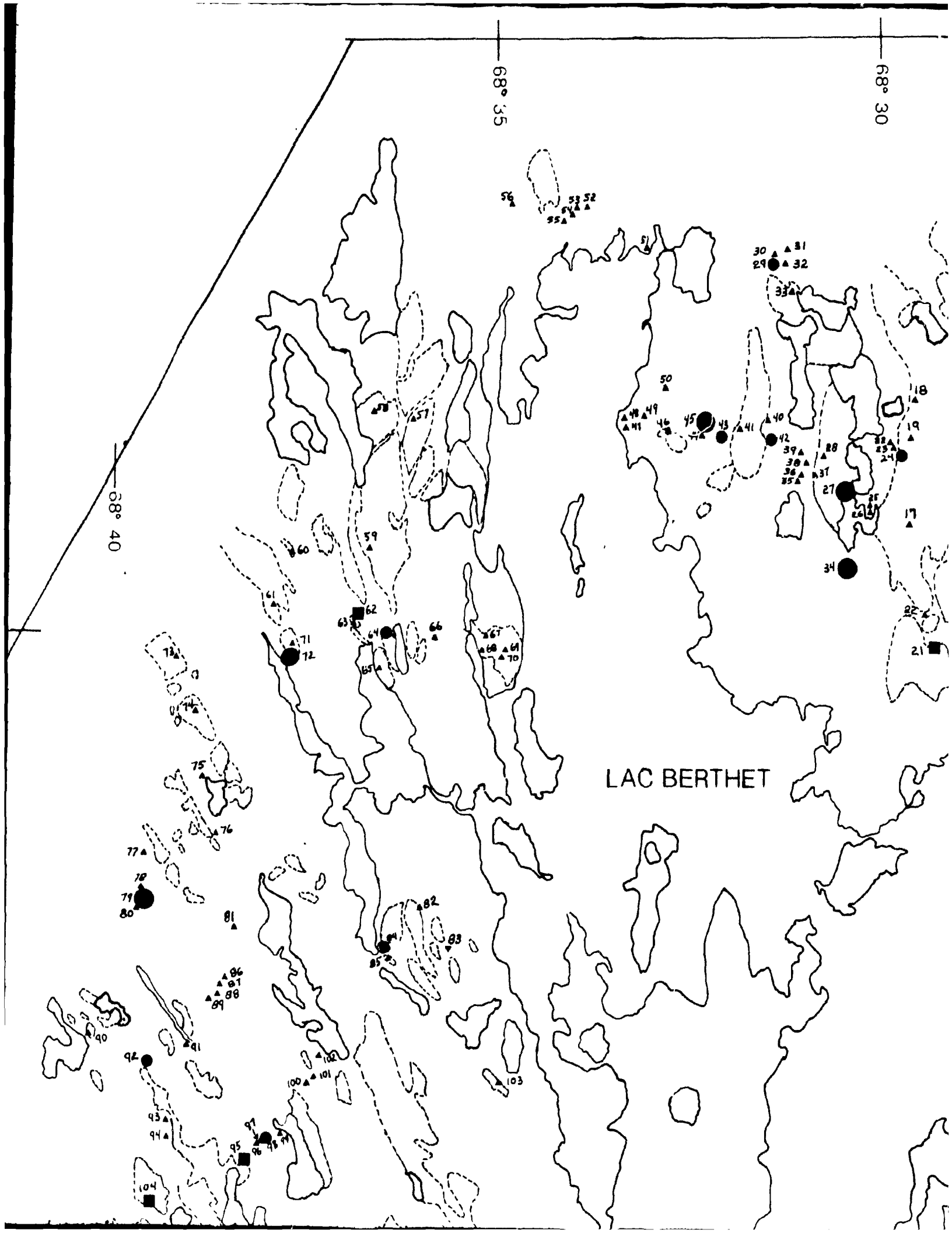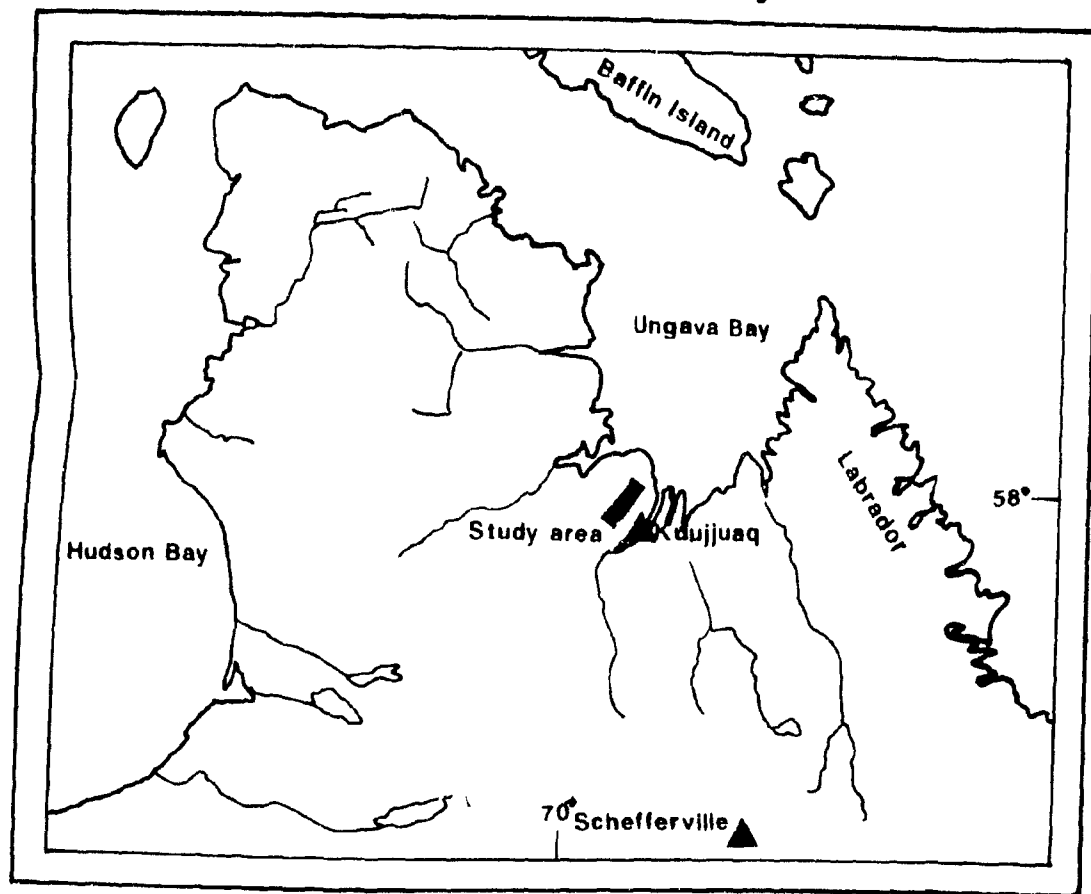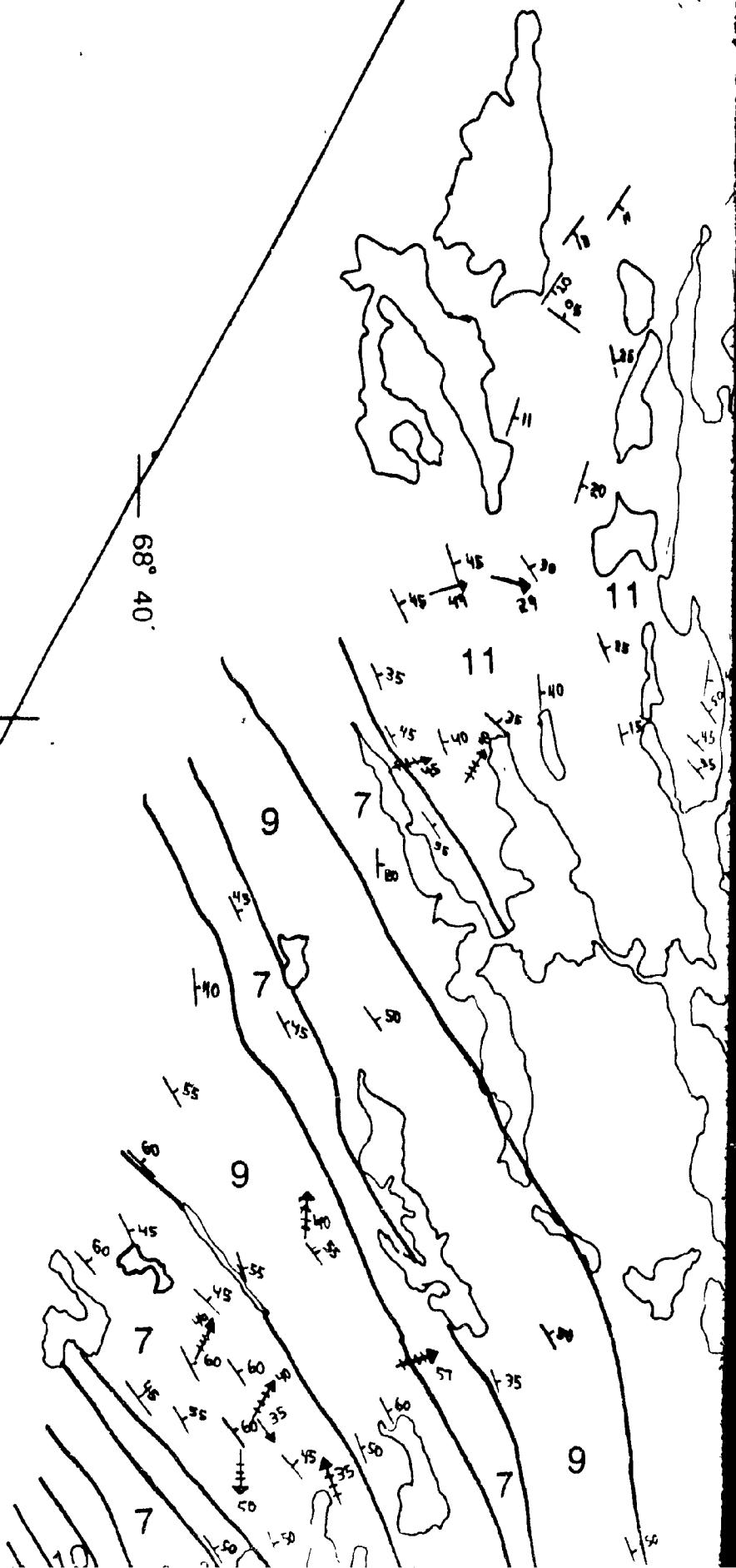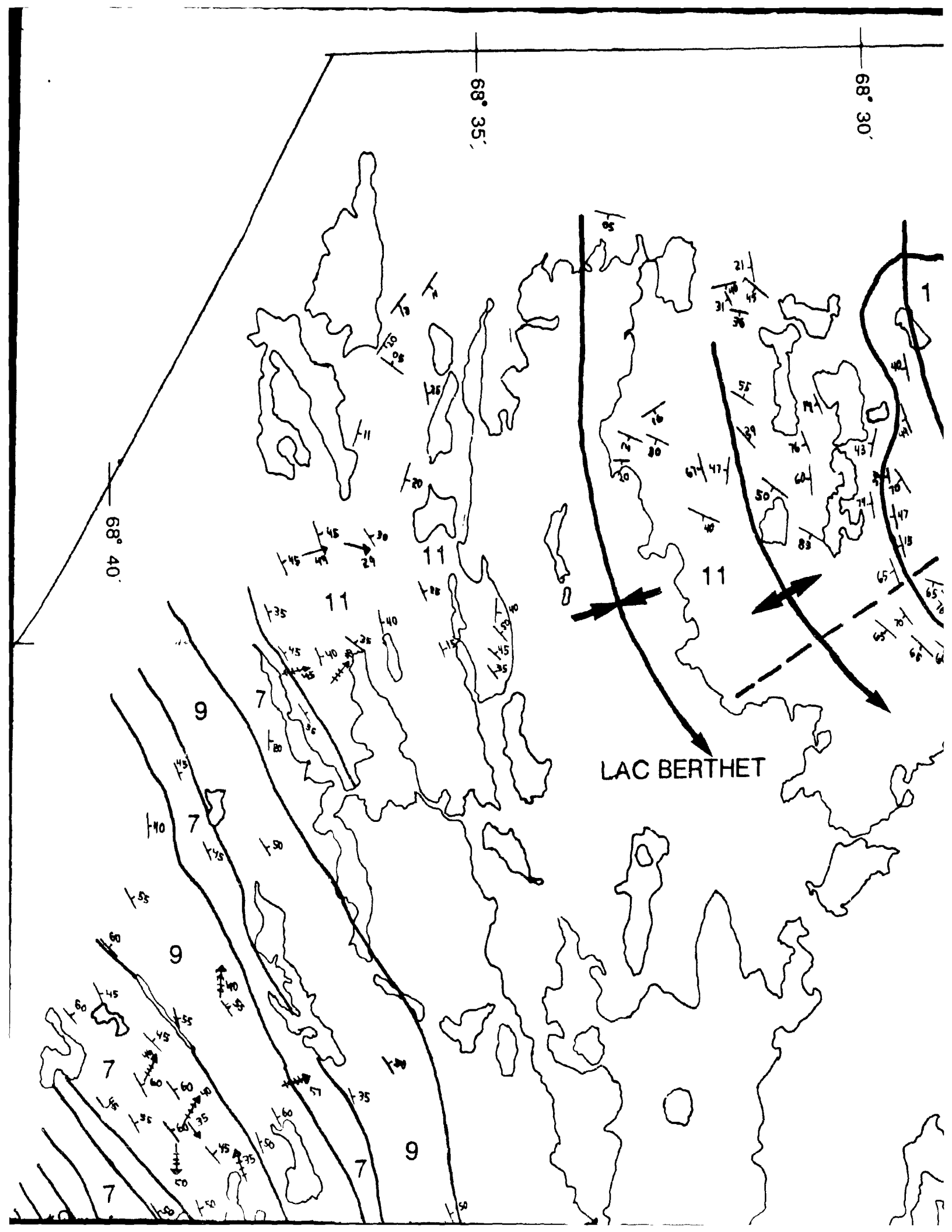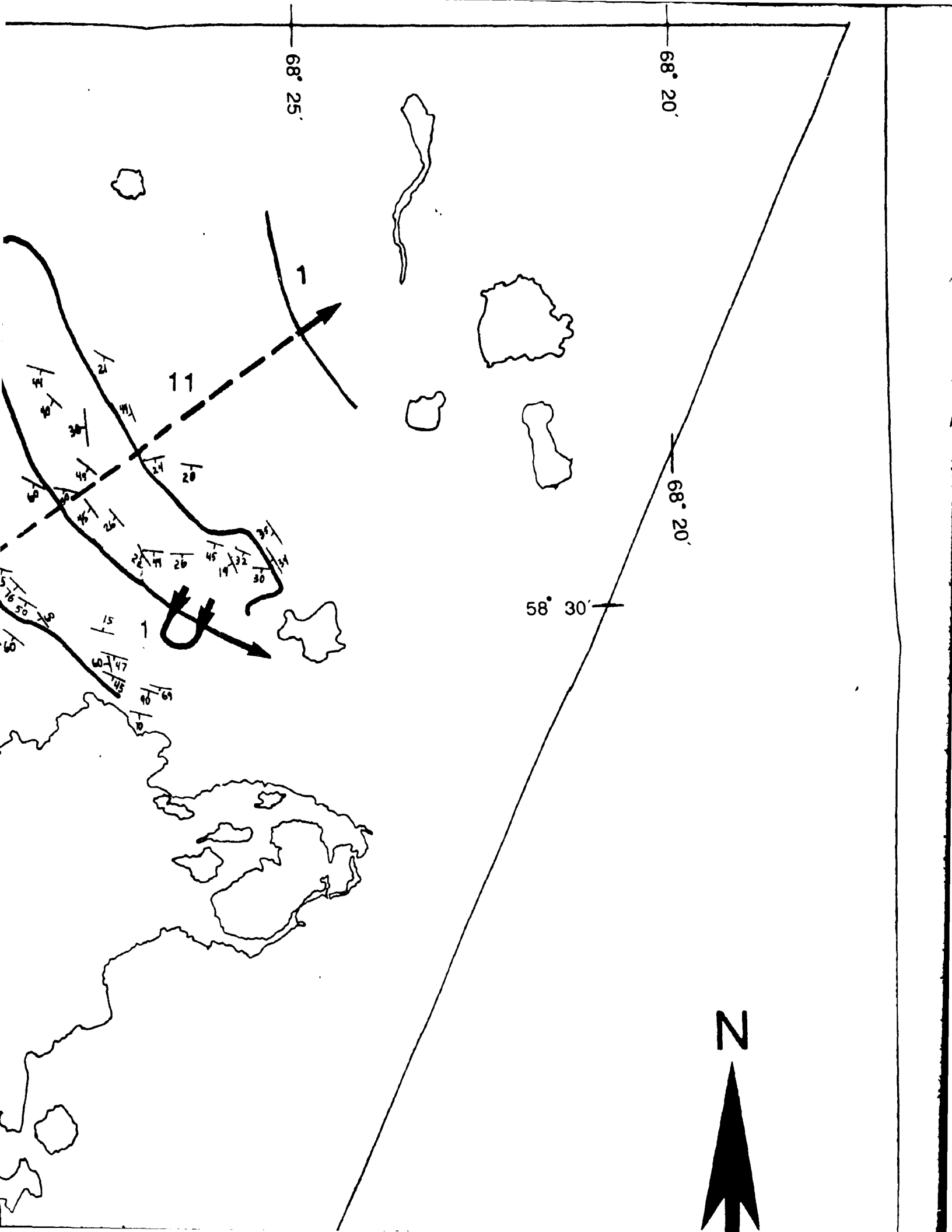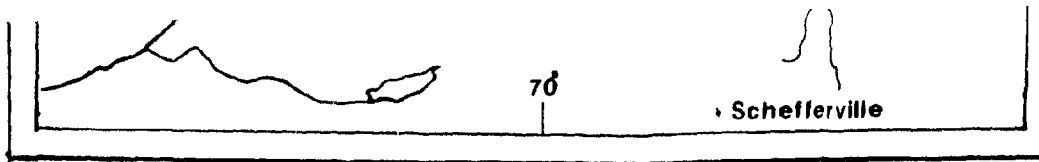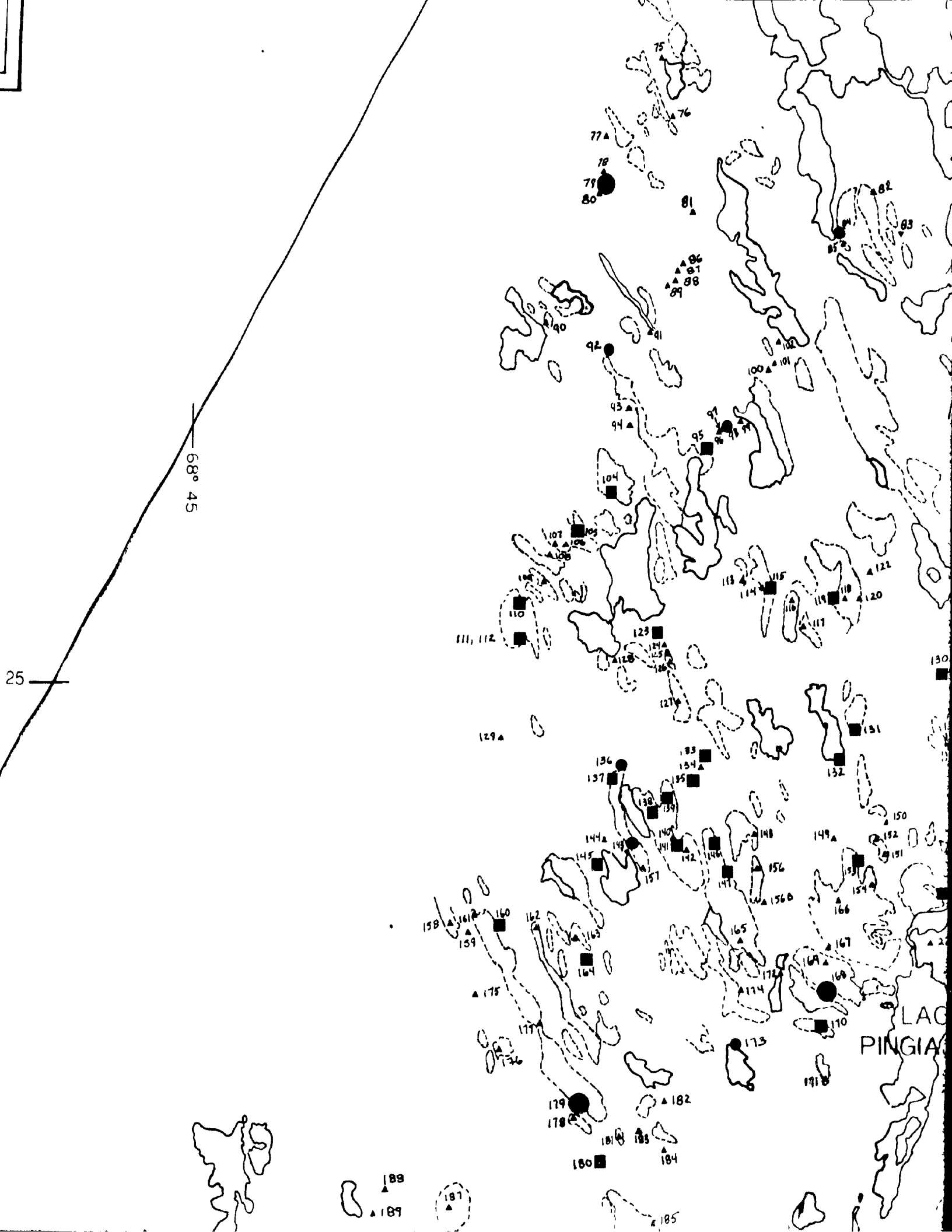
LAC BERTHET

LAC PINGIAJJULIK
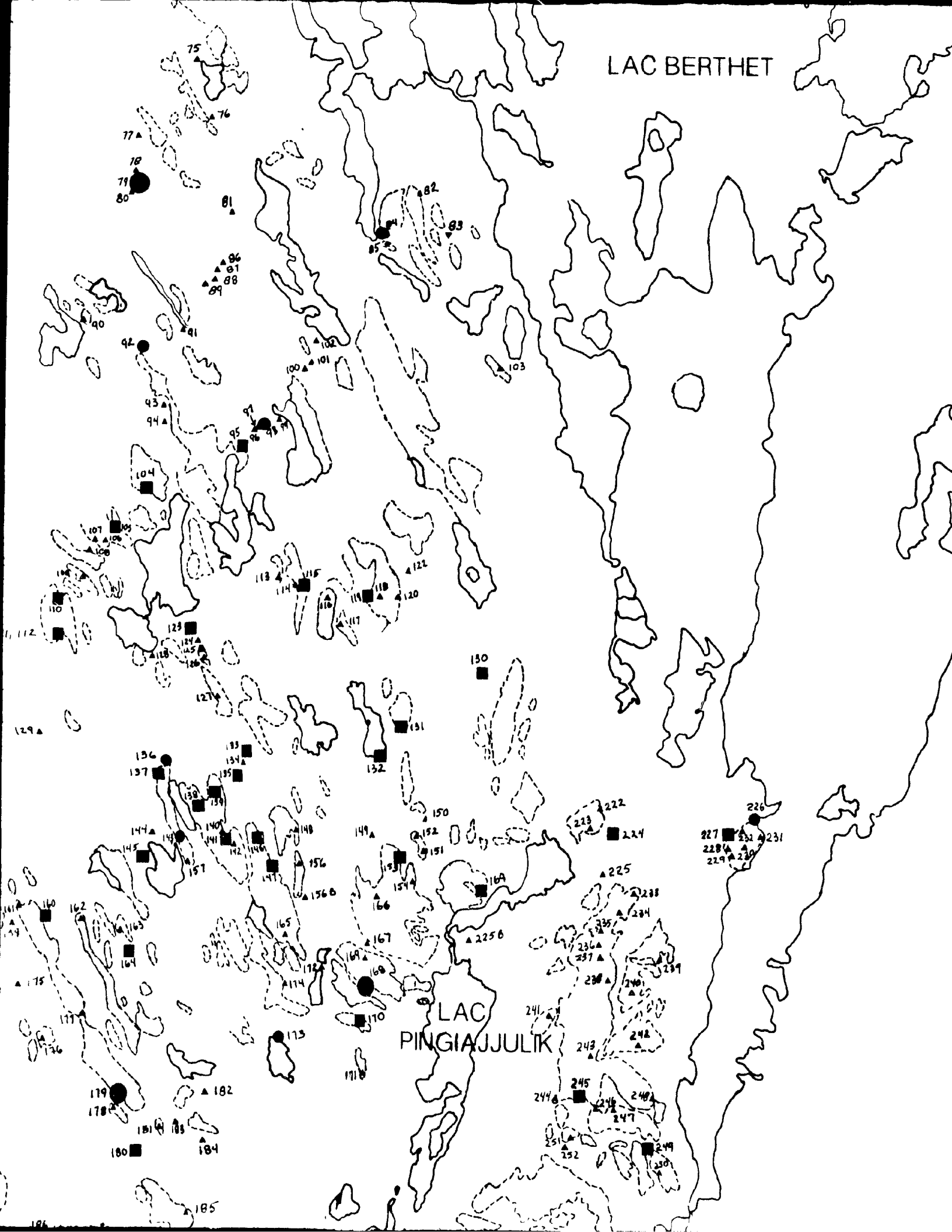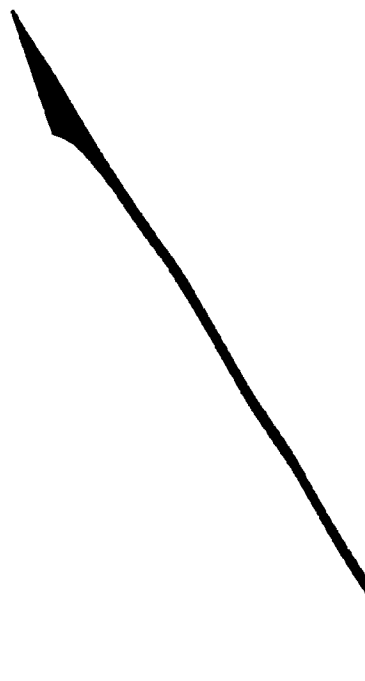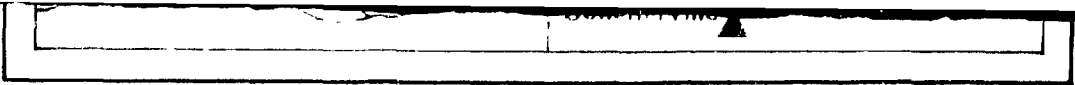
N

M. N.

58° 25 —|— 68° 25

58° 25´ -

68° 50´

Lac Pingiajjulik Fault

LAC
PINGIAJJULIK

58° 25′   68° 25′

N

M. N.

115

177
176

179
178
182

181 183
180
184

189
189

187

185

186

190
191 193
192
194 195
201
200
199
196
197
198
202

208
204
203
257 256
206
207
207
208
254

209
205 217
213
210 221
211 220
212 214
218 219
215
216

264
265
266

270

279

277
282
283

296

301

304
314 305
315 307 306
316 308
320 309
311 310
318
312
311
328 329
327 331
330 332
333 334
337 338 339
346

PINGIAJJULIK

LAC
PINGIAJJULIK

58 20'

68° 30'
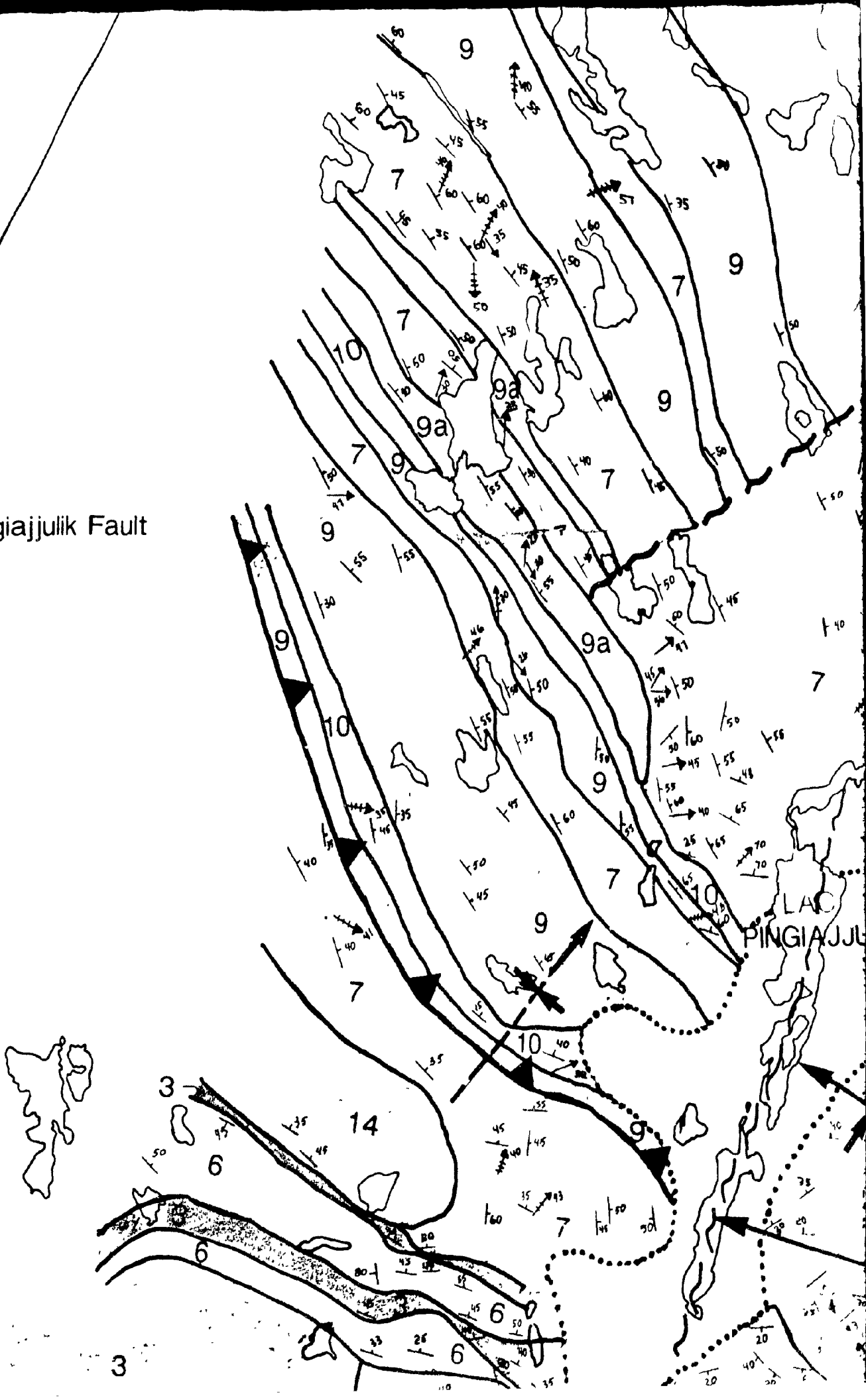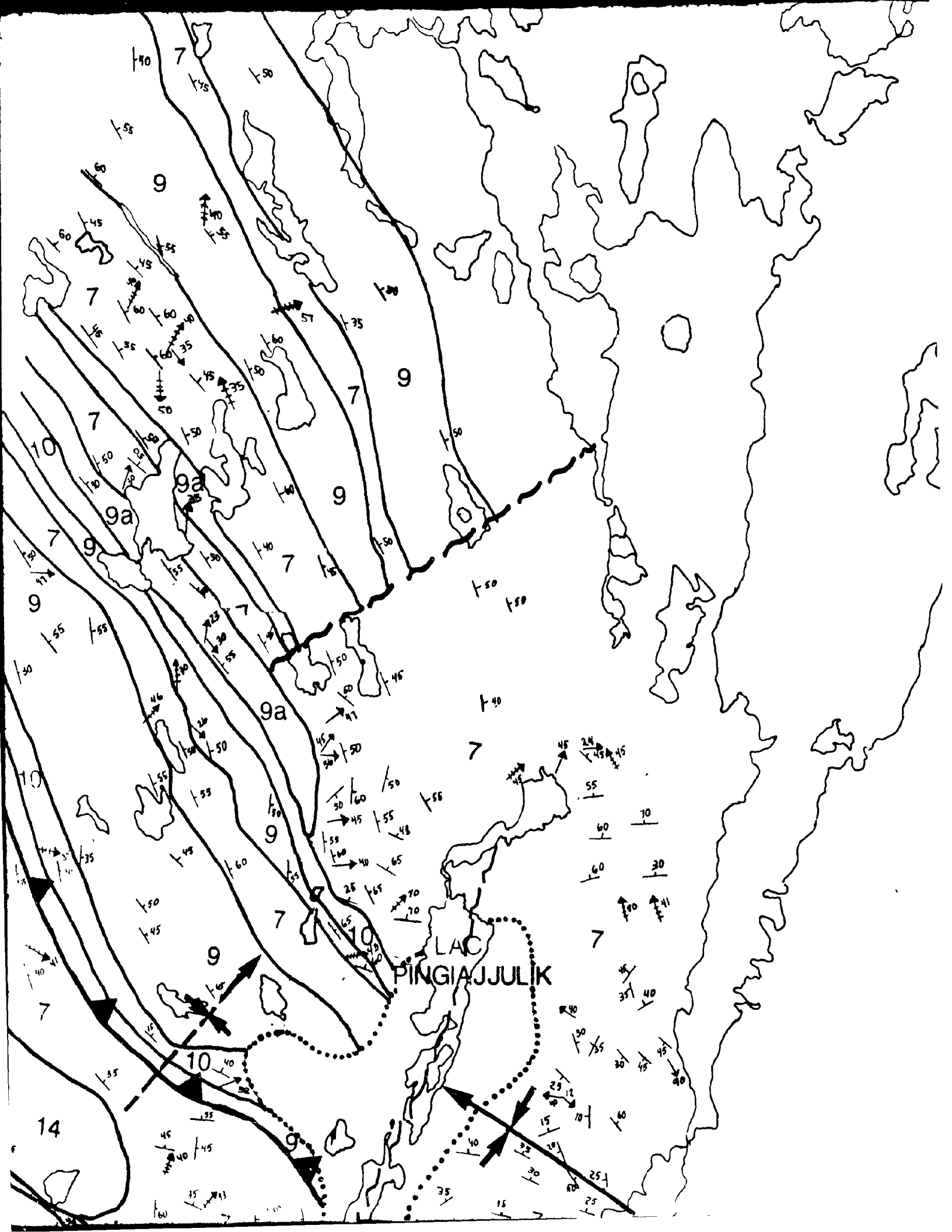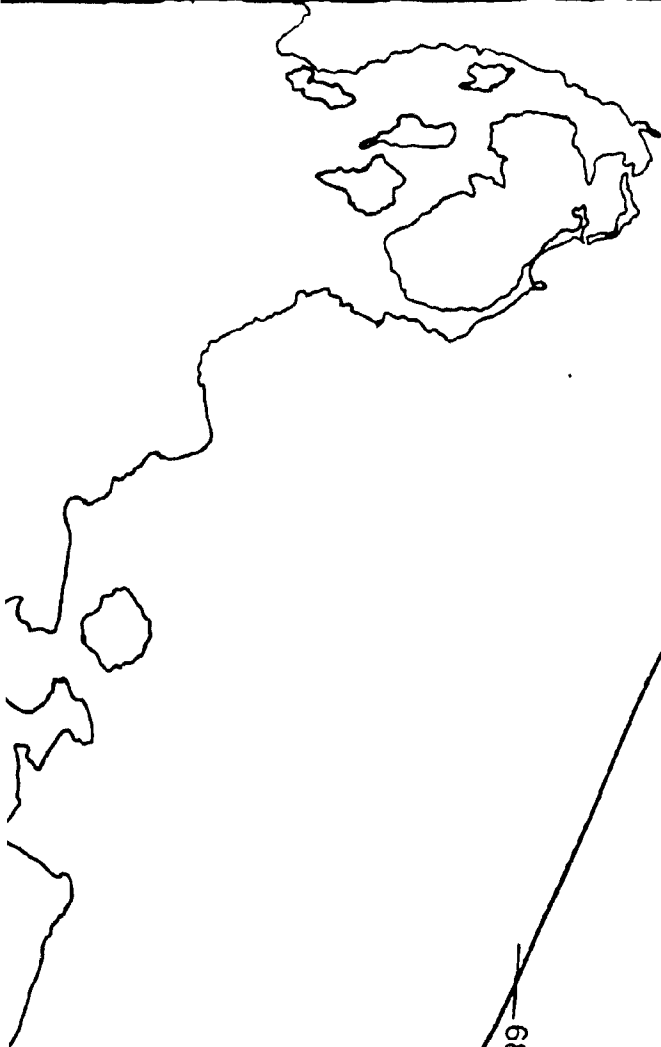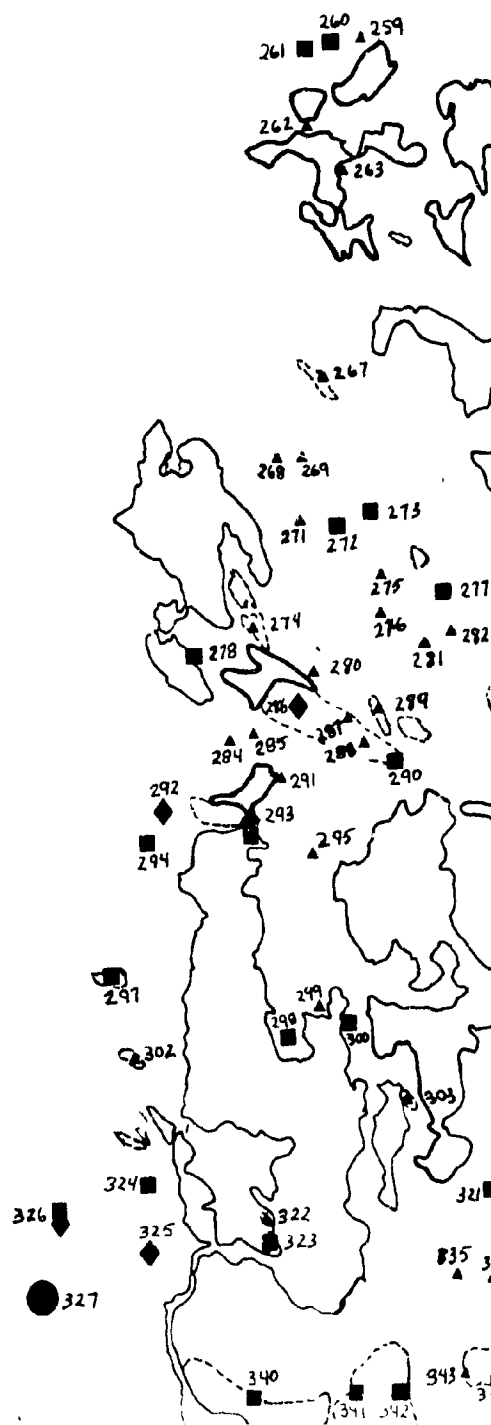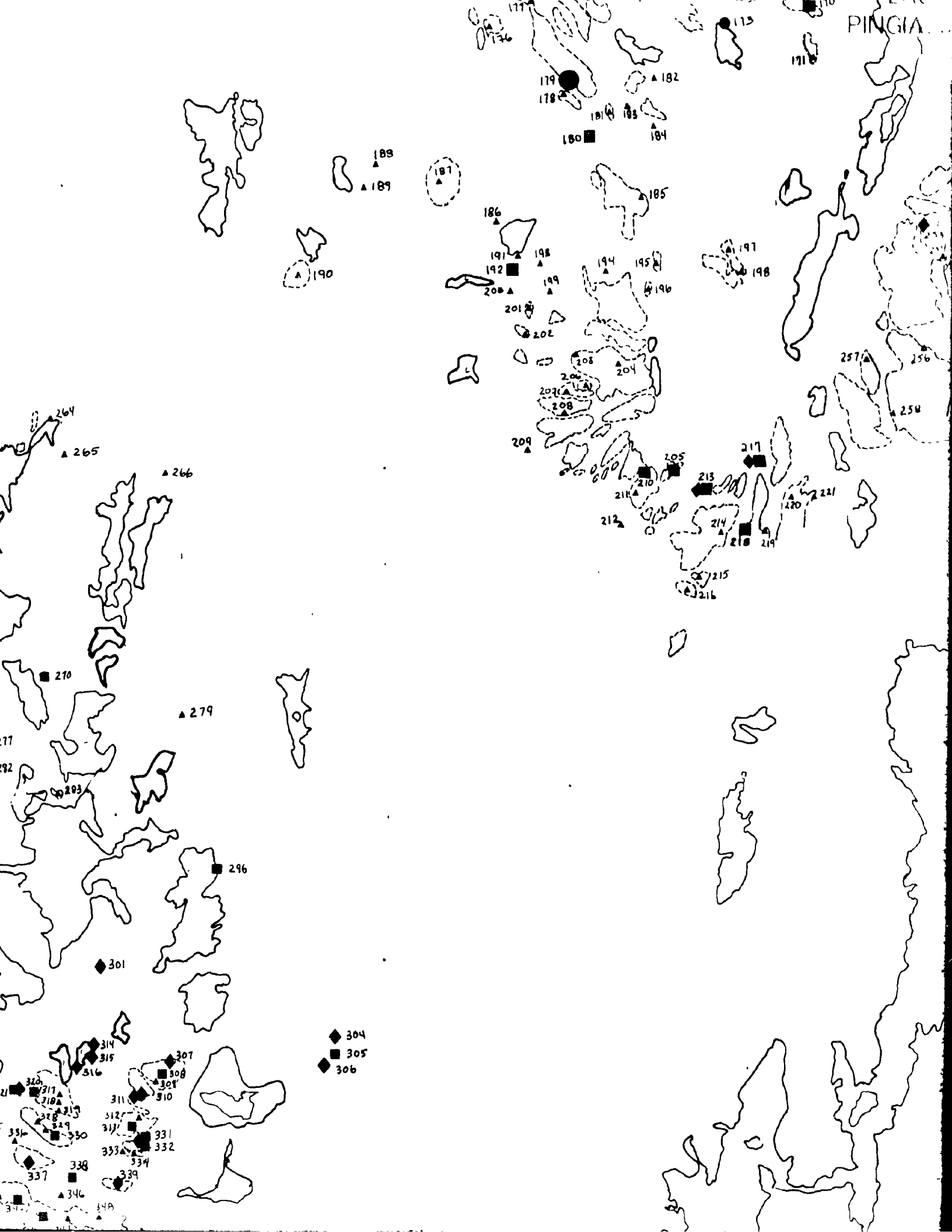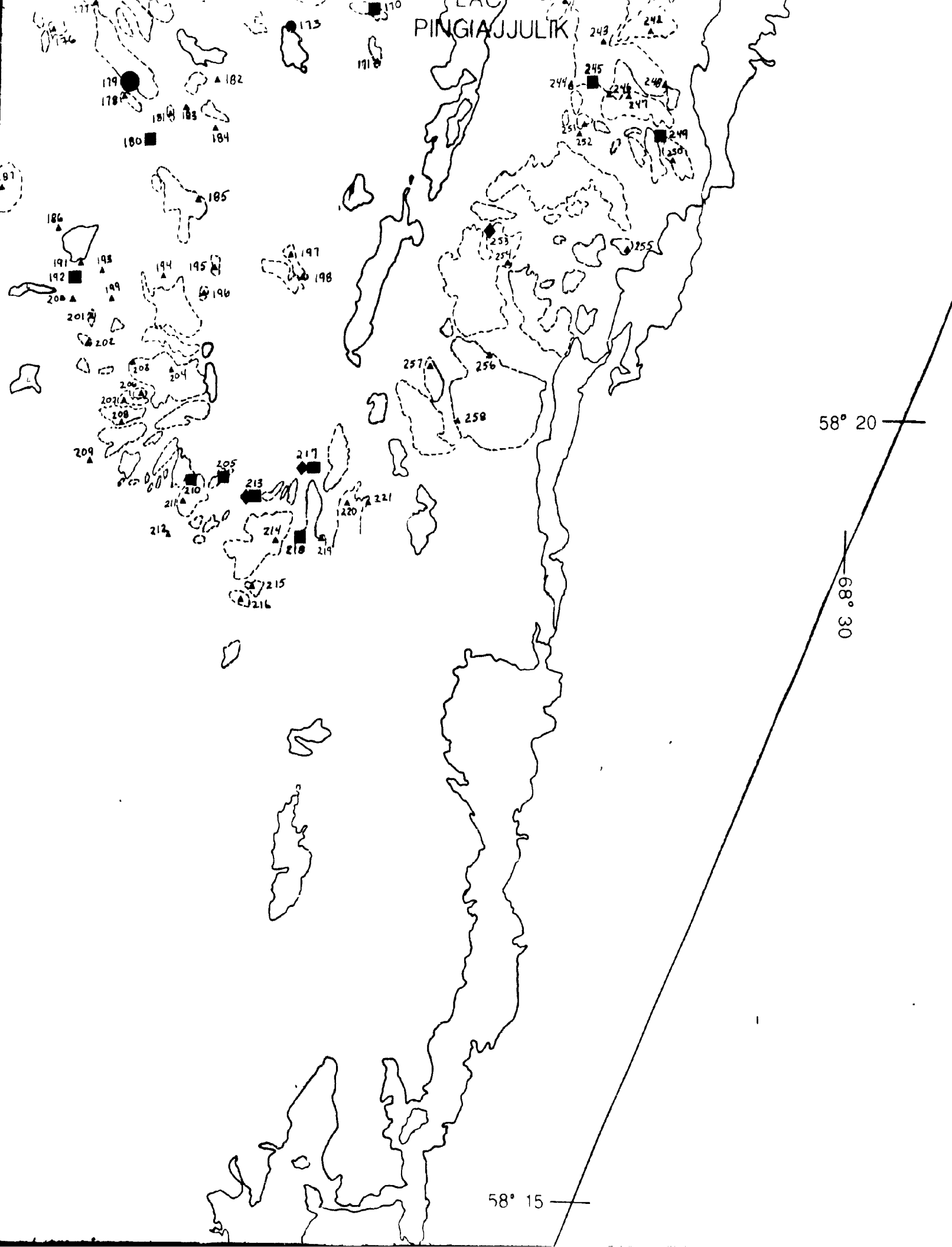
58° 15'
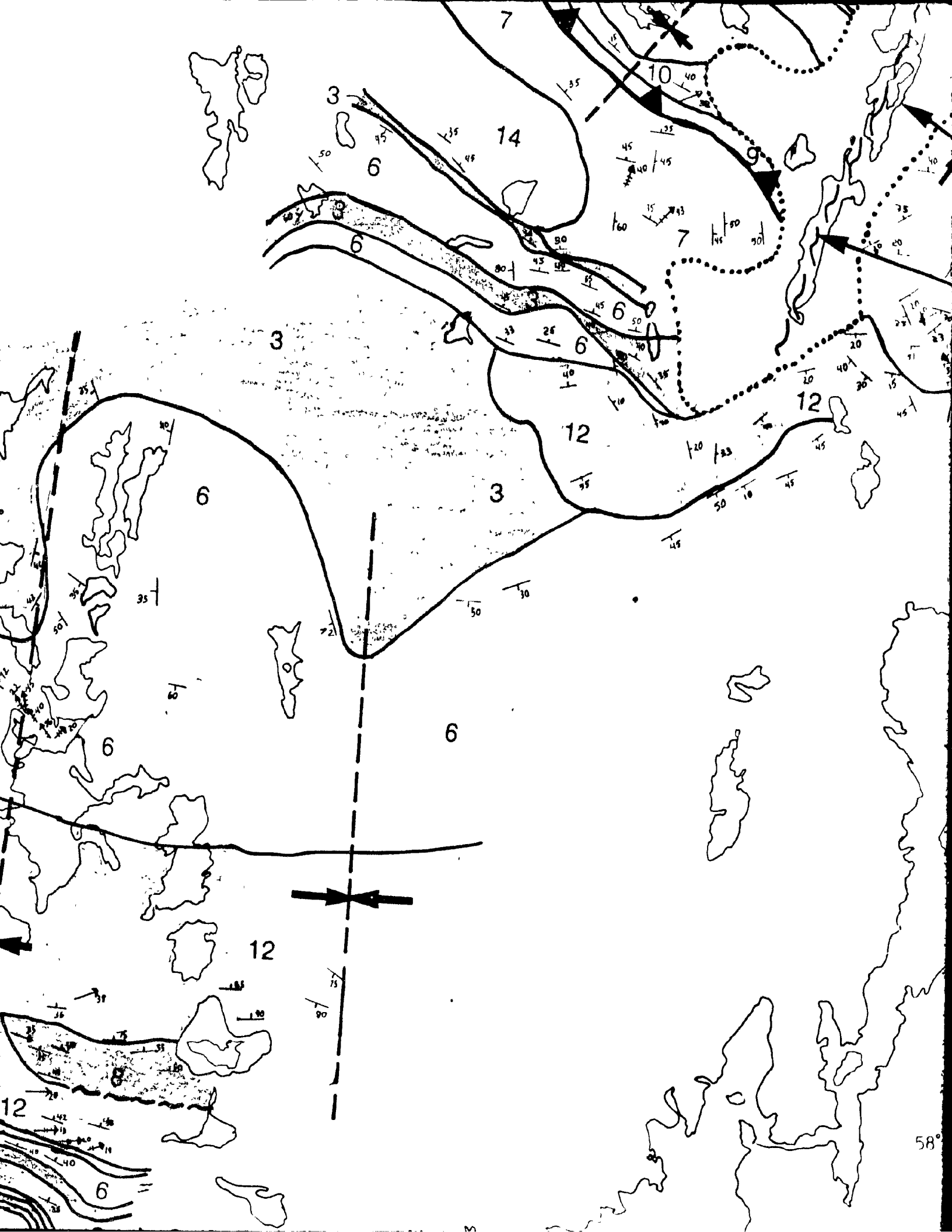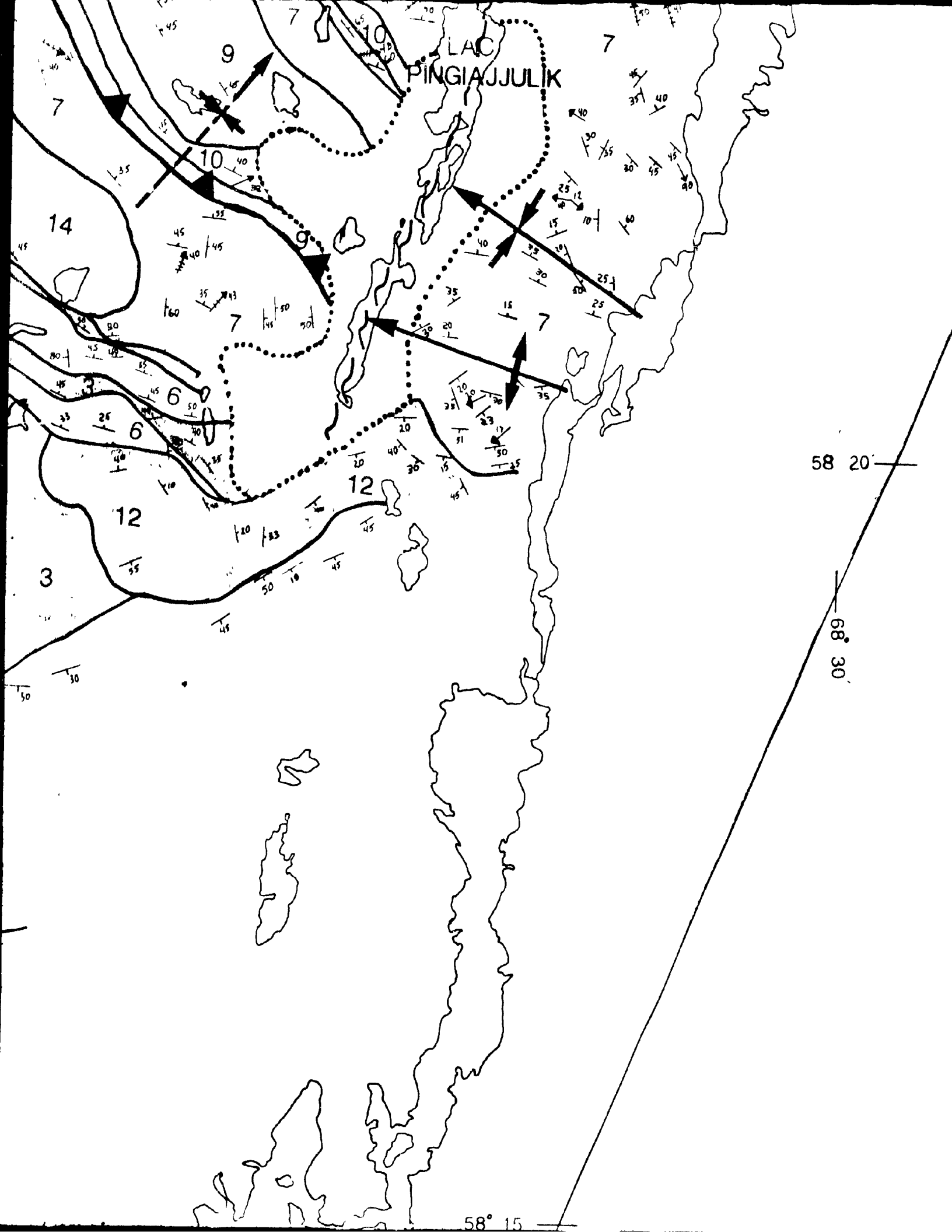
LEGEND

Hudsonian Intrusives

14	Pegmatite and minor granite
13	Granite
12	Granodiorite and tonalite
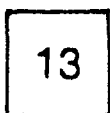
Aphebian Metamorphic Rocks

11	Undifferentiated metasediments (mainly amphibolites with minor quartzose gneiss)
10	Quartzofeldspathic gneiss
9	Epiclastic amphibolite; 9a Banded epiclastic amphibolite
8	Calc-silicate gneiss
7	Hornblende-Biotite paragneiss
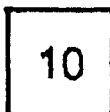
58° 15

291
249
299
300
302
303
324
326
325
322
323
835
327
340
341 342
343
349 350 350 B
350 A
351
LAC
352
353
A
FOIN
354
355
356
357
358
360
362
365

LAC FORTIN

366
367
368
369
311 370
388
374 373 372
375
387
380 383
386
391
376 371 381 384
385 390
392
318 374 382
393
389
401 397
400 398 395,396
404 402 394 409 410
406 403
407 405
LAC
408
MURRAY
411
412
416
415
413
417 414
418
421 419
426
422 420
427
428 430
423 429
424 431 432
425 433
434
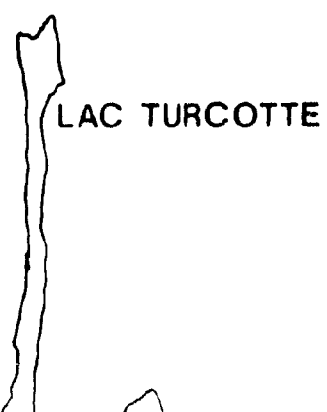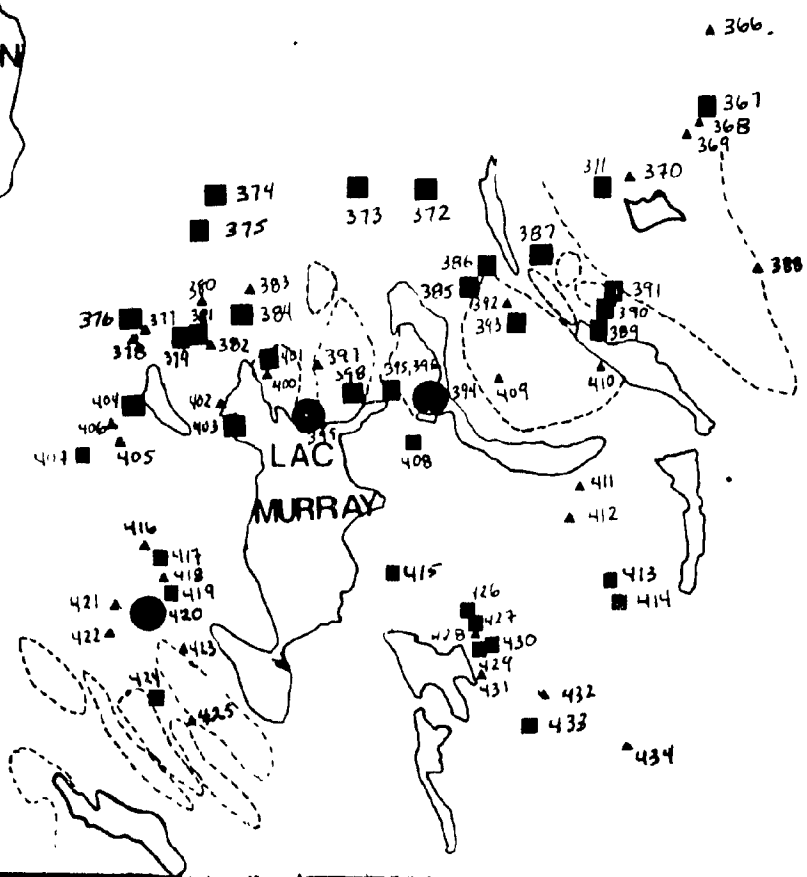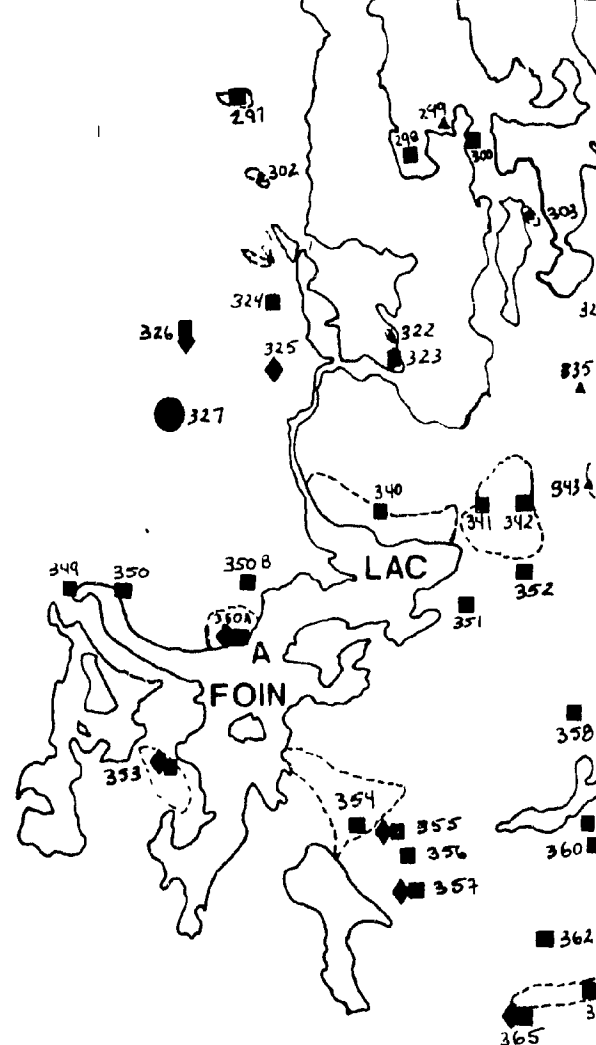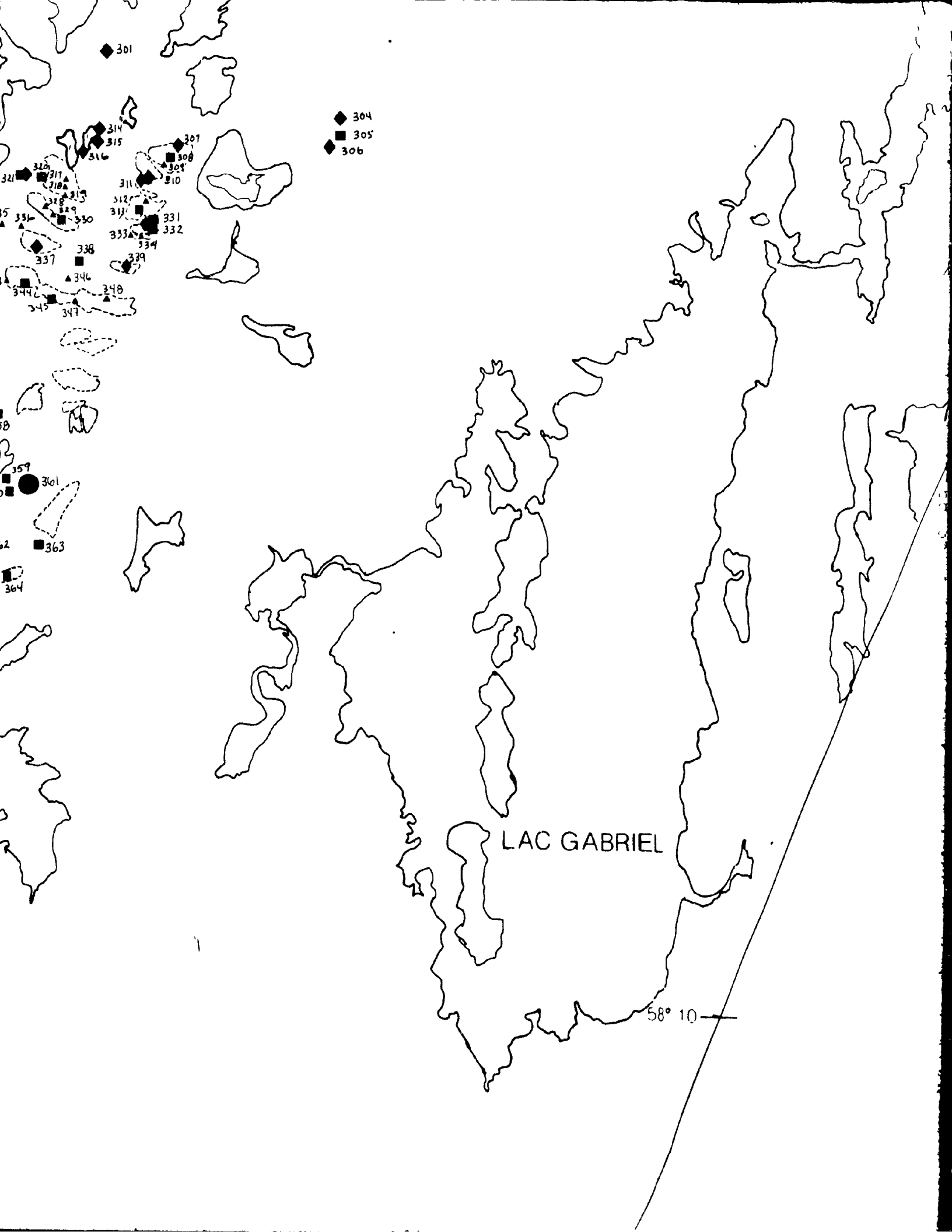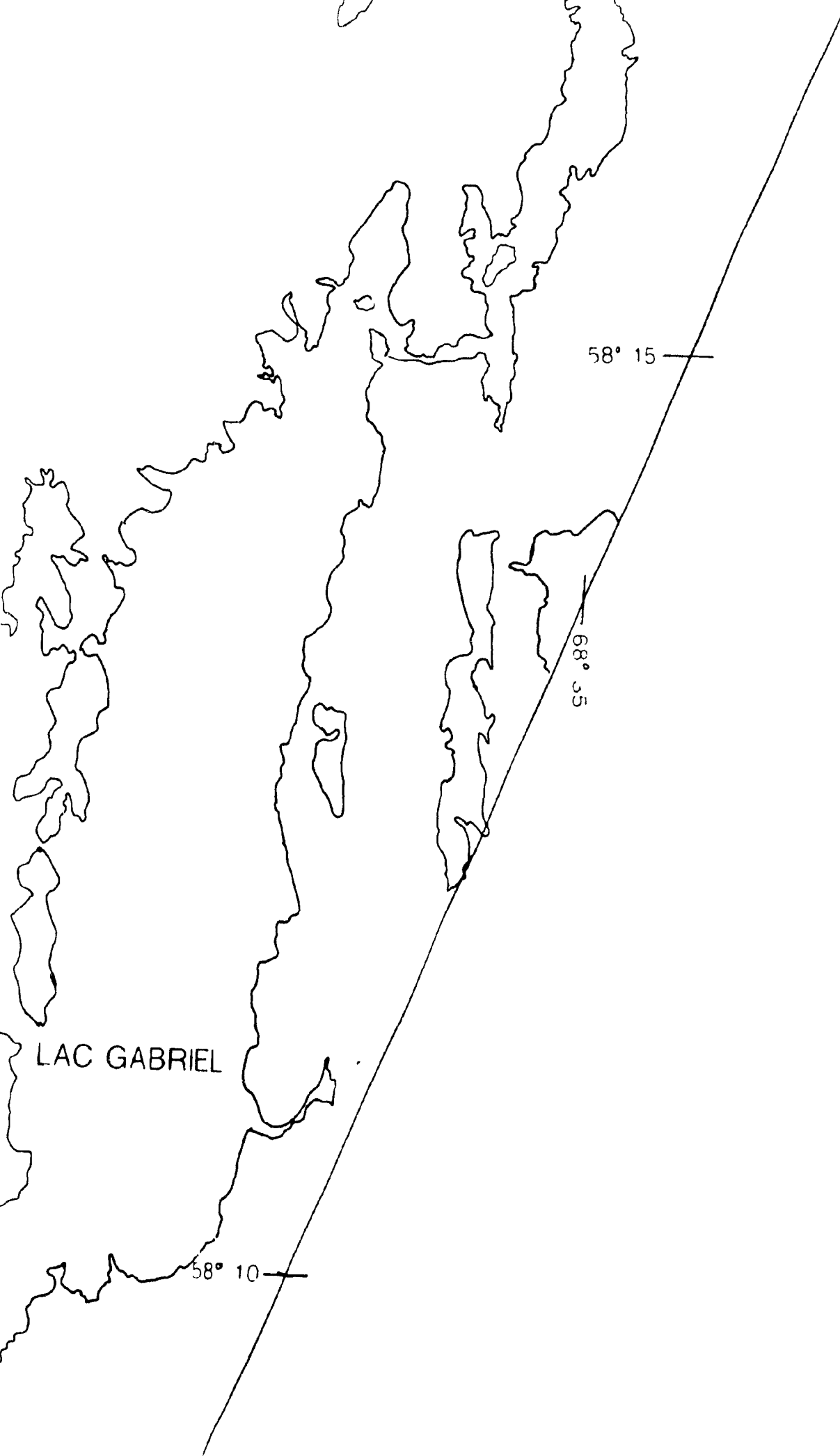
LAC TURCOTTE

LAC GABRIEL

58° 10

58° 15

68° 35

LAC GABRIEL

58° 10

SAMPLE KEY

▲   Rock Sample

■   Thin Section

●   Polished Thin Section

◆   Geochemistry Sample

●   Microprobed Sample

⬭   Large Outcrop
        (from aerial photographs)

Lac Turcotte Fault

Lac Olmstead
Fault

LAC FORTIN

LAC MURRAY

LAC TURCOTTE

58° 15'

LAC GABRIEL

58° 15′

68° 35′

LAC GABRIEL
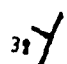
58° 10′

10	Quartzofeldspathic gneiss
9	Epiclastic amphibolite: 9a Banded epiclastic amphibolite
8	Calc-silicate gneiss
7	Hornblende-Biotite paragneiss
6	Gneissic metasandstone
5	Quartzose gneiss
4	Marble
3	Amphibolite
2	Pelitic to Semipelitic schist
1	Migmatized granitic to tonalitic gneiss (Archean?)

SYMBOLS

Strike and dip of foliation and or compostional layering

Lineation, trend and plunge

Minor fold, trend and plunge: F2. F3, generation unknown

Axial trace of major fold F2. F3

LAC FORTIN

LAC TURCOTTE

LAC
MURRAY

0   1   2   4

km

1 : 50,000

LAC GABRIEL

58° 10

68° 40

68° 45

8

LAC GABRIEL

68° 10

68° 40

♦ Geochemistry Sample

● Microprobed Sample

Large Outcrop
    (from aerial photographs)

GGP '89

LAC FORTIN

Lac Olmstead
Fault

LAC MURRAY

LAC TURCOTTE

68° 55'

68° 50'

0   2   4

km

1 : 50,000

LAC GABRIEL

58° 10'

68° 40'

68° 45'

Additional geology from Gelinas

8

LAC GABRIEL

58° 10'

68° 40'
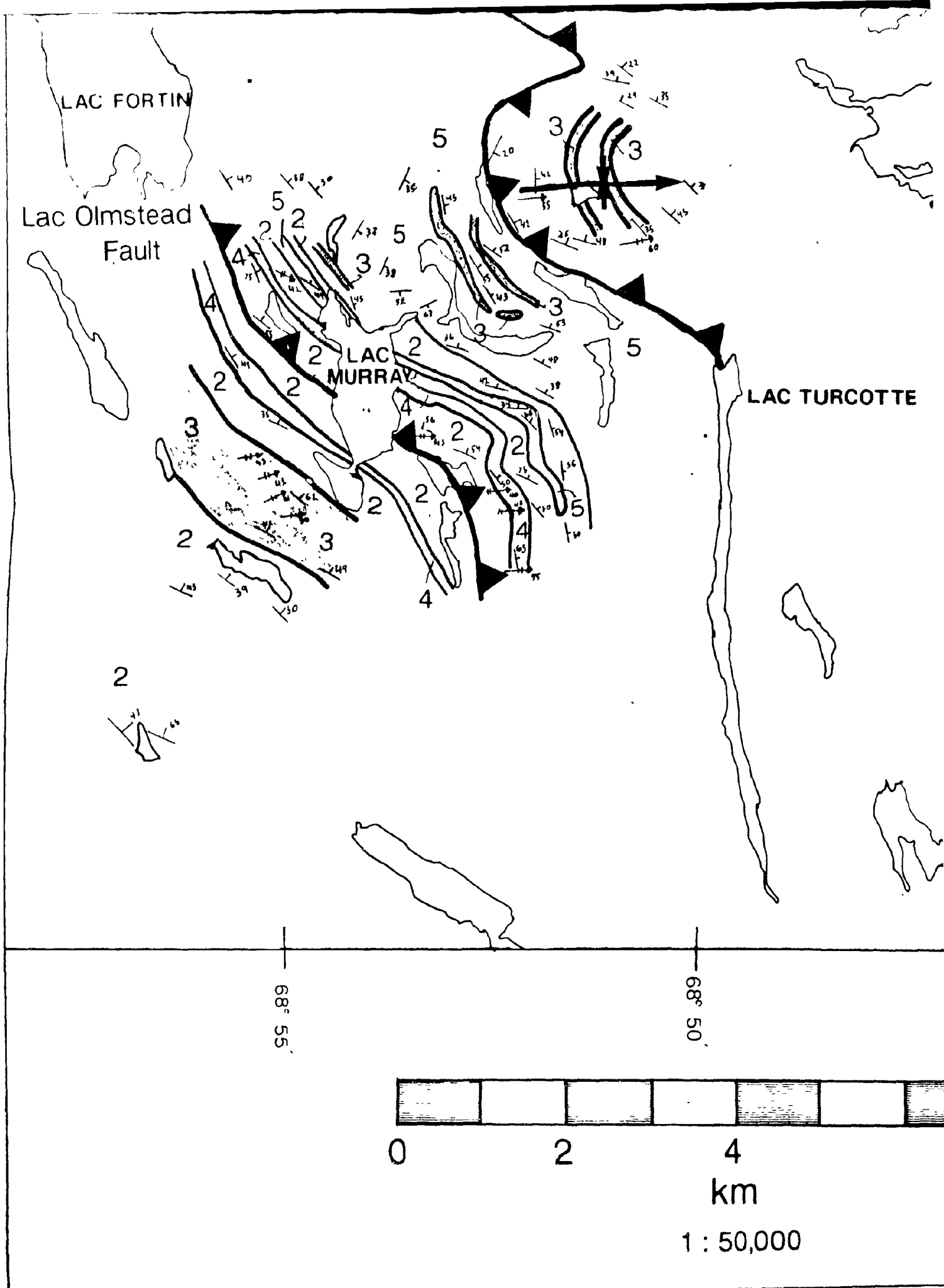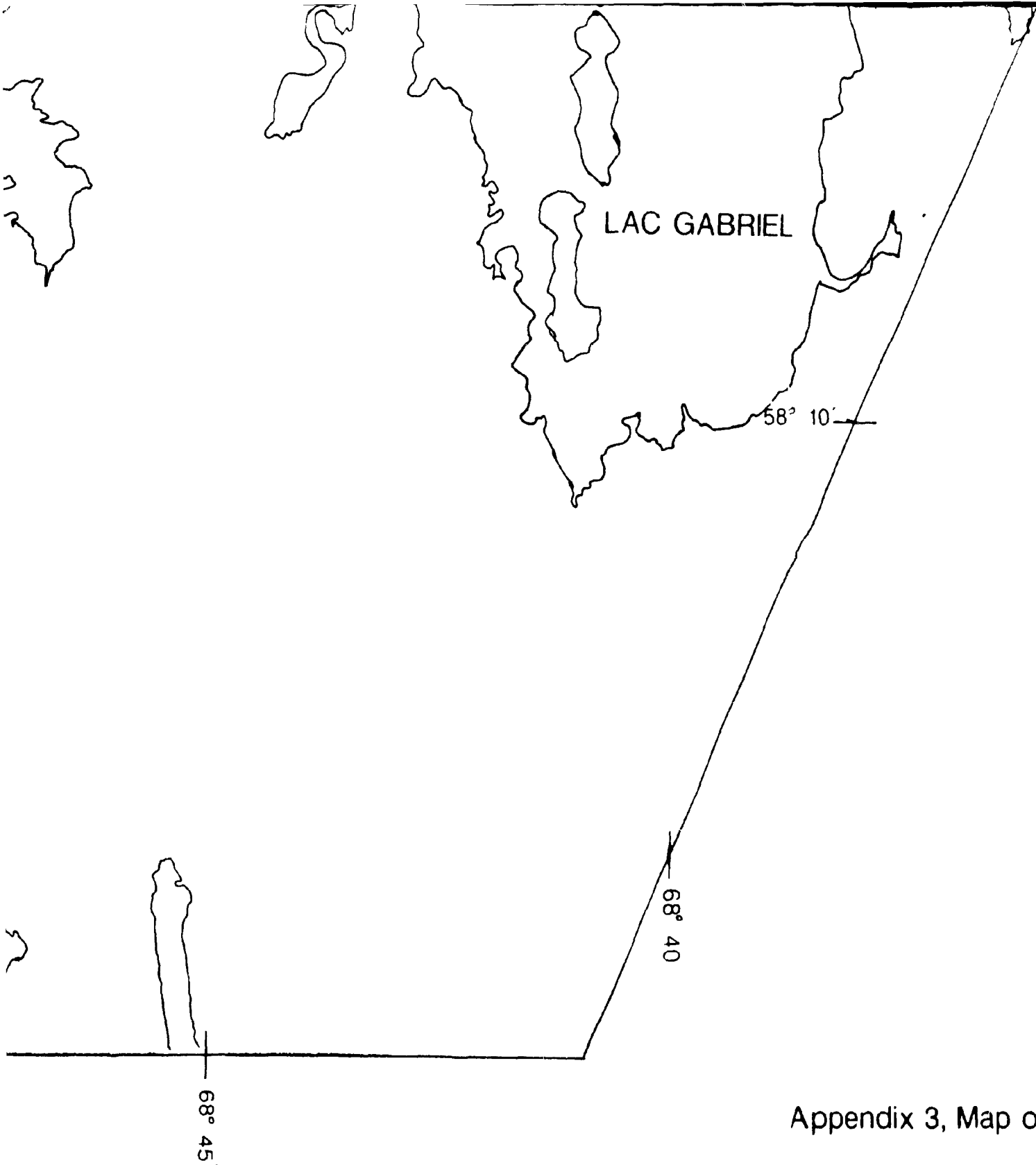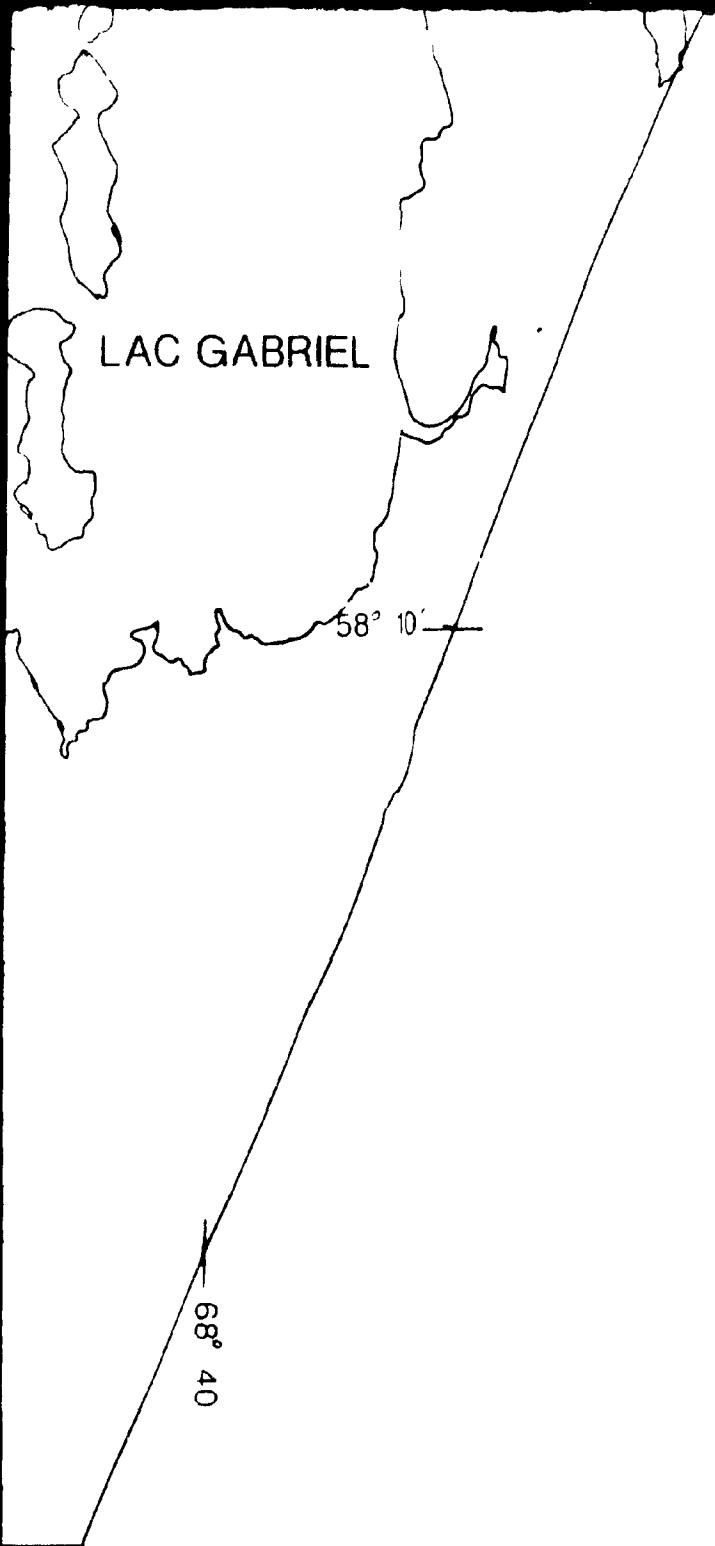
Appendix 3, Map of Study area with geology and structural data

Additional geology from Gelinas (1959) and Bosdachin (1986) (Lac a Foin area)

2	Pelitic to Semipelitic schist

1	Migmatized granitic to tonalitic gneiss (Archean?)

SYMBOLS

Strike and dip of foliation and or compostional layering

Lineation, trend and plunge
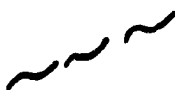
Minor fold, trend and plunge: F2, F3, generation unknown

Axial trace of major fold: F2. F3

Synform, Antiform, Overturned synform

Major fault, teeth point in dip direction

Minor fault

GGP '89